SOUND TRANSMISSION ANALYSIS BY SOUND INTENSIMETRY

by

Barend Gideon van Zyl

Submitted in partial fulfilment of the requirements for the degree of Doctor of Philosophy, in the

Department of Electronic Engineering
University of Natal
1985

Pretoria
1985

PREFACE

The experimental and theoretical research described in this thesis was carried out by the author in the Acoustics Division of the National Physical Research Laboratory (NPRL) of the South African Council for Scientific and Industrial Research (CSIR) during the period September 1982 to April 1985. Work in this division was performed under the supervision of Dr F. Anderson.

These studies represent original work by the author and have not been submitted in any form to another University. Where use was made of work carried out by others, it has been duly acknowledged in the text.

ACKNOWLEDGEMENTS

The work presented in this thesis was carried out under supervision of Professor A.D. Broadhurst of the Electronic Engineering Department, University of Natal. I wish to thank Professor Broadhurst for his advice and guidance in the course of this study.

The experimental part of this study is based upon measurements performed by the author in the acoustical laboratories of the NPRL. Permission by the CSIR to utilize the results of these measurements in the compilation of this thesis is gratefully acknowledged. The support and encouragement given by the Director of the NPRL, Dr G.J. Ritter, is appreciated.

I am greatly indebted to my colleague, Mr P.J. Erasmus, for his help and advice during all stages of the project. The precision and thoroughness of his approach contributed substantially to the reliability of test results and the high quality of graphs and drawings in this thesis.

Acknowledgement and a word of thanks are due to Mr J.F. Rossouw who has sacrificed precious time to perform independent sound insulation tests on the 220 mm brick filler wall.

The author wishes to thank Mrs I.T. Uytenbogaardt who, with great efficiency and excellence, has converted the text from analog to digital.

This thesis would not have been possible without the encouragement and positive attitude of my wife Jane, nor without the understanding and patience of my children, Adèle and Deon.

ABSTRACT

This thesis represents the development and evaluation of a theory for sound transmission analysis by sound intensimetry. In the context of this study sound transmission analysis is understood to embrace the following:

(1) The measurement of sound reduction indices.
(2) Diagnostic analysis of sound transmission through panels and structures.

The sound intensity method is examined against the theoretical background of the classic two-room method which forms the basis of currently used international standards. The flanking problem, which is one of the principle limiting factors in the use of the classic method, is analyzed.

The standard formulation of the intensity method is expanded to account for leakage error, boundary interference effects and calibration mismatch. It is shown that the commonly observed low-frequency discrepancy between intensity and classic method results is resolved by application of the Waterhouse correction.

Sound absorption by the test object on the receiving side is shown to cause an error which increases with the flanking factor and with the fraction of the receiving room absorption located on the surface of the test object. Guidelines are developed for the assessment and control of absorption error in practical situations.

Using the common mode rejection index as a performance rating for sound intensity meters, the measurement of sound transmission in reactive fields is investigated. Derivation of a formula for the reactivity near the surface of a transmitting panel surrounded by a flanking structure in a reverberant field, leads to the development of a theore-

tical framework and criteria for the planning and evaluation of test arrangements for sound transmission analysis. Guidelines are given for the calculation of minimum receiving room absorption and the microphone spacing required in practical situations.

A study of the characteristic properties of sound intensity fields in diffuse and non-diffuse environments is used as a basis in formulating a new method of measuring directional diffusivity. Based on the relationship between reactivity and the degree of directional balance in a sound intensity field, this method involves spatial averaging of the pressure level and determination of the magnitude of the total intensity vector at the point under consideration. A direct-reading diffusivity meter has been developed and employed in assessing diffusivity in practical situations.

The effect of a lack of directional diffusivity on the accuracy of sound transmission analysis in reactive fields is examined. Criteria for calculating minimum diffusivity requirements in the source and receiving room are developed and evaluated experimentally.

TABLE OF CONTENTS

Page

Page

Page

CHAPTER 4 : EXPERIMENTAL WORK

Page

Page

Page

LIST OF TABLES

Page

Page

Page

APPENDIX

LIST OF FIGURES AND PLATES

Page

CHAPTER 2

CHAPTER 3

Page

Page

CHAPTER 4

Page

APPENDIX

LIST OF PRINCIPAL SYMBOLS

A	Surface area of test object $[m^2]$
A_2	Surface area of measurement surface $[m^2]$
A_F	Surface area of flanking surface $[m^2]$
b	Linear dimension of a square test object $[m]$
B	Atmospheric pressure $[mb]$
$B(f)$	Signal bandwidth $[Hz]$
B_r	Atmospheric pressure implied in calibration $[mb]$
B_{ro}	Reference atmospheric pressure of 1013 mb
c	Speed of sound in air $[ms^{-1}]$
c_r	Speed of sound implied in calibration $[ms^{-1}]$
c_τ	Speed of sound simulated electronically $[ms^{-1}]$
d	Degree of directional diffusivity; %
e	Sampling error
f	Frequency $[Hz]$
f_c	Room cut-off frequency $[Hz]$
$f(t)$	Instantaneous force $[N]$
G_1, G_2	Calibration gain factors
h	Transmission factor, (direct power)/(total power)
h_F	Flanking factor, (flanking power)/(direct power)
$H(\gamma)$	Directivity function
$i(t)$	Instantaneous sound intensity $[W/m^2]$
I	Time-averaged sound intensity $[W/m^2]$
I'	Incident intensity; directivity method
I_0	Sound intensity reference level; $1pW/m^2$
I_A	Active intensity $[W/m^2]$
I_d	Direct sound intensity $[W/m^2]$
I_i	Net sound intensity incident on elemental surface dA $[W/m^2]$
I_{IN}	Average incident sound intensity $[W/m^2]$
I_n	Net intensity $[W/m^2]$
I_r	Net reverberant intensity $[W/m^2]$
I_R	Reactive intensity $[W/m^2]$
J_0	Zero order Bessel function
k	Wave number $[m^{-1}]$
Lc	Calibration correction term in dB

Le	Error in dB
Le_F	Estimation error in dB in sound reduction of flanking wall
Lei	Calibration error in dB
Le_R	Estimation error in dB in sound reduction index of test object
$Le_{R'}$	Estimation error in dB in apparent sound reduction index of test object
Le_{RT}	Total estimation error in dB in sound reduction index of test object
LI	Sound intensity level in dB re 1pW/m^2
LId	Intrinsic sound intensity level of a field in dB re 1pW/m^2
LIm	Measured sound intensity level in dB re 1pW/m^2
LP	Sound pressure level in dB re 20 μ Pa
LP1	Sound pressure level in dB re 20 μ Pa; source room
LP1m	Measured sound pressure level in dB re 20 μ Pa; source room
LP2	Sound pressure level in dB re 20 μ Pa; receiving room
LPm	Measured sound pressure level in dB re 20 μ Pa
LR	Reactivity of a sound field in dB
LRd	Intrinsic reactivity of a sound field in dB
LRm	Common mode rejection index in dB
LW	Sound power level in dB re 1pW
m	Reactivity factor or power factor
m_α	Air attenuation factor [m^{-1}]
M	Average absolute deviation of incident intensity from average value
M_0	The value of M in a free field
n	Integer variable
N	Number of measurements or samples
p_1	Instantaneous sound pressure; source room [Pa]
p_2	Instantaneous sound pressure; receiving room [Pa]
p(t)	Instantaneous sound pressure [Pa]
P_0	Reference sound pressure level, 20 μ Pa
P_1	Root mean square sound pressure; source room [Pa]
P_2	Root mean square sound pressure; receiving room [Pa]
P(r)	Rms sound pressure as a function of distance r [Pa]
P_{Ro}	Reverberant sound pressure; centre of room [Pa]

$Q(\theta)$	Directivity factor
r	Distance [m]
r_m	Maximum distance between plane measurement surface and test object [m]
r_{mo}	Minimum distance between source and microphone [m]
$r(\theta)$	Distance between source and a point on the test object in a direction θ [m]
R	Sound reduction index in dB
R'	Apparent sound reduction index in dB
$R_{1,2}$	Cross-correlation coefficient
R_F	Sound reduction index of flanking wall in dB
Rm	Measured sound reduction index in dB
R_α	Room constant; receiving room [m^2]
$R_{\alpha 1}$	Room constant; source room [m^2]
S	Total surface area, receiving room [m^2]
S_1	Total surface area, source room [m^2]
t	Time [s]
T	Reverberation time [s]
T	Temperature [K]
T_r	Temperature implied in calibration [K]
T_{ro}	Reference calibration temperature, 293 K
u_r	Instantaneous particle velocity in direction r [ms^{-1}]
$u(t)$	Instantaneous particle velocity [ms^{-1}]
U	Rms particle velocity [ms^{-1}]
U_0	Reference particle velocity level, 50 nm/s
V	Room volume [m^3]
V_1	Source room volume [m^3]
$w(t)$	Instantaneous sound power [W]
W	Total sound power [W]
W'	Apparent transmission power [W]
W_0	Reference sound power level, 1pW
W_D	Direct transmission power [W]
W_{D1}	Portion of direct power passing through the measurement surface [W]
W_{D2}	Portion of direct power missing the measurement surface [W]
W_F	Flanking power [W]

W_{F1} Portion of flanking power missing the measurement surface [W]

W_{F2} Portion of flanking power passing through measurement surface [W]

W_{FD} Portion of flanking power reaching the measurement surface via the test object [W]

W_{IN} Power incident on test object; source room [W]

W_{INd} Incident power from direct field [W]

W_{INr} Incident power from reverberant field [W]

W_n Net sound power [W]

Z Specific acoustic impedance [Ns m^{-3}]

α Average absorption coefficient

α_0 Effective boundary absorption coefficient

α_A Average sound absorption coefficient of the test object

β Phase mismatch error in output stage of a sound intensity meter [radians; degrees]

γ Angle of incidence

δ Total energy density [Jm^{-3}]

δ_0 Asymptotic value of energy density at a remote point [Jm^{-3}]

$\delta(0+)$ Energy density when the source is turned off [Jm^{-3}]

δ_1 Space-and-time averaged energy density in the source room [Jm^{-3}]

δ_d Direct energy density [Jm^{-3}]

δ_r Reverberant energy density [Jm^{-3}]

ΔL Safety margin in dB

Δr Distance between the centres of the two microphones in the intensity probe [m]

Δr_0 Maximum microphone spacing in a plane wave to limit intensity error to Le dB [m]

$\Delta(s)$ Laplace transform of $\delta(t)$

$\Delta\theta$ Acoustic phase difference between microphones [radians; degrees]

$\Delta\phi$ Phase of particle velocity re sound pressure [radians; degrees]

ε	Phase mismatch error [radians; degrees]
ζ	Angle of incidence; correlation method [degrees]
θ	Angle of incidence [degrees]
θ	Acoustic phase difference (Chapter 3) [radians; degrees]
λ	Wavelength [m]
ρ	Density of air [kg m^{-3}]
ρ_r	Density of air implied in calibration [kg m^{-3}]
σ	Standard deviation
τ	Time delay [s]
ω	Angular frequency [rad s^{-1}]
Ω	Solid angle [sr]
Ω_0	Fixed solid angle [sr]

CHAPTER 1

INTRODUCTION

1.1 THE ROLE OF THE AUTHOR IN THE DEVELOPMENT OF SOUND INTENSIMETRY

Sound power is a principle parameter in the radiation and transmission of sound. Reliable information on the power-radiation characteristics of sources such as musical instruments, household appliances, industrial plants and sound insulating partitions is constantly needed by acoustic engineers in devising solutions to acoustic design and noise control problems. In principle, since real sources are generally non-isotropic, the sound power radiated by a source situated in a free field has to be estimated by determination of the power per unit area (sound intensity) at a number of points on a measurement surface enclosing the source. In practice, sound power determination generally involves a much more elaborate procedure, for until recently it had not been possible to measure sound intensity directly. Even today, notwithstanding considerable advances which are taking place in sound intensimetry, standard methods of sound power determination are still based on indirect determination of sound intensity by sound pressure measurement. If the source is located in a reverberant or a semi-reverberant room, as for example when the sound transmission through a wall is examined, sound power measurement is compounded by uncertainties as to the actual relationship between sound intensity and sound pressure.

The need for sound intensimetry is further accentuated by the appearance of sound intensity and sound power as key parameters in the definitions of basic acoustic properties such as sound absorption, diffusion and sound insulation. Realizing this, Olson [1] described the principle of an instrument for measuring sound intensity in a patent issued to him in 1932. The first attempt to construct such a device was reported in 1941 by Clapp and Firestone [2] who used a crystal microphone and a ribbon microphone to measure the sound pressure and particle velocity, respectively. The results showed promise, but lacking the support of adequate electronic and microphone technology, this principle failed to pass the threshold of practical viability. Two

further attempts by Baker [3] and Schultz [4] in 1955 and 1956, respectively, marked the end of the first phase in the evolution of sound intensimetry.

A year after he had joined the CSIR in 1971, the author had the opportunity to resume a project on sound power determination which had formed the subject of his thesis in the final year of study for the B.Sc. degree in electrical engineering at the University of Pretoria. It was soon realized that a satisfactory solution to the problem of sound power determination would not be reached by further refinement of methods based on sound pressure measurement. Under supervision of Dr J.F. Burger, the then head of the Acoustics Division of the NPRL, a research project on the development of a practical sound intensity meter was initiated.

Setting out with the aim to develop a self-contained portable sound intensity meter with practically useful specifications, it was decided to recommence with Olson's idea, taking full advantage of the technological advances in electronics which had in the meantime taken place. The first prototype, using a dynamic STC 4035 pressure microphone and an STC 4038 velocity microphone, was battery-operated and self-contained but had a very limited frequency range. Even so, the instrument was used to demonstrate that sound power determination by sound intensity measurement could be accomplished in any type of acoustic environment [5].

A considerable improvement in bandwidth was accomplished by using a microphone assembly consisting of a 7 mm-diameter electret condenser microphone mounted in front of the ribbon of an STC 4038 velocity microphone, with the diaphragm facing the ribbon and spaced 2mm from it. In a series of experiments conducted in 1973 [6,7], it was possible by using this instrument, to obtain experimental proof of Gauss' theorem as applied to sound power determination [8]. In providing a means for selective sound power determination, this principle lays the foundation for sound transmission analysis by sound intensimetry.

These measurements, together with results obtained in field applica-

tions [9,10] removed all doubts as to the practical value of sound intensimetry. But it also became evident that the instrumentation suffered from fundamental limitations which disqualified it from further development into a field instrument. The extreme sensitivity of the dynamic velocity microphone to wind and mechanical vibration rendered it unsuitable for general-purpose field work. This is rather unfortunate inasmuch as the electronic instrumentation needed in conjunction with a pressure and velocity-sensitive pair of microphones is relatively simple and could easily have been developed into a compact field instrument.

By making use of Schultz's method to derive particle velocity from two pressure signals [4], a new series of instruments were developed. With the first prototype completed in 1973, it was concluded that the two-microphone principle, as it is called today, was basically sound and suited to use in field instruments. Although a considerable amount of development was still needed to perfect the intensity probe, the real problem now resided in the design of the electronic equipment which became much more involved, owing to the technical complexity of computing particle velocity by the two-microphone principle. Initially, the accomplishment of sufficient accuracy, dynamic range and bandwidth in a portable battery-operated instrument appeared to be beyond reach of the available technology, but eventually the problem was largely solved by careful arrangement of the sequence in which operations are executed in regard to the computation of sound intensity. The theory in support of this work as well as the findings of an experimental investigation of the sound intensity method of sound power determination were presented in an M.Sc. dissertation by the author in 1974 [6].

In 1978 the author was invited to participate in a large-scale project conducted in the Netherlands to evaluate sound intensimetry and its application to sound power determination. Using the model A77 SIM portable intensity meter which had then just been completed [11], it was demonstrated that the principle of selective sound power determination following Gauss' theorem was practicable for small as well as large sources, such as factories and industrial plants [12,13]. Further refinement and optimization of the measurement system resulted in Model A80 SIM [14] and created the opportunity to participate in a project on

sound intensity measurement at Brüel & Kjaer in Denmark. The latest system, Model A83 SIM, is now being manufactured on a small scale at the CSIR.

In the course of developing the CSIR-intensity meter, the author has devoted himself to the development of new applications and to the enhancement of sound intensimetry in general **[15-31]**. Contributions have thus been made to the development of the following applications of sound intensimetry:

(1) The determination of the sound power radiated by small and large sources [5-7,12,13].

(2) Determination of normal free-wave sound absorption coefficients [23].

(3) Determination of random incidence sound absorption coefficients [24].

(4) Sound field mapping [15].

(5) The measurement of very low noise levels [5].

(6) The measurement of diffusivity [17-19].

(7) The measurement of sound insulation [22,25-29].

Since the work of Schultz in 1956 no investigations other than those conducted at the CSIR were reported, until 1975 **[32]** when a renewed interest in sound intensimetry emerged. It is clear, in view of the exponential increase in the number of papers and publications on the subject, that sound intensimetry is now acquiring a standing of its own in modern acoustics. Considerable progress has been made in the development of new measurement techniques **[33-68]**. Today, practical sound intensity measurement is accomplished primarily by either of the following two methods:

(1) The cross-spectral density method [34] which can be implemented with the aid of 2-channel FFT analyzers. This technique, which gives a frequency line spectrum, does not allow real-time sound intensity measurement.

(2) Time domain processing by the sum-and-difference method [6,48,49]. This principle, which is implemented by analog processing in portable instruments and by digital processing in larger systems, allows real-time sound intensity measurement.

Although the computation is completely different in the aforementioned cases, the methods are based on the same underlying principle, namely the use of two pressure-sensitive microphones to sense the acoustic phase gradient at the measurement point. Fundamental characteristics such as directional response, frequency range and measurement error are identical for measurement systems employing either of the two methods.

1.2 THE NEED FOR SOUND TRANSMISSION ANALYSIS

The measurement and control of sound insulation is one of the fundamental aspects of noise control engineering. Defined as ten times the logarithm of the ratio of the sound power incident on one side of a partition to the power transmitted to the other side, the sound reduction index R is a measure of the ability of that partition to attenuate sound energy. Sound reduction indices of materials, partitions and miscellaneous building elements are extensively used by acousticians in controlling sound for such purposes as the prevention of hearing damage, the creation of pleasant acoustic environments and for the enhancement of speech intelligibility.

In order to be of any practical use, a test method for determining sound reduction indices must be applicable in the frequency range 100 Hz to 4kHz. In order to account for the dependence of sound insulation on the angle of incidence, the test object must be exposed to a sound field which is directionally diffuse. Moreover, since the sound insulation is affected by the size and the mounting of the test object,

great care has to be taken in designing the test arrangement and in using the test results in practical applications.

Apart from the necessity for a well-founded basic test method, there is a definite need for a more comprehensive technique of sound transmission analysis. The performance of a sound insulating element is almost invariably counteracted by the occurrence of flanking transmission through the surrounding building structure. By sound transmission analysis it would be possible to distinguish quantitatively between direct and flanking sources and to measure the relative amounts of sound power transmitted by a composite test object.

The classic two-room method **[69,70]**, which has been standardized by the International Organization for Standardization (ISO) **[71]**, involves sound pressure measurement in the source room as well as the receiving room. Whereas sound pressure is conditionally related to the magnitude only of the power flux per unit area, it is impossible to distinguish between different sources of sound radiation in the receiving room, except by sequential testing of constructions which respectively include and exclude the source under consideration. The classic method is therefore not considered to offer a practical solution to the problem of sound transmission analysis.

The development of a portable sound intensity meter by the candidate at the CSIR [5-7,9-31] and subsequent advances in sound intensimetry [32-68] have now made it possible to perform sound insulation measurements which no longer rely upon restricting statistical assumptions in determining the sound power radiated by the test object **[72]**. Based on a series of laboratory investigations [29] this dissertation represents the first known attempt to develop a comprehensive theory in respect of sound transmission analysis by sound intensimetry.

1.3 THE PURPOSE AND SCOPE OF THIS THESIS

This thesis presents a theoretical and an experimental evaluation of sound transmission analysis by sound intensimetry. In the context of this study, sound transmission analysis is understood to embrace the

following:

(1) The determination of performance figures for sound insulating elements such as walls, partitions and building elements. (In this document the performance of sound insulating partitions is expressed in terms of the **sound reduction index** R, while the term **sound insulation** refers to the physical property in general.)

(2) Diagnostic analysis of sound transmission through composite structures. This involves the examination and measurement of the relative amounts of sound power transmitted by the test object, by flanking elements or by components of either. The main applications of diagnostic analysis are the detection of construction faults and the evaluation of the design and construction of sound insulating elements.

For reasons which will be explained in Chapter 2, the classic two-room method of determining sound reduction indices, albeit the most practical one available, is rather inflexible and limited in its application. A considerable degree of simplification and improvement may be accomplished if the sound power transmitted by the test object is determined by direct measurement of sound intensity [72]. Diagnostic sound transmission analysis, which is not feasible by techniques based on the classic-method principle, may be accomplished by sound intensimetry. As yet, however, no comprehensive theoretical study has been made to establish the limiting factors and the practical bounds of the sound intensity method.

The evaluation of the sound intensity method presented in this thesis involves the following:

(1) Because the sound intensity method of determining sound reduction indices has certain basic aspects in common with the classic method, the theoretical basis of the classic method is thoroughly examined. This also provides a basis for comparison of the two methods. An independent analysis is made

of estimation errors arising when the true sound reduction index of a partition is determined by consecutive measurement of the sound transmitted by the flanking structure alone and that transmitted by the flanking structure whilst containing the test object.

(2) Proceeding from principle formulations [72], a theory is developed for sound transmission analysis by sound intensimetry. The main purpose of this theory, which pertains to the measurement of sound reduction indices as well as diagnostic sound transmission analysis, is to establish a basis and a framework for the evaluation of the sound intensity method.

(3) A comparative study by means of experimental investigation is made of the classic method and the sound intensity method of measuring sound reduction indices.

(4) The application of sound intensimetry to diagnostic sound transmission analysis is evaluated experimentally.

The classic two-room method and the sound intensity method for measuring sound reduction indices are evaluated on a comparative basis. Upon derivation of the classic method, it is shown in Chapter 2 that flanking transmission is one of the major causes of error and uncertainty, especially if the sound insulation of the test object is exceptionally high. The sound intensity method is formulated in Chapter 3, whereupon the advantages and the practical limitations of the method are investigated. Originality is claimed for the formulation and the experimental verification of fundamental equations relating the accuracy and validity of sound transmission analysis by sound intensimetry to the following factors, some of which are interactive:

(1) The reactivity at the surface of the test object and the common mode rejection index of the measurement system.

(2) The ratio of flanking power to direct power.

(3) The amount and distribution of sound absorption in the receiving room.

(4) Leakage due to incomplete coverage of the radiated power by the measurement surface (non-compliance with the conditions of Gauss' law).

In addition to these contributions, this thesis presents a new method of measuring the degree of directional diffusivity in a sound field. One of the principle preconditions of the classic method is that the source room as well as the receiving room must be spatially and directionally diffuse. The sound intensity method, on the other hand, only requires the source room to be diffuse. In the absence of practicable methods of assessing directional diffusion, this property (although it is presumably taken into consideration in the design of test rooms) is usually not verified experimentally except by indirect observation of the general performance of the test rooms. Since directional diffusion relates to the directional distribution of the incident sound power, it stands to reason that some relation should exist between the net sound intensity and the degree of directional diffusion at a given point. In order to establish whether sound intensimetry could be utilized in assessing directional diffusion in test rooms, a study of the sound intensity characteristics of diffuse fields was undertaken.

Whereas an exhaustive treatment of diffusion would amount to a dissertation in its own right, the scope of this investigation was confined to the following:

(1) A study of the principles of diffusion as expounded in the literature. Since the classic method and the sound intensity method are subject to the same requirements in respect of diffusion in the source room, this study is presented as part of the classic theory in Chapter 2.

(2) Formulation of a descriptive model of the sound intensity field in various types of acoustic environment and development of a new method for direct measurement of the degree of

directional diffusivity. As this work is based on sound intensity techniques, it is presented as a section of Chapter 3 which pertains to sound transmission analysis by sound intensimetry.

(3) Application of the newly developed criterion for assessing directional diffusion to sound transmission analysis by sound intensimetry.

(4) Development of an instrument for the direct measurement of the degree of directional diffusivity, presented in Chapter 3.

(5) Experimental evaluation of the new method, presented with the rest of the experimental work of this thesis in Chapter 4.

The formulation of physical quantities in this thesis is consistent with the International System of Units (SI). As far as possible, symbols, notations and terminology are consistent with the general usage observed in the literature. In further clarification of notations used in this thesis, the following aspects should be noted:

(1) Instantaneous values of quantities which vary with time or distance are denoted by small roman letters.

E.g. - instantaneous sound pressure; p.

(2) Where considered necessary and meaningful, the variable of the instantaneous quantity will be given in brackets.

E.g. - instantaneous pressure as a function of time; $p(t)$.
- instantaneous pressure as a function of distance; $p(r)$.

(3) Root mean square (rms) values are denoted by roman capitals.

E.g. - rms sound pressure; P.
- rms sound pressure as a function of distance; P(r).

(4) Logarithmic (decibel) levels are denoted by the letter L. Suffixes and subscripts are added to define the variable.

E.g. - sound level in general; L dB.
- sound pressure level ; LP dB.

(5) Where considered purposeful, averaged values will be denoted by including the function in pointed brackets, with the averaging variable denoted by a subscript.

E.g. - time-averaged pressure ; $\langle p \rangle_t$.
- distance-averaged pressure; $\langle p \rangle_r$.

This notation will only be used when it is necessary to emphasize the method by which the function is measured. Normally, in view of the clumsiness of the notation it will be avoided by using the notation referring to the theoretical value of the quantity under consideration.

E.g. - LP will normally be used to denote the sound pressure level, even though the time-averaged sound pressure level may be implied.

Finally, to emphasize the sequence in which references are cited, a reference number is given in bold type when it appears for the first time and in normal type when it recurs.

E.g. - The reference [16, 18, **104**] cites two references [16] and [18] which have already occurred, and one reference **[104]** occurring for the first time.

CHAPTER 2

THE CLASSIC TWO-ROOM METHOD

2.1 INTRODUCTION

Since the earliest reports on the development of test methods for assessing the sound insulation of partitions [69, 73-78], sound measurement technology has undergone considerable advances. The basic procedure and the test arrangement, however, have remained virtually unchanged. The determination of sound reduction indices requires a skeleton test facility, the acoustical properties of which are dictated by the peculiarities of sound transmission rather than the sophistication of the instrumentation or the physical parameters which are chosen to be measured. First of all, since the sound insulation of a partition depends on the angle of sound incidence, the test object must be subjected to sound approaching from all directions. The best way to achieve this, while at the same time ensuring that the incident power is constant everywhere on the surface of the test object, is to use a directionally and spatially diffuse source room. The acoustic properties of the receiving room are established once the measurement parameters have been decided on.

The classic two-room method [69,70] which has been standardized by ISO [71] is based entirely on sound pressure measurement. In the source room this is advantageous inasmuch as the well-defined statistic relationship between the average sound pressure in the supposedly diffuse source room and the power per unit area incident on the boundaries, simplifies the determination of incident power. On the receiving room side, however, dependence on pressure microphones imposes a restriction in that it dictates the use of a second diffuse room for determining the transmitted sound power.

To ensure conformity of test results obtained in different laboratories and to obtain figures which are applicable to conditions in actual buildings, standardization of test facilities and measurement procedures is imperative. According to ISO 140/I, which provides a statement of laboratory requirements, it should in the first instance be en-

sured that the two test rooms are diffuse. The latter condition may be regarded as the corner-stone of the classic method and is almost invariably emphasized in the treatment of sound insulation test principles. It is rather surprising therefore, that practical guidelines for the accomplishment and for the assessment of diffusion are virtually non-existent. ISO 140, for example, contends with a statement that diffusing elements, if necessary, should be installed in the rooms to obtain a diffuse sound field. It is recognized though, that this standard does provide for diffusion in that it specifies room conditions which are conducive to diffusion. The ratios of room dimensions should be such that the natural frequencies in the low-frequency region are spaced as uniformly as possible. It is also required that the shape of the two rooms be dissimilar and that the volumes differ by at least 10 %.

Error and uncertainty in sound transmission loss tests arise from a number of factors, some of which cannot be considered as shortcomings of the classic method per se. Guy et al. [79] and others [80-93] have shown theoretically and experimentally that the sound reduction index of a panel is dependent upon different boundary conditions. Below the coincidence frequency the transmission loss decreases with increasing panel dimensions.

Room dimensions and the ratio of test room sizes in particular, have been found to influence test results. There is some measure of disagreement, however, as to the nature and extent of influence observed in practice [81,83,93]. The mounting-orientation and boundary conditions of the panel not only affects the transmission properties of the test panel, but it may have a considerable influence on the establishment of flanking paths as well.

Thin panels mounted in thick walls create a niche towards one of the two test rooms. Guy [79] found that the sound transmission loss of such panels is generally higher when the panel is mounted on the source room side with the niche facing the receiving room. It has been pointed out in Chapter 1 that the sound reduction index of a partition depends upon the angle of sound incidence. Although this behaviour is

accounted for by subjecting the test panel to a diffuse incident field, the application of test figures in acoustic designs may still be subject to uncertainties in regard to the expected performance of the panel in semi-reverberant non-diffuse environments.

Mariner [94] has shown that significant errors may occur in the case of thin panels if the pressure level difference between the test rooms is less than about 10 dB. This deficiency of the classic method results in consequence of the ignorance of the energy exchange which takes place between the two rooms when reverberation times are measured. At high rates of energy exchange it is not possible to obtain a true estimate of the total amount of sound absorption in the receiving room. The error may be reduced, however, by adjusting the test room properties to obtain sufficiently large pressure level differences.

Since the classic method implicitly involves the determination of transmitted power by the reverberation room method, results are subject to the limitations of the latter method. Brüel [95] and Larsen [96] investigated the causes of error in sound power measurements and concluded that inaccuracies in reverberation time measurements were mainly responsible for the discrepancies often reported in the literature. Larsen [97] pointed out that for sound insulation tests, this error was nevertheless smaller than the estimation error in respect of the level difference between the rooms. The reverberation time error may be avoided by measuring the transmitted power by the substitution method, which is based on the use of a reference sound power source.

The main deficiency of the classic two-room method is that it cannot distinguish directly between direct and flanking power. ISO 140 is based on the premise that flanking transmission is either suppressed to negligible levels, or considered to be characteristic of the particular combination of test object and flanking walls, which must resemble the construction of the intended application. It is often impracticable to suppress flanking transmission to negligible levels, especially if the test object is small while having a high sound transmission loss. Moreover, it is sometimes desirable to assess the performance of a test object (such as a door) selectively. With the classic method this can

only be achieved by successive testing of constructions which respectively include and exclude the test object. In the majority of cases, with sound reduction indices falling in the range 20-50 dB, this procedure yields quite satisfactory results. It is shown in this thesis, however, that the method becomes prone to uncertainty and error whenever the total amount of flanking power is approximately equal to, or if it exceeds the amount of direct power radiated by the test object. In practice, if the test object has an airborne sound insulation index Ia > 55 dB (double massive panels with air cavities, for example) great difficulty may be experienced in controlling and assessing the amount of flanking power as required for accurate determination of the true sound reduction index of the test object.

In an attempt to overcome the limitations of the classic method and to develop techniques which are more suitable to field tests, various methods have been investigated. Some of these [98], being adaptions of the classic method, do not comply with ISO 140; others are based on different concepts altogether [99-103]. Methods based on correlation techniques [99,100] as well as those making use of vibration transducers to measure the velocity of radiating surfaces [102], have certain characteristics in common with the sound intensity method, the main subject of investigation of this thesis. Unlike the intensity method, these related techniques are rather specialized and cannot be considered as viable alternatives to the classic method in general purpose applications.

2.2 FORMULATION OF THE CLASSIC METHOD

This section presents the classic two-room method in its basic form [70, 104-106]. Practical considerations which may call for extension of the basic formulation are treated in subsequent sections. Consider a sound insulation test on a partition mounted in a test aperture between a source room and a receiving room as shown in Fig. 2.1. The test object may be smaller than the test opening, in which case it is mounted in a filler wall designed to have a sound insulation superior to that of the test object. ISO 140 requires that flanking transmission be reduced to levels which are negligible compared with the sound

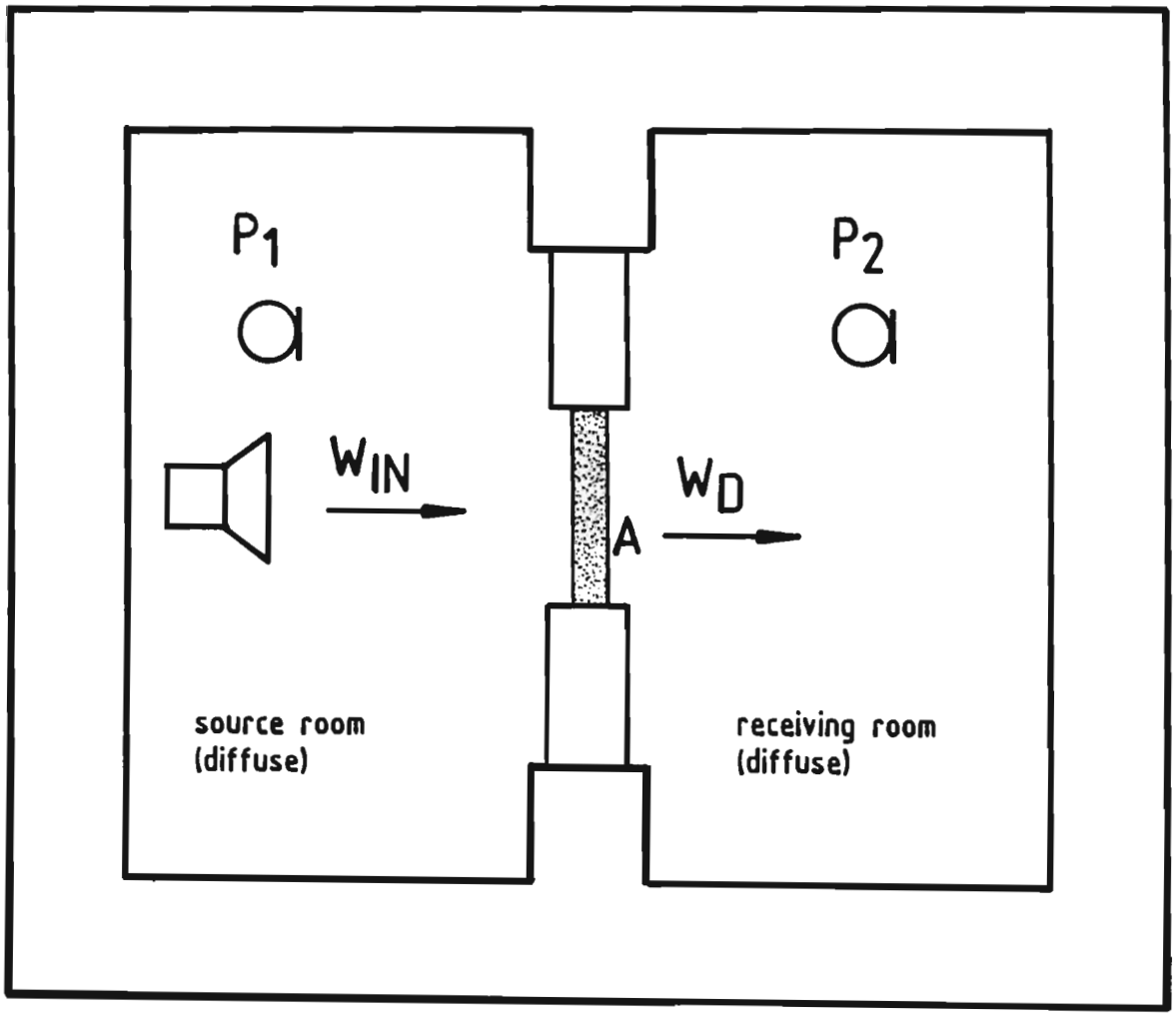

Figure 2.1

Test arrangement used for the determination of sound reduction indices by the classic two-room method.

transmitted by the test object, unless the combination of test object and flanking walls purports to resemble the situation in the intended application of the test object. In the latter case the flanking power is viewed as if radiated, in addition to the direct power, by the test object. Hence, in formulating the basic method, flanking transmission may be regarded as part of the direct transmission. The problem of distinguishing between the two quantities will be considered in Section 2.8.

The sound reduction index R of the test object, defined in terms of the incident power W_{IN} and the transmitted power W_D, is

$$R = 10 \log (W_{IN}/W_D) \quad \text{dB} \quad . \tag{2.1}$$

To account for the dependence of sound insulation on the angle of incidence and to attain constant average incident intensity everywhere on the surface of the test object, the source room is made directionally and spatially diffuse. Directional diffusion prevails if the rate of incidence of sound energy at a given point is the same for all directions, while spatial diffusion refers to a condition of constant energy per unit volume (constant energy density) throughout the field. The average incident intensity at the boundaries of a diffuse source room is [107]

$$I_{IN} = \delta_1 c/4 \tag{2.2}$$

where δ_1 is the space-and-time averaged energy density in the source room and c is the velocity of sound in air. The power incident on a test object which has a surface area A, is

$$W_{IN} = (\delta_1 c/4)A \quad . \tag{2.3}$$

The classic method is based on sound pressure measurement. In terms of the space-and-time averaged rms sound pressure P_1 in the source room, Eq. (2.3) becomes

$$W_{IN} = (P_1^2/4\rho c)A \qquad (2.4)$$

where ρ is the static density of air. In the receiving room the sound insulation test implicitly involves the determination of the transmitted power W_D by means of sound pressure measurement. The most practical solution, considering the size of the test object, is to use the reverberation room method. It is for this reason that the classic method requires the receiving room to be diffuse as well. In terms of the space-and-time averaged sound pressure P_2 in the receiving room, the transmitted power is given by [105]

$$W_D = P_2^2 R_\alpha /4\rho c \qquad (2.5)$$

where R_α is the room constant of the receiving room, defined as

$$R_\alpha = S\alpha/(1 - \alpha) \quad . \qquad (2.6)$$

S is the total internal surface, α is the average absorption coefficient and $S\alpha$ represents the total absorption, also known as the effective absorption area of the receiving room. The sound reduction index is obtained by substituting Eqs. (2.4) and (2.5) into Eq. (2.1). Hence,

$$R = 10 \log (P_1^2/P_2^2) + 10 \log (A/R_\alpha) \quad . \qquad (2.7)$$

In terms of the sound pressure levels LP1 and LP2 in the source and receiving rooms, respectively,

$$R = LP1 - LP2 + 10 \log (A/R_\alpha) \quad . \qquad (2.8)$$

It now remains to derive a method by which R_α can be determined with the aid of a pressure-sensitive microphone. Sabine realized that when a sound source in a room is turned off, the rate of decay of energy density depends on the amount of absorption in the room [76,77]. This led to the standard practice of measuring the reverberation time T, defined as the time required for the energy density to fall to a level 60 dB below its steady state value [108,109]. The power balance in a re-

ceiving room of volume V the moment before the source is turned off, is given by

$$V\frac{d}{dt}\delta(t) + \frac{c\,S\alpha}{4}\delta(t) = W(1-\alpha) \qquad (2.9)$$

$$\left(\begin{matrix}\text{Rate of energy}\\ \text{build-up or decay}\end{matrix}\right) + \left(\begin{matrix}\text{Power absorbed}\\ \text{at boundaries}\end{matrix}\right) = \left(\begin{matrix}\text{Power delivered to}\\ \text{reverberant field}\end{matrix}\right)$$

where $\delta(t)$ is the instantaneous energy density in the room. In the steady state the first term in Eq. (2.9) tends to zero. Note that Eq. (2.9) pertains to the reverberant field only; hence the use of $S\alpha$ rather than R_α in the absorption term. When the source is turned off the power input term falls away. Division by V then yields

$$\frac{d}{dt}\delta(t) + \frac{c\,S\alpha}{4V}\delta(t) = 0 \quad . \qquad (2.10)$$

Laplace transformation of Eq. (2.10) gives [110]

$$S\Delta(s) - \delta(0+) + \frac{c\,S\alpha}{4V}\Delta(s) = 0 \qquad (2.11)$$

where $\delta(0+)$ is the value of the energy density at the moment when the source is turned off. The solution for $\Delta(s)$ is

$$\Delta(s) = \delta(0+)/(S + c\,S\alpha/4V) \quad . \qquad (2.12)$$

The time-domain solution, obtained by inverse Laplace transformation is

$$\delta(t) = \delta(0+)\,e^{-(c\,S\alpha/4V)t} \quad . \qquad (2.13)$$

At $t = T$ the energy density has fallen to a level 60 dB below $\delta(0+)$. Hence,

$$\delta(0+)\,e^{-(c\,S\alpha/4V)T} = 10^{-6}\delta(0+) \quad . \qquad (2.14)$$

The solution for $S\alpha$ results in the Sabine reverberation formula

$$S\alpha = 24V\,[\,\ln(10)\,]/c\,T = 0{,}16\,V/T \quad . \qquad (2.15)$$

The constant 0,16 is valid in the temperature range 6 - 43 °C. Note that Eq. (2.8) calls for R_α rather than $S\alpha$. An expression for R_α in terms of reverberation time T is obtained by multiplying the numerator and the denominator of Eq. (2.6) by S and by substituting Eq. (2.15) into the result. This yields

$$R_\alpha = S\alpha S/(S - S\alpha) = S/(TS/0,16V - 1) \quad . \tag{2.16}$$

In terms of practically measurable parameters the sound reduction index, obtained by substituting Eq. (2.16) into Eq. (2.8), is

$$R = LP1 - LP2 + 10 \log [AS/(TS/0,16V - 1)] \quad . \tag{2.17}$$

Since the receiving room is presumably diffuse, $\alpha \ll 1$ and $R_\alpha \approx S\alpha$. Hence it has become standard practice to use

$$R = LP1 - LP2 + 10 \log (A/S\alpha) \quad . \tag{2.18}$$

Substitution of Eq. (2.15) into Eq. (2.18) gives

$$R = LP1 - LP2 + 10 \log (AT/0,16V) \quad . \tag{2.19}$$

In terms of Eq. (2.19), the classic two-room method and for that matter also the ISO 140-test procedure [71], involves measurement of the following parameters:

(1) The space-and-time averaged sound pressure level LP1 in the source room.

(2) The space-and-time averaged sound pressure level LP2 in the receiving room.

(3) The reverberation time T of the receiving room.

It is possible by using a reference sound source, to determine the effective absorption area $S\alpha$ of the receiving room by sound pressure, instead of reverberation time measurements [97].

2.3 RECEIVING ROOM ABSORPTION

The physical meaning of the average absorption coefficient α in Eq. (2.6) and the significance of the related quantities R_α, $S\alpha$ and T in Eqs. (2.8) to (2.19) deserves further attention. In the first place, α is not only determined by boundary absorption, but by absorption of sound energy in the air as well. As a result of air attentuation m_α per metre and as a result of the effective boundary absorption coefficient α_o, α attains a value given by [105]

$$\alpha = 4m_\alpha V/S + \alpha_o \quad . \tag{2.20}$$

Moreover, it is evident by inspection of the Sabine formula, Eq. (2.15), that the true absorption coefficient α_m of the boundary surfaces, which can only take on values in the range $0 \leq \alpha_m \leq 1$, cannot be regarded as α in calculating the effective room absorption $S\alpha$. For an anechoic room ($T \to 0$), this would yield a finite value for $S\alpha$ and therefore, by Eq. (2.15), a reverberation time $T \neq 0$. The danger of misinterpretation arises in Eq. (2.9) in that the discrete nature of sound absorption owing to the mean free path traverses between reflections, is not accounted for. If absorption is considered to occur in discrete steps, assuming that the absorption taking place at each reflection is α_m, the effective boundary absorption coefficient becomes [105]

$$\alpha_o = -\ln(1 - \alpha_m) \quad . \tag{2.21}$$

The average absorption coefficient

$$\alpha = 4m_\alpha V/S - \ln(1 - \alpha_m) \tag{2.22}$$

and the corresponding absorption area

$$S\alpha = S[4m_\alpha V/S - \ln(1 - \alpha_m)] = 0{,}16V/T \quad . \tag{2.23}$$

For the condition {$\alpha \ll 1$ and $V \simeq 50 - 100\ m^3$} implied in the classic two-room method, $-\ln(1 - \alpha_m) \simeq \alpha$ and $4m_\alpha V/S \simeq 0$ so that for all practical purposes the Sabine formula may be used as in Section 2.2, assuming $\alpha = \alpha_m$. The meaning of α as explained in this section attains greater significance if sound reduction indices are determined by sound intensimetry, since in that case the receiving room is allowed to be comparatively absorptive.

2.4 SPATIAL AVERAGING OF THE REVERBERANT ENERGY DENSITY

2.4.1 Criteria relating to direct-field error

In formulating the classic method, it was implicitly assumed in Eqs. (2.2) to (2.5) that the contribution to the total energy density in each room by direct field radiation was negligible. In reality, the total energy density δ is given by the sum of the reverberant energy density δ_r and the direct energy density δ_d. In the source room the total sound power incident on the test object W_{IN} is the net result of a reverberant component W_{INr} and a direct component W_{INd}. Summation in the latter order yields

$$W_{IN} = A\, W_1/R_{\alpha 1} + \iint_A [W_1 Q(\theta)/4\pi r^2(\theta)]\,dA \qquad (2.24)$$

where A = Surface area of the test object;
W_1 = total power input, source room;
$R_{\alpha 1}$ = room constant, source room;
$Q(\theta)$= directivity factor of the source;
θ = angle at which direct sound impinges on the test object;
$r(\theta)$= distance between the source and a point on the test object in a direction θ.

The direct field contribution to W_{IN} is undesirable, as it defeats the purpose of diffusion. To avoid this, the source must be situated at a safe distance r_0 from the surface of the test object. For the purpose of calculating r_0, the direct-power term may be expressed in terms of a fixed angle of incidence θ_0 for which $Q(\theta_0) = Q_0$ and

$$W_{INd} = AW_1 Q_0/4\pi r_0^2 \quad . \tag{2.25}$$

The direct-field contribution to W_{IN} will be less than Le dB if

$$AW_1/R_{\alpha 1} > [(AW_1 Q_0/4\pi r_0^2)/(10^{Le/10} - 1)] \quad . \tag{2.26}$$

In the source room the minimum distance between source and test object, as implied in Eq. (2.26), is

$$r_0 > 0{,}28\,[Q_0 R_{\alpha 1}/(10^{Le/10} - 1)]^{0,5} \quad . \tag{2.27}$$

Likewise, the minimum distance r_{mo} between the measuring microphone and the source, implied by the condition

$$\delta_r > \delta_d/(10^{Le/10} - 1) \quad , \tag{2.28}$$

is

$$r_{mo} > 0{,}14[Q_0 R_{\alpha 1}/(10^{Le/10} - 1)]^{0,5} \quad . \tag{2.29}$$

Example 2.1. The minimum distances between an omnidirectional source and the test object and between the source and the microphone in a source room of volume V = 100 m^3 and T = 2 seconds, for a direct field error Le < 1,0 dB, are shown in Table 2.1 for various positions of the source in relation to the room boundaries.

Table 2.1

Minimum distances to be maintained between (a) the source and the test object and (b) between the source and the microphone in a source room of volume V = 100 m^3 and T = 2 s.

Source position	Q_0	(a) r_0 (m)	(b) r_{mo} (m)
Centre of room	1	1,58	0,78
Near wall	2	2,26	1,10
Two-wall corner	4	3,20	1,56
Three-wall corner	8	4,53	2,20

This example illustrates the danger of direct-field error if the source is located in a corner of the source room. It is advisable when using a directional loudspeaker source, to direct it away from the test object.

In the receiving room, the direct field is set up by the sound power W_D emanating from the surface of the test object. At the surface of the test object the total energy density, assuming plane-wave radiation, is given by [105,106]

$$\delta = \delta_d + \delta_r = W_D/c\ A + 4W_D cR_\alpha \quad . \tag{2.30}$$

The variables were defined in Section 2.2. The condition

$$\delta_r > \delta_d/(10^{Le/10} - 1) \tag{2.31}$$

yields

$$R_\alpha/A > 4(10^{Le/10} - 1) \quad . \tag{2.32}$$

For Le > 1 dB this requirement becomes $R_\alpha > 4A$. Donato [111] showed that the direct energy density falls more or less by an exponential law with the distance from the test object. Hence, the criterion implied in Eq. (2.32) accounts for the maximum direct-field error.

2.4.2 Criteria relating to interference effects

It stands to reason that the number of measurements and the spacing between measurement points required to obtain the average energy density in a room with a specified accuracy, depends on the spatial variation of the sound pressure field. Cook [112] has shown that the cross-correlation coefficient of the sound pressures at points separated by a distance r in a random field is given by

$$R_{1,2} = (\sin kr)/kr \tag{2.33}$$

where k is the wave number.

It follows by examination of Eq. (2.33) that the measured values at two points will be statistically independent if the points are at least $\lambda/2$ apart. Waterhouse **[113]** showed that the energy density near reflecting boundaries is distributed into interference patterns exhibiting the same characteristic as $R_{1,2}$, though at twice the repetition rate. The energy density near a wall

$$\delta = \delta_0[1 + (\sin 2kr)/2kr] \tag{2.34}$$

where r is the distance from the wall and δ_0 is the asymptotic value of the energy density at a remote point. The energy densities at a wall, in a two-wall corner and in a three-wall corner are respectively 3 dB, 6 dB and 9 dB above the average level at the centre of the room. Standard sound insulation test procedures are based on spatial averaging of the energy density around the centre of the room. To obtain this average with an error of less than 1 dB, the microphones should not be located closer than 0,7 λ from corners and edges and 0,25 λ from the walls of the room. Strictly speaking, an estimate of the average energy density in the room should also take into account the energy stored in the interference field. This may be accomplished by adding the Waterhouse correction $10\log(1 + \lambda S/8V)$ to the average sound pressure level obtained by measurement near the centre of the room [113]. In practice, however, the Waterhouse correction for the source and receiving rooms have negligible net effect on the results of sound insulation tests because of their mutually opposing effect when introduced in Eq. (2.19).

Crocker **[114]** presents a criterion for calculating the number of measurements N required to sample the sound pressure in a reverberant field which has a variance σ^2. For a sampling error e and a confidence level of 98.75 %, the number of measurements

$$N \geq (2,5\ \sigma/e)^2 \quad . \tag{2.35}$$

An approximation of the variance given by Crocker [114] is

$$\sigma^2 = 1/[1 + B(f)T/6,9] \tag{2.36}$$

where B(f) is the signal bandwidth and T is the reverberation time of the room. In order that the values are statistically independent, the points must be separated by a distance of at least $\lambda/2$ (Eq. (2.33)). In the third-octave band centred at 100 Hz, assuming T = 2 seconds and allowing a maximum error of 1 dB, this criterion requires $N > 7$ for measurement points separated by 2,2 m. In addition to increasing the signal bandwidth and the reverberation time of the room, the spatial variance may be reduced by using a moving reflector, by using a frequency-modulated signal and by varying the position of the source- **[115]**. Continuous averaging with a moving microphone does not yield a variance as low as that obtained by discrete measurements at points separated by $\lambda/2$, but the method is commonly used in practice for two reasons:

(1) It is a time-saving method.
(2) Consistent application of the $\lambda/2$-criterion would require a different set of measurement points for each third-octave band, a procedure which is impracticable in most applications.

ISO 140/III [71] specifies a minimum distance between the microphone and reflecting surfaces of 0,7 m and allows continuous averaging, using a rotating microphone with a sweep radius between 1,0 m and 1,5 m and an averaging time of at least 30 s.

The well-defined behaviour of the energy density interference pattern at the walls and in the corners of a reverberant room suggests that the spatial average of the energy density be determined by sound pressure measurement close to the walls or in the corners and by applying the appropriate Waterhouse correction. Bartel **[116]** found that the variation in energy density and in reverberation time was much less among corners than among interior locations, for frequencies below the 200 Hz third-octave band. This practice, however, is not recommended in ISO 140.

2.5 DIFFUSION

2.5.1 Definition and purpose of diffusion

Ideally, a diffuse sound field is defined as one which has the following two characteristics:

(1) The energy density is constant throughout the field.
(2) The rate of energy incident on an elemental sphere at any given point in the field is constant for all directions of incidence.

In bringing this definition within closer reach of practical realities, it should be borne in mind that the behaviour of real sound fields cannot be fully described in terms of a model whereby sound energy is propagated in completely uncorrelated rays. A more practical definition of a diffuse sound field is as follows [108,113,114]:

(1) Sound energy is distributed uniformly throuhout the field. This condition is defined as **spatial diffusion.**
(2) On a time-average basis, an elemental sphere at any given point in the field receives the same average energy per second from each element of solid angle by sound waves of random amplitude and phase distribution. The sound field is said to be **directionally diffuse.**

The specification of diffuse source and receiving rooms in the formulation of the classic two-room method serves a twofold purpose. In the source room a diffuse field is employed in order that a practically meaningful estimate be obtained of the sound insulation of the partition, a property which depends on the angle of sound incidence. In the receiving room a diffuse field is implied by employment of the reverberation room method as the most practical and cost-effective means of determining the sound power radiated by the typically large surface of the test object. Commitment to diffusion is built into Eqs. (2.2), (2.5) and (2.13). It is rather difficult to make any specific predictions in regard to the consequences of a lack of diffusion. In gene-

ral, however, it may be stated that a lack of diffusion in the source room would result in non-uniform distribution of sound energy across the surface of the test object as well as non-uniform directional distribution at some points on the surface. The sound reduction index thus obtained would not represent the true surface-averaged and directionally-averaged performance of the test object. In the receiving room a lack of diffusion would affect the accuracy and validity of sound pressure as well as reverberation time measurements.

There is no absolute criterion for the formulation of a quantitative measure of diffusion. As a practical rule, spatial diffusion may be regarded as adequate for classic room tests if the standard deviation of the sound pressure level in the internal field (at least $\lambda/2$ from the nearest boundary) is less than 1 dB. This criterion is implied, for instance, by the requirements for test room qualification for sound power measurements in reverberation rooms according to ISO 3741. As to be explained in Section 2.6, various criteria have been employed in methods for evaluating directional diffusion. Most of these, however, do not yield results which can be quantitatively related to the degree of directional diffusivity and cannot be used on a comparative basis.

De Bruijn [117] investigated the influence of diffusivity on the transmission loss of a single-leaf panel. It turns out that diffusion is quite important below coincidence where a change in diffusivity could cause a shift of up to 5 dB in the sound insulation-curve. No significant effect was observed at coincidence, while no specific trend could be identified above coincidence.

2.5.2 Practical considerations

A highly reverberant sound field is not necessarily diffuse; there are quite a number of factors which affect the distribution of sound energy in a room. Consideration of these factors in the following discussion leads to the conclusion that a state of diffusion, even as implied in the "practical definition" given in the previous section, can never be fully realized in practice. Fortunately, however, it is not too diffi-

cult to achieve a state of diffusion which is completely adequate for practical purposes. The purpose of the remainder of this section is to examine the factors which effect and affect diffusion and which should be considered in planning measurements in existing test facilities.

(a) **Room size and shape** The baseline condition for diffusion is that the room be large enough to have sufficiently high modal density at the lowest frequency of interest. Using a modal overlap index $M_f = 1/3$, the room cut-off frequency is given by [114]

$$f_c = 680(T/V)^{0,5} \quad . \tag{2.37}$$

For f_c = 100 Hz, Eq. (2.37) yields V/T = 46. Provided the modal density is high enough, the shape of the room is of secondary importance; cubical shapes, though, should be avoided [79,114, **118**].

(b) **Room modes** If a sound source exciting a diffuse field is turned off, the classic reverberation formula (Eq. (2.13)) predicts an exponential discharge of energy equivalent to the situation when a capacitor is discharged through a resistor. In reality, the sound energy is not stored in a single capacitive volume but rather in a large number of independent resonators associated with the normal modes of the room [105]. A wide band source will excite narrow bands of frequencies centred at the normal frequencies, the bandwidths depending on the damping associated with each mode. Hence, when the source is turned off, each mode discharges at its own exponential rate, giving a net result which is no longer accurately described by Eq. (2.13).

Modal density may be increased by using irregularly shaped rooms and by making use of modal enrichment panels [108,114]. At low frequencies it may be necessary to increase the amount of absorption in the room. This has the effect of extending the bandwidth of individual modes and of increasing modal overlap. As a first line of approach, boundary absorption should be uniformly distributed to attain constant damping for all modes. However, the damping is determined, not only by the amount

of absorption, but by the mean free path and the angle of incidence as well [96]. At low frequencies, reverberation is primarily controlled by axial modes on account of their relative abundance and on account of the fact that their damping constants are smaller than those of tangential and oblique modes. The relatively low damping of axial modes is due to their longer than average mean free path and due to the fact that minimum absorption occurs at normal incidence. Uniform distribution of boundary absorption will therefore not guarantee perfectly uniform damping at all frequencies.

A limit is set to modal-damping control by the increase of spatial variance with increasing absorption. In addition to the risk of direct-field error (Section 2.4.1), increased absorption tends to cause a negative energy density gradient from the centre of the room towards the boundaries [119]. A maximum absorption coefficient of 0,16 is a commonly used criterion.

(c) **Boundary characteristics** It has been shown theoretically [108] that boundary reflection according to Lambert's law results in an isotropic reverberant field with homogeneous energy density; that is to say, the sound field in a room with diffusely reflecting boundaries is itself diffuse. Carrol has shown [120] that the reverberant portion of the wall intensity in such a room is uniform, even if the absorption is not uniformly distributed. If the absorption is uniform, the reverberant field is diffuse irrespective of the source location.

In practice, diffuse reflection according to Lambert's law can only be attained to a very limited degree; even roughly surfaced walls exhibit specular rather than diffuse behaviour. Notwithstanding this, diffusion is not affected too seriously by a large degree of specular reflection, provided the boundary absorption is kept low [108]. Fujiwara [121] has recently shown that variation of the specular content of boundary reflection could result in a 1,2 dB variation in the energy density and could have a noticeable effect on the directional distribution of sound energy. It has also been demonstrated [122] that the error due to inadequate description of steady-state conditions by classic theory only becomes significant in rooms with highly non-uniform distribution of absorption. This situation is hardly ever encountered in

laboratory measurement of sound insulation.

(d) **Diffusers** Failure to achieve diffuse boundary reflection by room and boundary design may be compensated by introducing sound reflecting panels in the room. The use of irregularly curved stationary diffusers suspended randomly in a room effects a significant improvement in diffusivity, especially at low frequencies where additional modes are created below the cut-off frequency of the room. The panels must have a weight of at least 4,8 kg/m^2 and must have dimensions comparable with the wavelength of the lowest frequency of interest [114]. Balachandran **[123]** has indicated that the presence of diffusing panels makes the positions of the source and the microphones less critical and enhances diffuse energy decay.

(e) **Coupling to other rooms** The effect of coupling is to add a reverberation term which in general has a different damping constant than the test room. This may affect the decay curve in a variety of ways, resulting in false estimates of the reverberation times of the test room [108]. The effect of energy exchange between source and receiving rooms has been examined by Mariner [94]. At high rates of energy exchange estimation of room absorption by measurement of reverberation times becomes inaccurate. It turns out that significant errors in estimates of sound reduction indices occur if the level difference between the test rooms is less than 10 dB. Some control of this error is possible by adjustment of room properties in order that the level difference between the test rooms is increased.

(f) **Interference effects** The notion of a spatially diffuse field is only conceivable by a model of geometrical room acoustics. It is evident from the discussion in Section 2.4.2 that a perfectly homogeneous energy density field can never be realized in practice due to the wave nature of real fields. Sufficiently accurate estimation of the average energy density in the field can be accomplished though, by following the rules set out in Section 2.4.2.

(g) **Direct-field influence** The inevitable presence of the direct field in the steady state, as discussed in Section 2.4.1, is another

factor which rules out the realization of a perfectly diffuse field. The direct field has an adverse effect on diffusivity in that it causes a gradient in the energy density field as well as a distortion of the directional distribution of sound energy. The direct-field influence is minimized by keeping a safe minimum distance between the source and the test object as well as between the source and the microphone, as explained in Section 2.4.1.

2.6 TECHNIQUES FOR MEASURING DIFFUSION

2.6.1 Assessment of diffusion by the directivity method

Thiele and Meyer [124-126] developed a criterion for the assessment of directional diffusion which can be directly related to the definition of this property. The percentage directional diffusion d is defined as

$$d = 100(1 - M/M_0)\ \% \tag{2.38}$$

where

$$M = (1/4\pi\langle I'\rangle_{4\pi})\iint \left| I' - \langle I'\rangle_{4\pi} \right| d\,\Omega \quad . \tag{2.39}$$

The factor M is the average absolute deviation of the incident intensity I' in a solid angle d Ω, from the average intensity $\langle I'\rangle_{4\pi}$ in a solid angle 4π. Normalization is accomplished by the factor M_0, the value given by Eq. (2.39) in a free field. This criterion yields d = 0 % in a free field and d = 100 % if the incident energy distribution is completely uniform in three dimensions.

Practical implementation of this method involves measurement of the incident "intensity" I' in a large number of evenly distributed directions at each point of interest. Two principle limitations of this method are that it is extremely cumbersome and that the result depends on the directional characteristics of the microphone. Results may therefore only be compared if obtained by measurement with similar microphones. Directional discrimination has been accomplished by using a microphone situated at the centre of a large parabolic reflector

[124]. Broadhurst [127] developed an acoustic telescope based on a beamforming technique whereby the output signals of an array of microphones are spatially filtered. Using an array of 25 microphones, a half-power bandwidth of 32 ^{o} was obtained in the 1 kHz octave band. A big saving in microphones was shown to be possible by using a sparse-array configuration [128].

2.6.2 The correlation method

It has been demonstrated [108,112] that the variation with distance of the cross-correlation coefficient of the steady-state sound pressures p_1 and p_2 at two points separated by a distance r, has a characteristic value if the sound field is diffuse. The cross-correlation coefficient is defined as

$$R_{1,2} = \langle p_1 p_2 \rangle_t / (\langle p_1^2 \rangle_t . \langle p_2^2 \rangle_t)^{0,5} \quad . \tag{2.40}$$

For three-dimensional diffusion

$$R_{1,2}(3\ d) = (\sin kr)/kr \quad . \tag{2.41}$$

The case of two-dimensional diffusion serves to define a reference condition for $R_{1,2}$. (A field with uniform directional distribution but with all the waves travelling along lines parallel to a single plane is said to be diffuse in two dimensions.) If both measurement points lie in the aforementioned plane, then

$$R_{1,2}(2\ d) = (1/2\pi) \int_0^{2\pi} \cos\ (kr \cos \zeta) d\zeta \ - \ J_0(kr) \tag{2.42}$$

where ζ is the angle of incidence relative to the line connecting the two measurement points. J_0 is the zero order Bessel function. Computation of $R_{1,2}$ according to Eq. (2.40) does not require too specialized equipment, though it is essential to use reasonably well matched microphones and preamplifiers. A phase mismatch error of ε radians results in

$$R_{1,2}(\varepsilon) = [\sin(kr + \varepsilon)]/kr \tag{2.43}$$

To limit the error at zero-crossings ($kr = n\pi$; $n = 1,2,...$) to 0,02, the phase mismatch error should not exceed 3,6 °.

The correlation method has been applied with success to study some of the factors which control diffusion. Balachandran [123] has demonstrated that the correlation method may be used to examine diffusion in the steady state as well as the decaying state of a reverberant field. In the latter case it was found that the initial portion of the decay curve was the most suitable for performing correlation measurements.

Although the correlation method is not quite as time-consuming as the directivity method discussed in the previous section, it is still too elaborate for general-purpose use. It has also been pointed out [117, 129] that the sensitivity of the correlation method in finding deficiencies in diffusivity is restricted; only the zero-crossing points of the correlation curve are suitable to indicate the extent of deviation. Although the (sin kr)/kr - characteristic is implied by diffusion, it has not yet been established if the converse is true; does compliance with the (sin kr)/kr - condition prove perfect three-dimensional diffusion? Neither is it clear how many measurements are required to assess threedimensional diffusion.

2.6.3 Indirect indicators of the state of diffusion in a field

In the absence of simple methods for direct measurement of diffusion, the state of diffusion in a room is often assessed by observation of its secondary effects. The condition yielding the highest values of sound absorption coefficient by the reverberation room method has been suggested as a measure to indicate optimum diffusion [130]. The variation in the steady-state sound pressure level with frequency has also been considered as a possible measure of the lack of diffusion in a room [131]. Bolt [132] observed that improvement of the diffusivity in a room results in a reduction of the roughness of the steady-state transmission curve (pressure as a function of frequency). The interpretation of the results obtained by this method is difficult.

2.7 MICROPHONE CALIBRATION

Sound pressure levels in the source and receiving rooms should be measured with the same microphone or with microphones having the same relative calibration. As the sound reduction index is calculated from the difference between these two levels, absolute calibration is not required.

2.8 FLANKING [25-31]

2.8.1 The need to distinguish between direct and flanking transmission

Determination of sound reduction indices in accordance with ISO 140 [71] requires that the total amount of flanking power be reduced to a level well below the level of the direct power transmitted by the test object, unless the flanking structure is considered to be part of the test object. Hence, in formulating the classic method, it was assumed in Section 2.2 that the sound pressure level in the receiving room is caused by direct transmission only. In some applications great difficulty is experienced in attaining sufficient suppression of flanking transmission in order to justify this assumption. The filler wall containing the test object and the surrounding permanent structure are not perfect sound insulators and moreover, their combined surface area may be a few times larger than that of the test object. In such cases, if only the performance of the test object per se is of interest, the apparent sound transmission of the test object must be corrected by subtraction of the flanking portion.

2.8.2 Formulation of flanking parameters

Consider the case depicted in Fig. 2.2 where the total power W entering the receiving room consists of two parts; the direct power W_D transmitted by the test object

$$W_D = hW \tag{2.44}$$

and the flanking power W_F transmitted by the surrounding structure

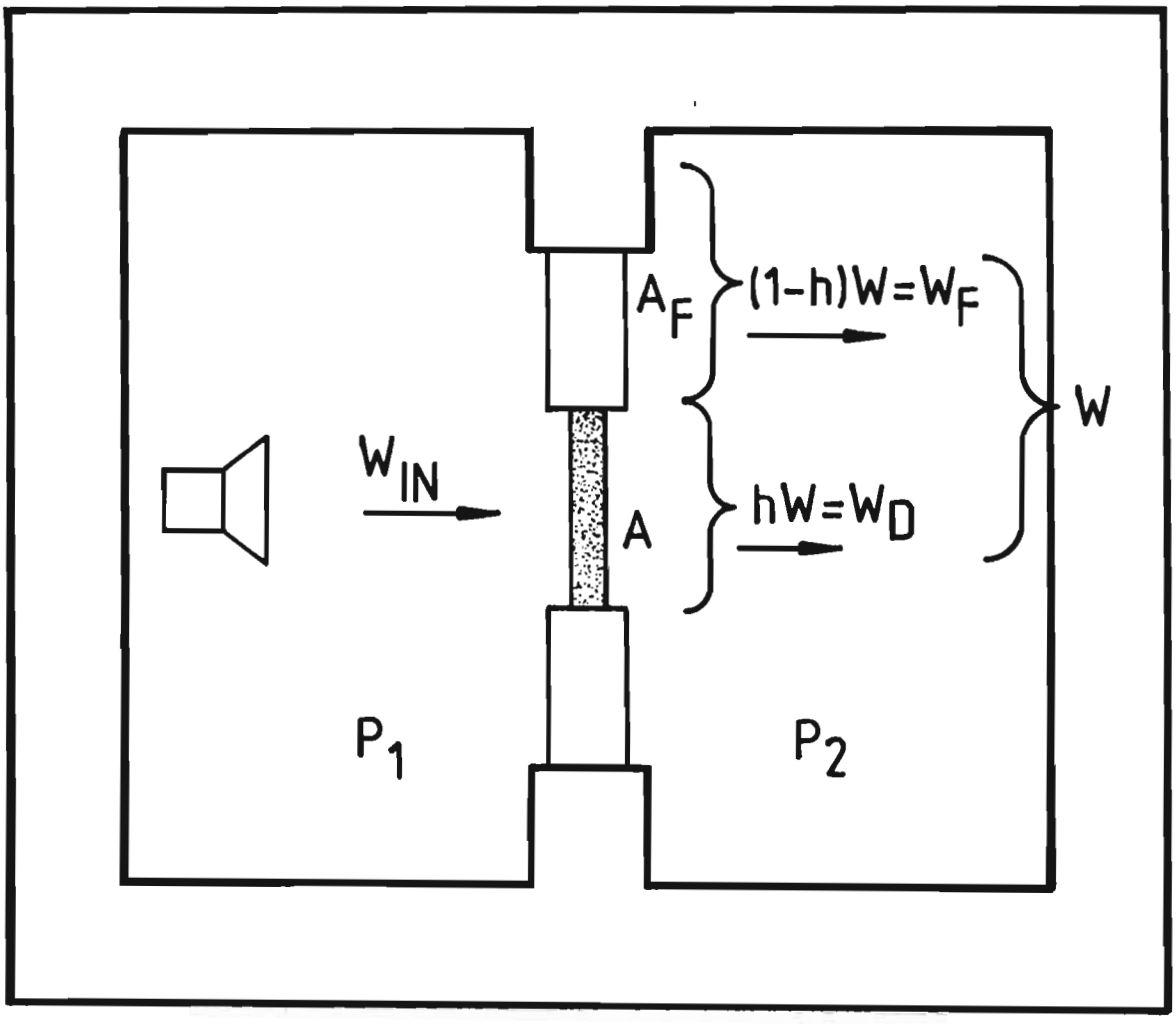

Figure 2.2

The contribution of direct power W_D and flanking power W_F to the total power W.

$$W_F = (1 - h)W \tag{2.45}$$

where

$$h = (\text{direct power})/(\text{total power}) = W_D/W \quad . \tag{2.46}$$

Since the total rms sound pressure in the receiving room P_2 is maintained by the sum of the direct power and the flanking power, the sound reduction index of the test object R, if calculated by Eq. (2.8) without applying any correction for flanking, is underestimated. The estimation error is

$$Le = 10 \log h \quad dB \quad . \tag{2.47}$$

Although the permanent structure of the test facility may in extreme cases contribute significantly to the flanking power, the flanking problem may usually be attributed to the filler wall. In the following, flanking transmission will be accounted for in terms of the flanking reduction index R_F of the flanking structure which has a surface area A_F. Unless otherwise indicated, R_F is understood to be the sound re-reduction index of the filler wall. As the flanking surface and the surface area A of the test object are exposed to the same average incident intensity I_{IN}, h as defined in Eq. (2.46) becomes

$$h = \left(I_{IN}\, A\, 10^{-R/10}\right)/\left(I_{IN} A\, 10^{-R/10} + I_{IN}\, A_F\, 10^{-R_F/10}\right) \tag{2.48}$$

and upon simplification

$$h = 1/\left(\frac{A_F}{A}\, 10^{-(R_F - R)/10} + 1\right) \quad . \tag{2.49}$$

It is also useful to define the flanking ratio

$$h_F = (\text{flanking power})/(\text{direct power}) = W_F/W_D \tag{2.50}$$

which is given by

$$h_F = (A_F/A)10^{-(R_F - R)/10} \quad . \tag{2.51}$$

The relationship between h and h_F is

$$h = 1/(h_F + 1) \tag{2.52}$$

or

$$h_F = (1 - h)/h \quad . \tag{2.53}$$

2.8.3 Determination of the sound reduction index of a test object in the presence of flanking transmission

Selective determination of the sound reduction index of a test object in the presence of flanking transmission calls for two consecutive sound insulation tests. The first test is preformed on the flanking structure alone to determine the flanking reduction index R_F; the second test, performed on the flanking structure whilst containing the test object, yields an apparent sound reduction index R', calculated by attributing the total transmission power W to the surface area A of the test object. Thus,

$$R' = 10 \log (W_{IN}/W) \quad \text{dB.} \tag{2.54}$$

The true sound reduction index of the test object, taking note of Eq. (2.47), is

$$R = R' - Le = R' - 10 \log h \quad \text{dB.} \tag{2.55}$$

By substitution of Eq. (2.49) into Eq. (2.55) and upon simplification it is found that the true sound reduction index R is given in terms of R' and R_F by

$$R = -10 \log \left(10^{-R'/10} - \frac{A_F}{A} 10^{-R_F/10}\right) \quad \text{dB.} \tag{2.56}$$

The corresponding solution for R' is

$$R' = -10 \log \left(10^{-R/10} + \frac{A_F}{A} 10^{-R_F/10}\right) \quad \text{dB.} \tag{2.57}$$

The accuracy of the R-estimate depends upon h_F and upon the accuracies by which R_F and R' are determined. Consider the estimation error Le_R resulting from an error Le_F dB in the measured value of R_F. The estimated value of R given in Eq. (2.56) is

$$R + Le_R = -10 \log \left(10^{-R'/10} - \frac{A_F}{A} 10^{-(R_F + Le_F)/10}\right) \quad \text{dB.} \quad (2.58)$$

The estimation error is

$$Le_R = -10 \log \left(10^{R/10} \left[10^{-R'/10} - \frac{A_F}{A} 10^{-(R_F + Le_F)/10}\right]\right) \text{ dB.} (2.59)$$

For the purpose of planning sound insulation tests and for assessing the adequacy of filler walls it is useful to express Le_R in terms of R and R_F. By substitution of Eq. (2.57) into Eq. (2.59) and by rearrangement of the terms, the estimation error becomes

$$Le_R = -10 \log \left[1 + (1 - 10^{-Le_F/10}) \frac{A_F}{A} 10^{-(R_F - R)/10}\right] \quad \text{dB.} \quad (2.60)$$

Substitution of Eq. (2.51) into Eq. (2.60) yields the following result:

An error Le_F dB in the measured flanking reduction index R_F results in an error Le_R dB in the estimated value of the true sound reduction index R, where

$$Le_R = -10 \log \left[1 + h_F (1 - 10^{-Le_F/10})\right] \quad \text{dB.} \quad (2.61)$$

Eq. (2.61) is plotted in Figs. 2.3(a) and 2.3(b). In the same way it may be shown that:

An error $Le_{R'}$ dB in the measured apparent sound reduction index of the test object R' results in an error Le_R dB in the estimated value of the true sound reduction index R, where

$$Le_R = -10 \log \left[(1 + h_F) 10^{-Le_{R'}/10} - h_F\right] \quad \text{dB.} \quad (2.62)$$

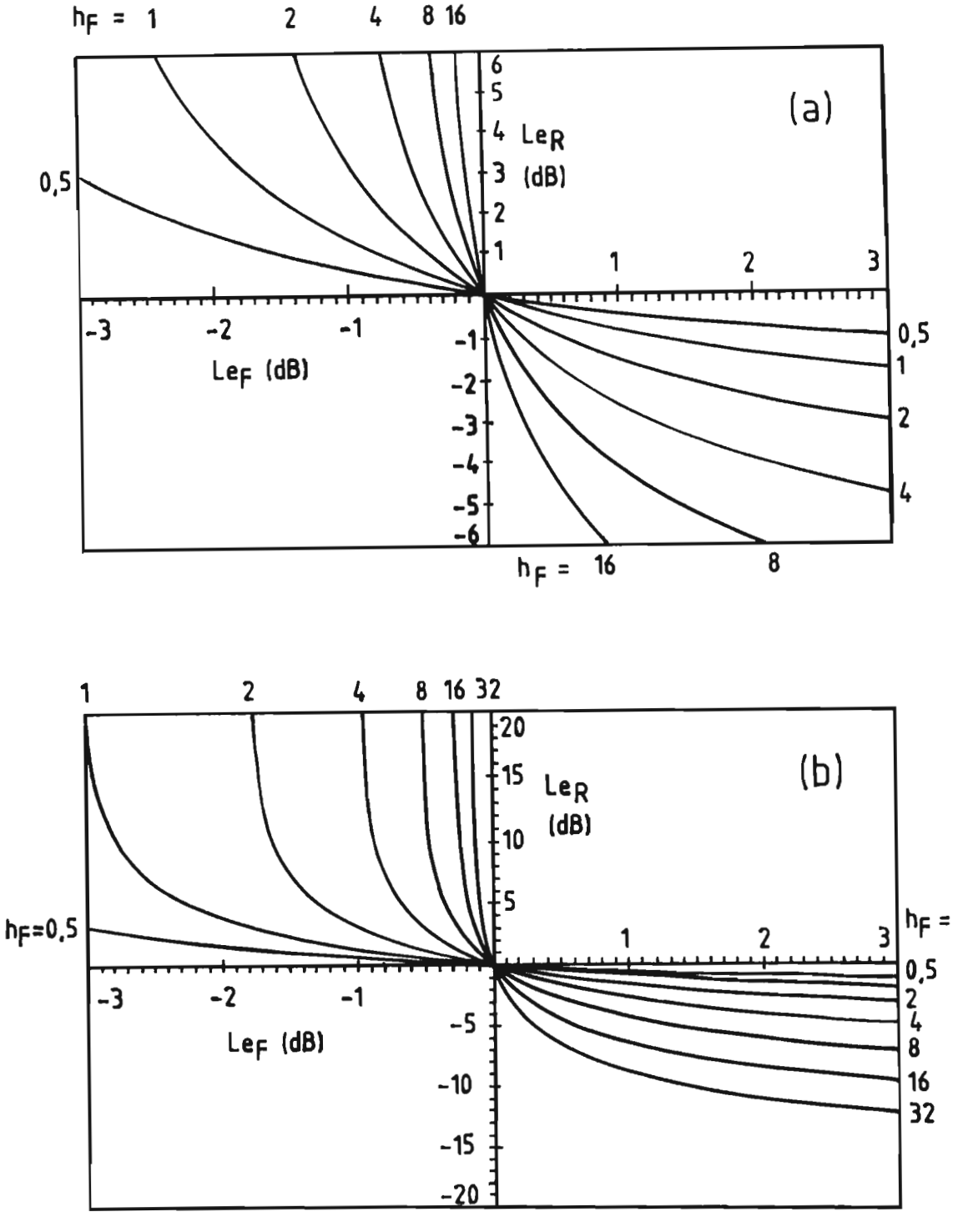

Figure 2.3

Estimation error Le_R dB in the sound reduction R of a test object, if an error Le_F dB occurs in the estimation of the sound reduction R_F of the flanking wall.
h_F = (flanking power)/(direct power)

(a) $|Le_R| \leq$ 6dB

(b) $|Le_R| \leq$ 20dB

Eq. (2.62) is plotted in Figs. 2.4(a) and 2.4(b). In practice Le_F and $Le_{R'}$ occur concurrently. The maximum total error is obtained if Le_F and $Le_{R'}$ have opposite signs. It is reasonable to assume that the magnitudes of the two errors are approximately equal and to define a single error $Le = Le_F = - Le_{R'}$. Using this value, the measured sound reduction index Rm is obtained by introducing Le into Eq. (2.56). Hence,

$$Rm = - 10 \log \left[10^{-(R' - Le)/10} - \frac{A_F}{A} 10^{-(R_F + Le)/10}\right] \quad dB. \quad (2.63)$$

The total error Le_{RT} in the estimated value of R, obtained by subtraction of Eqs. (2.63) and (2.56), is given by

$$Le_{RT} = Rm - R = 10\log\left[\frac{10^{-R'/10} - \frac{A_F}{A} 10^{-R_F/10}}{10^{-(R' - Le)/10} - \frac{A_F}{A} 10^{-(R_F + Le)/10}}\right]. \quad (2.64)$$

It follows by inspection of Eqs. (2.52) and (2.55) that

$$R' = R + 10 \log (1/(h_F + 1)) \quad . \quad (2.65)$$

Substitution of Eq. (2.65) into Eq. (2.64) and simplification yields the following result:

The total error Le_{RT} in the estimated value of the true sound reduction index R as a net result of an error Le dB in the measured flanking reduction index R_F and an error - Le dB in the measured apparent sound reduction index of the test object R' is

$$Le_{RT} = - 10 \log \left[(1 + h_F)10^{Le/10} - h_F 10^{-Le/10}\right] \quad dB. \quad (2.66)$$

The plots of Eq. (2.66) given in Figs. 2.5(a) and 2.5(b) illustrate how difficult it is to obtain an accurate estimate of R in the presence of flanking transmission, particularly in the case of high-performance test objects. If the test object has a high sound insulation index, while at the same time it has a surface area small in relation to the flanking surface, it may prove extremely difficult, if not impossible

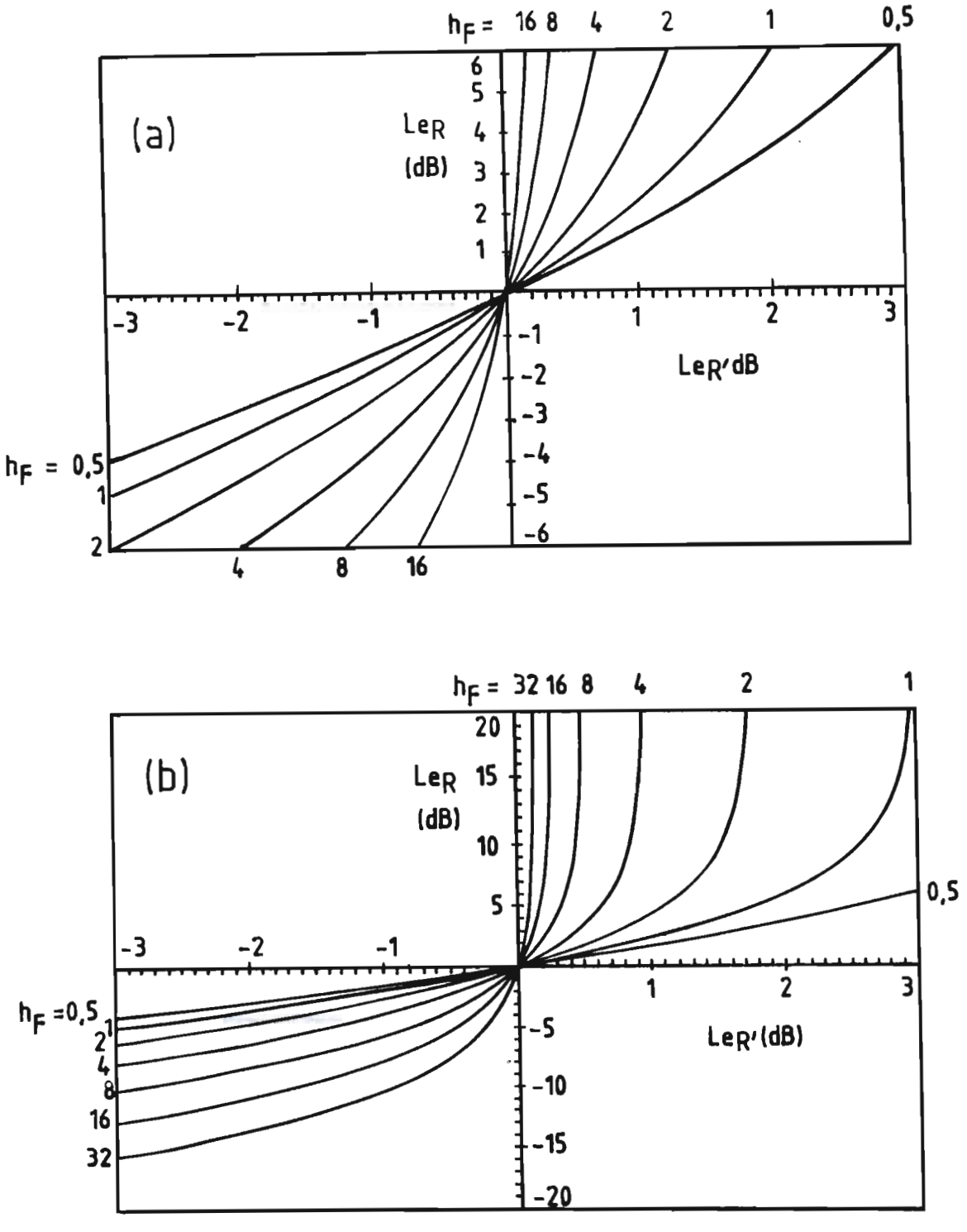

Figure 2.4

Estimation error Le_R dB in the sound reduction R of a test object, if an error $Le_{R'}$ dB occurs in the estimation of the apparent sound reduction R' of the test object.
h_F = (flanking power)/(direct power)

(a) $|Le_R| \leq$ 6dB

(b) $|Le_R| \leq$ 20dB

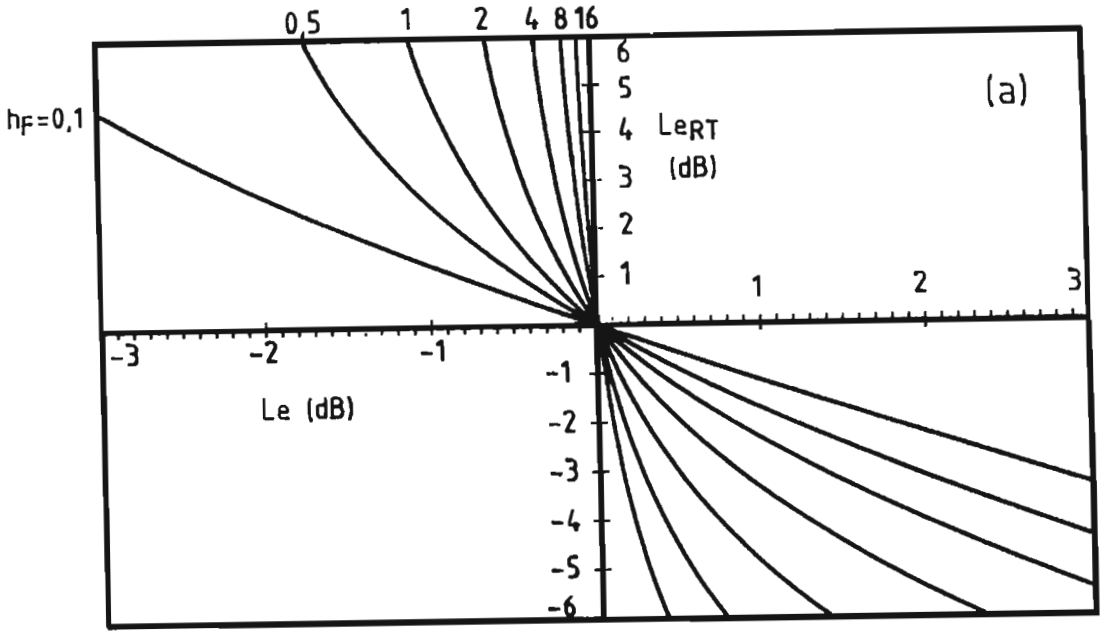

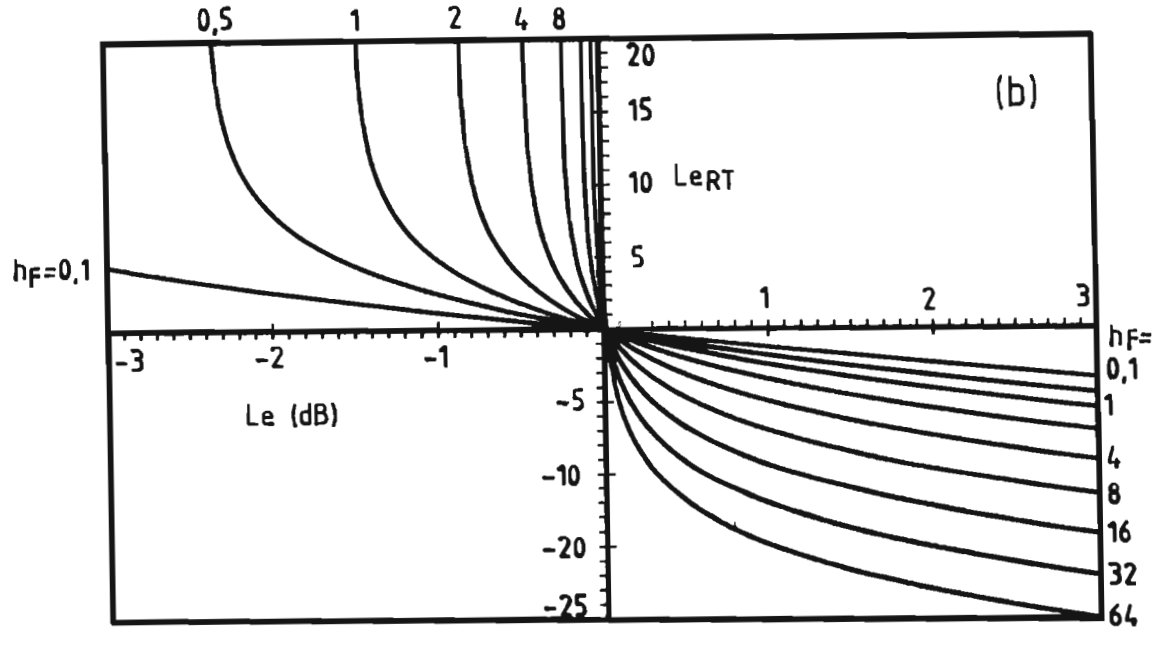

Figure 2.5

Estimation error Le_{RT} dB in the sound reduction R of a test object if an error Le dB occurs in the estimation of the sound reduction R_F of the flanking wall while at the same time an error - Le dB occurs in the estimation of the apparent index R′ of the test object.

(a) $|Le_R| \leq 6dB$

(b) $|Le_R| \leq 20dB$

to determine R with sufficient accuracy.

Note that the estimation errors given in Eqs. (2.61), (2.62) and (2.66) become infinitely large in the following cases:

$$Le_R \to \infty \quad \text{if} \quad Le_F < -10 \log (1 + 1/h_F) \quad \text{dB} \tag{2.67}$$

$$Le_R \to \infty \quad \text{if} \quad Le_{R'} > 10 \log (1 + 1/h_F) \quad \text{dB} \tag{2.68}$$

$$Le_{RT} \to \infty \quad \text{if} \quad Le < -10 \log (1 + 1/h_F)^{0,5} \quad \text{dB} \tag{2.69}$$

Example 2.2 Consider a sound insulation test performed on an experimental window to evaluate the effectiveness of its design. The latter is aimed at attaining a sound reduction index R = 56 dB at 400 Hz. Consider the consequences of measurement inaccuracies if the window (surface area A = 2,0 m^2) is mounted in a special brick cavity wall used as a filler in a 10,0 m^2 test aperture between two test rooms. The filler wall (A_F = 8,0 m^2) has a sound reduction index R_F = 60 dB at 400 Hz. The estimated measurement accuracy is ± 1,0 dB. The expected error in the estimate of R is summarized in Table 2.2

Table 2.2

Analysis of the problem in Example 2.2

Eq. (2.51)	h_F = 1,59
Eq. (2.61), using $\lvert Le_F \rvert$ < 1,0 dB	- 1,2 dB < Le_R < 2,3 dB
Eq. (2.62), using $\lvert Le_{R'} \rvert$ < 1,0 dB	- 2,2 dB < Le_R < 3,3 dB
Eq. (2.66), using $\lvert Le \rvert$ < 1,0 dB	- 3,0 dB < Le_{RT} < 12,5 dB

In order to limit the total error to Le_{RT} dB, the measurement error must comply with

$$|Le| < 10 \log \left[\frac{10^{-Le_{RT}/10} \pm \left(10^{-2Le_{RT}/10} + 4(1 + h_F)h_F\right)^{0,5}}{2(1 + h_F)}\right] \quad (2.70)$$

or the flanking transmission should be reduced to a level at which

$$h_F < [10^{-(Le_{RT} + Le)/10} - 1]/(1 - 10^{-2Le/10}) \quad . \quad (2.71)$$

Using

$$R_F = R - 10 \log (h_F \, A/A_F) \quad , \quad (2.72)$$

It follows that the sound reduction index of the flanking structure must be

$$R_F > R + 10\log\left[\frac{A_F}{A} (1 - 10^{-2Le/10})\right]/[(10^{-(Le_{RT} + Le)/10} - 1)] . \quad (2.73)$$

In the previous example the sound insulation of the already special filler wall is inadequate for the purpose of the test. In order that $|Le_{RT}| < 1,5$ dB, a filler wall is required which has a sound reduction index of at least 69 dB at 400 Hz, a figure which is extremely difficult and costly to attain. Note that according to Eq. (2.69) $Le_{RT} \to \infty$ if $|Le| > 1,1$ dB.

CHAPTER 3

SOUND TRANSMISSION ANALYSIS BY SOUND INTENSIMETRY

3.1 INTRODUCTION

It is clear from the analysis in Chapter 2 that the applicability of the classic two-room method is restricted by conditions arising from the implicit use of the reverberation room method in determining the transmitted sound power. A fundamental limitation of this method is that it gives no indication of either the relative amounts or the origins of the components contributing to the total transmitted power. For light-weight partitions the direct portion of the transmitted power can be determined with sufficient accuracy by supression of the flanking portion. In the case of high-performance test objects mounted in filler walls it is sometimes appropriate to consider the flanking portion as inevitable and to combine it with the direct portion. In many applications, however, it is essential to distinguish between direct transmission through the test object and flanking transmission through the filler wall in order to assess the performance of the test object per se. In addition, there is also a need for a technique by which sound transmission through composite panels may be analyzed in finer detail.

The decision to apply and to evaluate sound intensimetry as a means of performing sound insulation tests at the NPRL ensued from difficulties encountered in testing newly developed doors and windows intended for applications demanding exceptionally good sound insulation. The sound intensity method of measuring sound reduction indices was first introduced by Crocker [133,134]. The principles and advantages of this new method have since been demonstrated by several investigators by comparison with the classic method [14,29, 135,136]. It has been shown that the intensity method can be used very effectively for selective determination of sound reduction indices of different parts of a composite panel [29,134, 137] and that the direct transmission can be determined in the presence of flanking transmission [29, 138]. The intensity method has been used with success to determine sound

reduction indices selectively for flanking factors $h_F > 15$, whereas the classic method was found unreliable if $h_F > 1$ [27]. McGary [139] extended the sound intensity method and developed a technique for separating airborne and structureborne noise in propeller-driven aircraft.

Using the intensity method on a comparative basis with the classic two-room method to investigate the influence of room design and mounting conditions on the sound insulation of test objects, Cops et al. [140, 141] found that the sound insulation index could vary by as much as 5 dB, depending on the placement of the test panel in the niche. This stresses the point that sound insulation test results can be affected by factors bearing no relationship to the use of sound pressure or sound intensity as the basis of measurement.

While it is generally accepted that the intensity method does not require a diffuse receiving room, a certain degree of wariness is observed in the literature with regard to the use of reverberant receiving rooms. Investigators almost invariably state without explanation that the receiving room should be made relatively absorbent or that it had been made absorbent for the purpose of their investigations. This cautiousness is understandable, considering that no guidelines have yet been established for the assessment of receiving room adequacy. Although it is known that the accuracy of sound intensity measurement in reactive fields depends on phase mismatch errors introduced by the measurement system [6,138], no attempt has yet been made to relate minimum receiving room requirements to intensity meter performance figures.

It is the purpose of this chapter to identify and to define the principles involved in using sound intensimetry for sound transmission analysis in reactive fields, and to develop a theoretical framework for the assessment of the validity and accuracy of the intensity method in any given application. Section 3.2 begins by reviewing the principles of sound intensimetry with emphasis on the methods employed in conducting the experimental work in support of this thesis. The general characteristics of sound intensity meters are considered, followed by a

thorough treatment of sound intensity calibration.

The analyses in the remainder of this chapter represent original contributions by the author towards the development of a comprehensive theory on sound transmission analysis by sound intensimetry. The application and meaning of theoretical derivations are explained by examples presented in the course of the chapter.

The sound intensity method of determining sound reduction indices is formulated in Section 3.3. The method derived here, although basically identical to the one commonly referred to in the literature [133], gives account of factors which have until now been disregarded. These are:

(1) The effect of a difference in the surface area of the test object exposed to radiation in the source room and that of the measurement surface needed to cover the radiation from the surface of the test object into the receiving room completely.
(2) The storage of reverberant energy in the interference field near the boundaries of the source room.
(3) Calibration mismatch between the sound pressure and sound intensity measurement systems employed in determining sound reduction indices.

Section 3.3 proceeds to consider the leakage error resulting from the common practice of using a plane measurement surface at a finite distance from the surface of the test object and concludes with an examination of the effect of sound absorption by the test object on the accuracy of the intensity method.

The principles and theory of sound transmission analysis in reactive fields are developed in Section 3.4. Beginning with the problem of sound intensity measurement in reactive fields, the author identifies two types of phase error in measurement systems and shows that the intensity error is different in the two cases. In order to account for sound intensity meter limitations, the common mode rejection index is defined and used in conjunction with the concept of reactivity [142] in

assessing the validity of sound intensity measurements in sound transmission analysis. First, a general expression is derived for predicting the reactivity at the surface of a test object in a reverberant receiving room. It is then shown how the minimum amount of absorption in the receiving room, or the minimum microphone spacing may be calculated for any given application of the intensity method. Finally, the application of the theory to the assessment of flanking transmission is considered.

Section 3.5 presents a new method based on sound intensimetry, of assessing the degree of directional diffusivity in sound fields. Upon consideration of the general characteristics of the sound intensity field in relation to the sound pressure field in the vicinity of a point source located in various types of acoustic environment, a descriptive model of the intensity field in reverberant rooms is derived. This model is then used as a basis in developing a criterion for the assessment of the degree of diffusivity at a point on basis of sound intensity measurement. It is shown that either reactivity, or a diffusivity factor derived from the latter, can be used as a measure of the degree of diffusivity. A formula for calculating this factor is constructed and scaled to attain the best possible agreement between the intensity method and the directivity method discussed in Section 2.6.1. Finally, the influence of a lack of directional diffusivity on the accuracy of the intensity method is analyzed in terms of the criteria developed in the first part of Section 3.5.

3.2 PRINCIPLES OF SOUND INTENSIMETRY

3.2.1 Definition. The sound intensity in a specified direction is defined as the rate of acoustic energy flow per unit area normal to that direction. Hence, the instantaneous sound intensity

$$i(t) = \text{acoustic power/unit area} = w(t)/A \qquad (3.1)$$

where from elementary mechanics

$$w(t) = \text{force} \times \text{velocity} = f(t) \cdot u(t) \qquad (3.2)$$

And since f(t)/A = pressure, substitution of Eq. (3.2) into Eq. (3.1) yields the instantaneous intensity as a function of the instantaneous sound pressure p(t) and particle velocity u(t). Thus,

$$i(t) = [f(t) \cdot u(t)]/A = p(t) \cdot u(t) \quad . \tag{3.3}$$

The desired quantity for practical purposes is the time-averaged intensity

$$I = \langle i(t) \rangle_t = \langle p(t) \cdot u(t) \rangle_t \quad . \tag{3.4}$$

As sound power is propagated in a specific direction, sound intensity is a vector quantity specified in terms of its magnitude and direction.

3.2.2 Measurement techniques. Various schemes have been devised for sound intensity measurement, of which only a few proved to be practically viable. Considerable effort has been made to find solutions for particle velocity measurement. One approach is to obviate particle velocity measurement by manipulating the mathematical formulation of I to dispose of u(t) in its explicit form [34,35]. This has in fact resulted in new methods with totally different instrumentation requirements. The essence of the problem, however, is not changed by mathematical transformation; particle velocity is a function of the phase gradient, the principle and unavoidable parameter in sound intensity measurement. The two most widely used methods for sound intensity measurement are the cross-spectral density method and the direct method.

Cross-spectral density method [34]. Sound intensity as defined in Eq. (3.4) may be determined from the imaginary part of the cross-spectral density of two pressure microphone signals. This follows by noting that the time-averaged intensity may be expressed as a function of the cross-correlation between the two pressure signals and that the Fourier transformation of the latter results in the cross-spectral density $S_{12}(\omega)$ of the pressure signals. The expression for the time-averaged sound intensity becomes

$$I = - \frac{1}{\rho\omega\ \Delta r}\ \mathrm{Im}\{S_{12}(\omega)\} \qquad (3.5)$$

where Δr is the distance between the two pressure microphones. The main advantage of this technique is that it can be implemented on general purpose dual-channel FFT analyzers. There are two disadvantages:

(1) Measurements cannot be performed in real-time.
(2) The result is presented as a frequency line spectrum which has to be converted to octave or third-octave band levels by computation.

Direct method [6,48] This method is based on direct computation of particle velocity by solving Euler's equation

$$\frac{\partial p(t)}{\partial r} = - \rho\ \frac{\partial u(t)}{\partial t} \qquad (3.6)$$

for u(t). the time-averaged sound intensity, obtained by substituting the solution of u(t) into Eq. (3.4), is

$$I = \left\langle - \frac{1}{\rho} \left[p(t) \int \frac{\partial p(t)}{\partial r} dt \right] \right\rangle_t \qquad (3.7)$$

If the pressure differential in Eq. (3.7) is approximated by the difference $p_1(t) - p_2(t)$ between the sound pressures at two microphones spaced by a distance Δr and if the sound pressure p(t) is estimated by $[p_1(t) + p_2(t)]/2$, the time-averaged sound intensity becomes

$$I = \left\langle - \frac{1}{2\rho\Delta r} [p_1(t) + p_2(t)] \int [p_1(t) - p_2(t)] dt \right\rangle_t \quad . \qquad (3.8)$$

Equation (3.8) may be executed by analog computation [6] or by digital signal processing [48]. The experimental part of this investigation was performed with two sound intensity meters which both employed the direct principle; one by analog computation, the other by digital signal processing.

3.2.3 Fundamental characteristics of sound intensity meters

The fundamental characteristics of all sound intensity meters utilizing two pressure microphones are identical; frequency and directional characteristics are primarily governed by the distance Δr between the microphones. In addition to this limitation, practically all other errors are caused by phase mismatch errors distorting the true acoustic phase difference between the two microphones.

Directional characteristics The directional response of a sound intensity meter is given by [6]

$$H(\gamma) = 10 \log \left| \left[\sin\{(k\Delta r + \varepsilon)\cos\gamma\}/k\Delta r \right] \right| \quad \text{dB} \qquad (3.9)$$

where γ is the angle of incidence at the acoustic centre of the probe, measured with respect to the direction of maximum sensitivity, $\gamma = 0^{\circ}$ and ε is the phase error introduced by the instrument.

Frequency characteristics In a plane wave the fundamental intensity error due to the finite distance Δr between the microphones is [6]

$$Le = 10 \log \left[\frac{\sin(k\Delta r)}{k\Delta r} \right] \quad \text{dB} \qquad (3.10)$$

where $k\Delta r$ represents the true acoustic phase difference in radians between the microphones. If, due to phase mismatch, the measurement system introduces an additional phase shift ε radians, the error becomes

$$Le = 10\log\left[\frac{\sin(k\Delta r + \varepsilon)}{k\Delta r} \right] \overset{\text{at low frequencies}}{\approx} 10\log\left(1 + \frac{\varepsilon}{k\Delta r}\right) \quad \text{dB}. \qquad (3.11)$$

The finite distance approximation $k\Delta r$ is accurate at low frequencies but causes an error which increases with frequency. For all practical purposes the low frequency error is caused by the phase error ε only. Using the approximation $\sin k\Delta r \approx k\Delta r$, which is valid at low frequencies, Eq. (3.11) may be solved to find the minimum spacing Δr_0 (m) required to limit the error in a plane wave to Le dB. With ε in degrees

and using c = 346 m/s, the result is

$$\Delta r_0 = (0{,}96\varepsilon/f)/(10^{Le/10} - 1) \qquad (3.12)$$

where f is the frequency in Hz. The lowest third-octave band of interest for general-purpose sound insulation tests is 100 Hz. The minimum microphone spacing required to limit the plane wave error at 100 Hz to -1,0 dB if the measurement system has a phase error $\varepsilon = -0{,}3^{\circ}$, is Δr = 14 mm.

Equations (3.11) and (3.12) are valid for a plane wave. Analysis of the sound intensity method in this thesis is based on the assumption that the receiving room is allowed to be reverberant. For a fixed microphone spacing Δr, the acoustic phase difference in a reverberant field is only a fraction m of the value in a plane wave. Accuracy requirements for sound intensity measurement in reactive fields is examined in Section 3.4.

The high-frequency error is primarily determined by the microphone spacing. In order to limit the error Le in Eq. (3.11) to - 1,0 dB at 5kHz, a microphone spacing Δr = 12 mm is required. Frequency and directional characteristics measured for the NPRL sound intensity meter are presented in Appendix A1.

3.2.4 Calibration of sound intensity meters

Consistency of acoustic reference levels In applied acoustics sound power W is usually converted to a logarithmic scale. The sound power level in decibels is defined as

$$LW = 10 \log (W/W_0) \quad dB \qquad (3.13)$$

where the reference power level W_0 = 1pW. Likewise, the sound intensity level for a sound intensity I is defined as

$$LI = 10 \log (I/I_0) \quad dB \qquad (3.14)$$

where $I_0 = 1 pW/m^2$. If sound intensity is expressed in terms of the rms sound pressure P, the intensity level defined in Eq. (3.14) becomes

$$LI = 10 \log [(P^2/\rho c)/I_0] \quad dB \tag{3.15}$$

where ρc is the specific acoustic impedance at the temperature and atmospheric pressure prevailing at the point under consideration. Likewise, in terms of the rms particle velocity U,

$$LI = 10 \log [(U^2 \rho c)/I_0] \quad dB. \tag{3.16}$$

Using the standard consistent set of reference levels

$$S_0 = \{I_0 = 1 pW/m^2; P_0 = 20 \mu Pa; U_0 = 50 \text{ nm/s}; \rho_0 c_0 = 400 \text{ mks rayls}\} \tag{3.17}$$

it follows that

$$P_0^2/\rho_0 c_0 = V_0^2 \rho_0 c_0 = I_0 \quad . \tag{3.18}$$

If calibration complies with the set S_0, Eq. (3.15) becomes

$$LI = 10 \log [(P^2/\rho c)/(P_0^2/\rho_0 c_0)] \quad dB. \tag{3.19}$$

If $\rho c = \rho_0 c_0$, Eq. (3.19) reduces to

$$LI = 10 \log (P^2/P_0^2) = LP \quad dB. \tag{3.20}$$

The assumption $\rho c = \rho_0 c_0$, which is almost invariably made when acoustic power is related to sound pressure, implies that LP = LI in a plane wave. Since in reality $\rho c \simeq \rho_0 c_0$, there will be a small difference

$$Lep = LPm - LI = 10 \log (\rho_0 c_0/\rho c) \quad dB \tag{3.21}$$

between the reading LPm given by a sound level meter calibrated according to Eq. (3.20) and the true intensity level LI, defined in Eq. (3.14), at the measurement point. The specific acoustic impedance at the prevailing temperature T (K) and atmospheric pressure B (mb) may be calculated from

$$\rho c = 6.98\ B/\sqrt{T} \quad . \tag{3.22}$$

Calibration of sound intensity meters is complicated by a lack of practical techniques to generate accurately known intensity reference levels. Three calibration techniques will now be considered.

Method 1. (LP re 20 μ Pa; LI re 1pW/m^2 by free-field calibration) This involves standard pressure calibration of both microphones, followed by adjustment of the relative gain LI-LP such that

$$LI = LP + 10 \log (\rho_0 c_0/\rho_r c_r) \qquad dB \tag{3.23}$$

with the probe positioned in the far field of a small sound source located in an anechoic chamber. This calibrates the system for correct intensity level reading re 1pW/m^2 for $\rho c = \rho_r c_r$, the specific acoustic impedance at the temperature T_r and atmospheric pressure B_r prevailing during calibration.

If a sound intensity meter calibrated for T_r and B_r is used at T and B, an error Lei will occur. Some caution is required in calculating Lei. Consider the measurement of sound intensity according to Eq. (3.7). Computation by this formula yields a result of the form

$$I = -(1/\rho)(1/c)\langle f\{p(t)\}\rangle_t = -G_1 G_2 \langle f\{p(t)\}\rangle_t . \tag{3.24}$$

At calibration conditions T_r and B_r, sound intensity is measured faithfully as

$$I = -(2.873\ T_r/B_r)(1/20{,}05\ \sqrt{T_r})\langle f\{p(t)\}\rangle_t . \tag{3.25}$$

The presence of ρ in the gain factor G_1 originates from Euler's equation (Eq. (3.6)) where ρ appears as a constant. The speed of sound c in G_2 is generated by the operation $\frac{\partial p(t)}{\partial r}$ in Eq. (3.7). Hence, if environmental conditions change from T_r and B_r to T and B, respectively, I would be measured as

$$I_m = -(2.873\ T_r/B_r)(1/20{,}05\ \sqrt{T})\langle f\{p(t)\}\rangle_t . \tag{3.26}$$

The gain factor G_2 is seen to follow the change in temperature, while G_1 remains constant. The intensity measurement error

$$Lei = LIm - LI = 10 \log \left(\frac{BT_r}{B_r T}\right) \quad dB. \tag{3.27}$$

Method 2. (Pressure compensation method). The calibration procedure recommended by the manufacturer of the B & K 3360 analyzer, which has a fixed gain G_1G_2 set for $T_{ro} = 293$ K and $B_{ro} = 1013$ mb, is to off-set the pressure calibration by a factor B_{ro}/B_r. In this way Lei reduces to

$$Lei = 10 \log (T_{ro}/T_r) = 10 \log (293/T_r) \quad dB. \tag{3.28}$$

It should be borne in mind that the sound pressure calibration is slightly off-set by this procedure. If a system calibrated in this way is used for sound pressure level measurements, it will give a reading

$$LPm = LP + 10 \log (1013/B_r) \quad dB \tag{3.29}$$

where Lp is the sound pressure level obtained by standard calibration re 20 μ Pa.

Method 3. (Lp re 20 μ Pa; LI re 1pW/m^2 by electronic calibration). The Model A83 SIM sound intensity meter has an adjustable gain G_1 which may be set during calibration with the aid of an electronic calibrator, Model A83 CAL 2. This instrument generates two signals with an accurately defined time delay between them. In this way it is possible to calibrate LP and LI independently. For a time delay τ (s) intensity calibration for conditions T_r and B_r is obtained by adjusting G_1 to obtain a reading

$$LI = LP + 10 \log (400/\rho_r c_\tau) \tag{3.30}$$

where $c_\tau = \Delta r/\tau$ is the speed of sound implied by the time delay τ between the calibration signals, if a microphone spacing Δr is to be used. By inspection of Eqs. (3.24) to (3.26) it is concluded that, in

addition to pressure calibration re 20 μ Pa, G_1 should be adjusted to obtain

$$LI = LP + 10\log[(400)(2.87T_r/B_r)(1/c_\tau)] = LP + 10\log(1149\frac{T_r\tau}{B_r\Delta r})dB \quad (3.31)$$

with the electronic calibrator connected to the intensity meter. An instrument calibrated by this procedure measures LP re 20 μ Pa and LI re $1pW/m^2$ at a temperature T_r (K) and atmospheric pressure B_r (mb). (This method is equivalent to, though more accurate and faster than Method 1.)

3.3 DETERMINATION OF SOUND REDUCTION INDICES BY THE SOUND INTENSITY METHOD

3.3.1 Derivation of a test procedure based on sound intensimetry

The intensity method is based on the test arrangement shown in Fig. 3.1. The desired properties of the two rooms and a practical measurement procedure may be derived from the definition of sound reduction;

$$R = 10 \log (W_{IN}/W_D) = 10 \log (I_{IN}A/I_DA_2). \quad (3.32)$$

$W_{IN} = I_{IN}A$ is the acoustic power incident on the surface area A of the test object and $W_D = I_DA_2$ is the power transmitted by the test object. It is not assumed at this stage that $A = A_2$; A_2 being any surface subtended by the test object and which receives an average sound intensity I_D from it. The use of sound intensimetry in determining W_{IN} and W_D will now be investigated. Note that a sound intensity meter measures the net component of the acoustic power flow per unit area in the direction in which the microphone is pointed.

Source room: incident power. In the source room the nature of the sound field is dictated by the practical requirement that the sound reduction index should be valid for random sound incidence. To ensure that all surface elements of the test object are exposed to the same level of net incident intensity, it is essential to have constant energy density in the source room and to ensure omnidirectional sound inci-

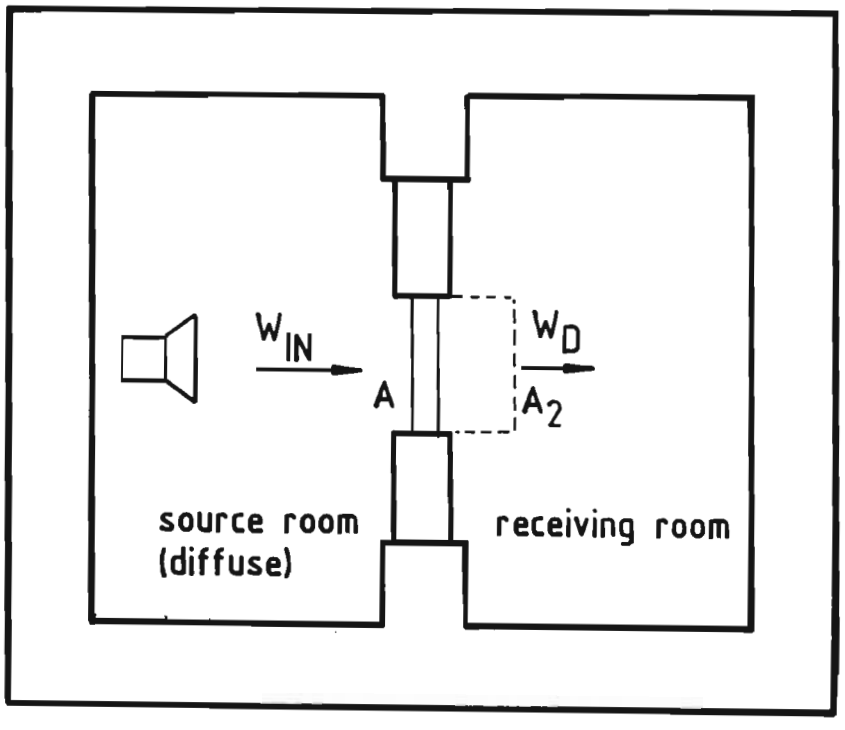

Figure 3.1

Test arrangement; sound intensity method

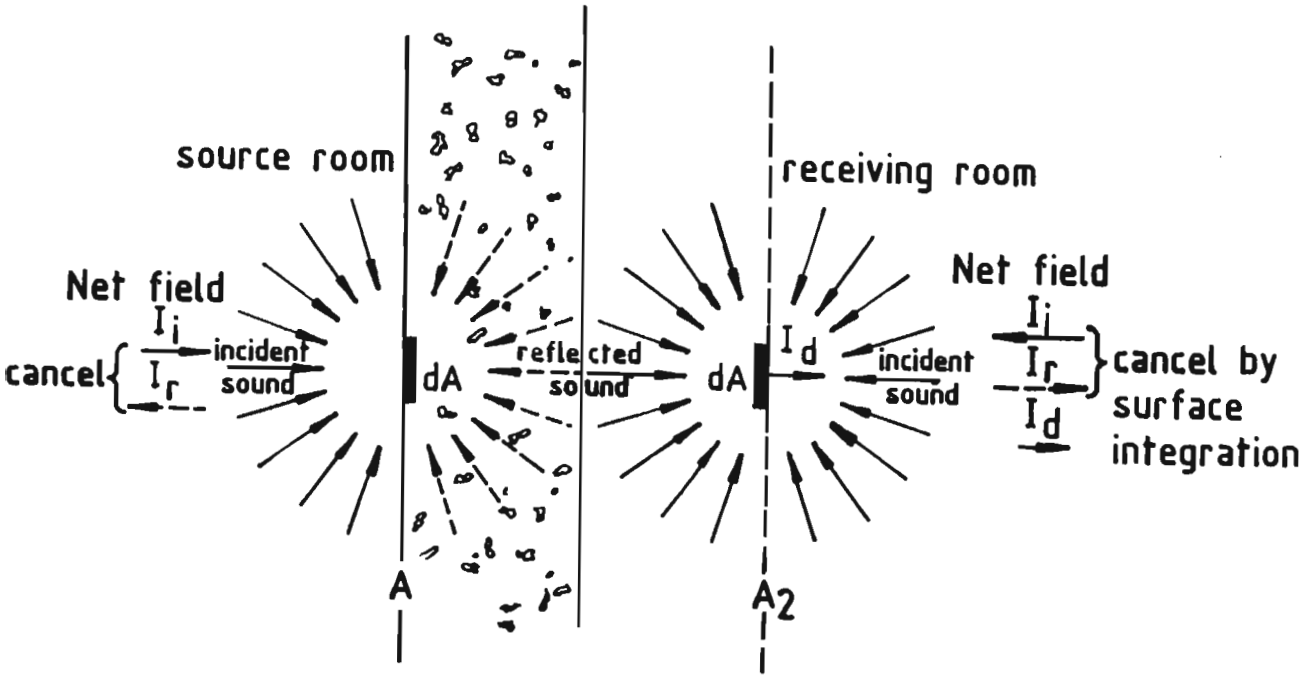

Figure 3.2

Composition of the sound intensity field at the surface of the test object A in the source room and at the measurement surface A_2 in the receiving room.

dence everywhere on the surface of the test object. These two requirements imply that the room should be diffuse.

The sound intensity field at the surface of the test object in the source room is depicted in Fig. 3.2. The reflected sound, which in reality is contained in the same half-space as the incident sound, is depicted separately. The collective effect of all the waves incident on the elemental surface dA may be described by a single vector I_i normal to the surface of the partition, and the corresponding vector for reflected waves by I_r. The total power incident on surface A, as required for implementation of Eq. (3.32) is

$$W_{IN} = \iint_A I_i \, dA. \tag{3.33}$$

The sound intensity meter, however, does not distinguish between I_i and I_r; it responds to the vector sum $I_i + I_r$. The net power obtained by surface integration of the sound intensity measured on the surface A, would be

$$W_n = \iint_A (I_i + I_r) \, dA \approx 0 \text{ if } \alpha \approx 0. \tag{3.34}$$

Thus, if the sound absorption coefficient of the test object $\alpha = 0$, the sound intensity meter should indicate zero net acoustic power flow; the measurement surface contains no sources or sinks. Although I_{IN} could be determined by sound intensity measurement at an open window provided temporarily in the dividing wall, the author found that the method was impracticable. The generally accepted procedure is to measure the sound pressure P_1 in the source room and to make use of the relationship in Eq. (2.4) repeated here as

$$W_{IN} = (P_1^2/4\rho c)A. \tag{3.35}$$

Hence, as regards the determination of the incident power, the intensity method is identical to the classic two-room method; it requires a diffuse source room and the incident power is determined by sound pressure measurement.

Receiving room: transmitted power. As shown in Fig. 3.2. the sound field in the receiving room contains a relatively strong direct intensity component I_d normal to the measurement surface, originating from the surface of the test object. The measurement surface A_2 includes the test object, which acts as a sound source, but excludes the flanking as well as all the mirror sources in the reverberant receiving room. Hence, by Gauss' theorem [8], surface integration of the normal component of the sound intensity on A_2 yields the total power transmitted by the test object; the power from extraneous sources.does not affect the result. The net power flowing through the surface A_2 is

$$W_n = \iint_{A_2} (I_i + I_r + I_d)dA = \iint_{A_2} (I_i + I_r)dA + \iint_{A_2} I_d \, dA. \tag{3.36}$$

By Gauss' theorem, if $\alpha = 0$,

$$W_n = \iint_{A_2} I_d \, dA = W_D = I_D A_2 \quad . \tag{3.37}$$

3.3.2 Formulation of the intensity method

The standard formulation of the intensity method is

$$R = LP1 - LI - 6 \quad \text{dB}. \tag{3.38}$$

If the sound reduction index R is determined by the procedure developed in the preceeding section, Eqs. (3.32), (3.35) and (3.37) may be combined, giving

$$R = 10 \log (AP_1^2/4\rho c A_2 I_D), \tag{3.39}$$

or in terms of the average sound pressure level in the source room LP1 and the average intensity level at the surface of the test object in the receiving room LI,

$$R = LP1 - LI + 10 \log (A/A_2) - 6 \quad \text{dB}. \tag{3.40}$$

Equation (3.40) does not account for the additional energy stored in

the interference field at the boundaries of the source room. Partial cancellation of the Waterhouse correction factors due to the difference LP1 - LP2 appearing in the classic formula, does not occur at all for the sound intensity method. Disregard of this correction results in underestimation of R at low frequencies, a phenomenon which in fact seems to appear in most results reported in the literature [25,26,134, 136-138,140]. By inclusion of the Waterhouse correction factor, Eq. (3.40) expands to

$$R = LP1 - LI + 10\log(A/A_2) + 10\log(1 + \lambda S_1/8V_1) - 6 \quad dB \quad (3.41)$$

where λ = wavelength (m);

S_1 = internal surface area of the source room (m^2);

V_1 = source room volume (m^3).

The final consideration in formulating the intensity method concerns calibration of the systems used for measuring LP1 and LI. As pointed out in Section 2.7, calibration in the case of the classic two-room method is greatly simplified because of the cancelling effect of the difference term LP1 - LP2. The sound intensity method involves two different types of measurement. The incident intensity is determined with a sound pressure level meter calibrated with respect to a reference level P_0 = 20 μ Pa, while the measurement of transmitted intensity is based on sound intensity calibration. To account for discrepancies between pressure and intensity calibration references, a calibration correction term Lc is introduced in Eq. (3.41). Hence,

$$R = LP1 - LI + 10\log(A/A_2) + 10\log(1 + \lambda S_1/8V_1) + Lc - 6 \text{ dB}. \quad (3.42)$$

In practice, Lc depends on the calibration technique used with the equipment employed in the tests. The general expression for Lc is

$$Lc = [(LP1m - 6) - LIm] - [(LP1 - 6 + 10\log \frac{400}{\rho c}) - LI] \text{ dB}. \quad (3.43)$$

where (LP1m - 6) and LIm are the measured levels of the incident and transmitted intensities, respectively and (LP1 - 6 + $10\log \frac{400}{\rho c}$) and LI

are the true levels re $1pW/m^2$. For instruments calibrated according to the procedures discussed in Section 3.2.4, the following corrections which presume that calibration values T_r and B_r correspond to environmental conditions prevailing during measurement, should be used in Eq. (3.42):

Method 1 (LP re 20 μ Pa; LI re $1pW/m^2$; free-field calibration).

$$Lc = 10 \log (\rho c/400) = 10 \log [B_r/(57.31 \sqrt{T_r})] \quad dB. \qquad (3.44)$$

Method 2 (Pressure compensation method)

$$Lc = 10 \log \left(\frac{1013}{B_r} \times \frac{T_r}{293} \times \frac{\rho c}{400}\right) = 10 \log (\sqrt{T_r}/16.58) \; dB. \qquad (3.45)$$

Method 3 (LP re 20 μ Pa; LI re $1pW/m^2$; electronic calibration)

$$Lc = 10 \log (\rho c/400) = 10 \log [B_r/(57.31\sqrt{T_r})]. \qquad (3.46)$$

3.3.3 Selectivity of the intensity method

Determination of sound reduction indices involves measurement of the power radiated by the test object into the receiving room. The fundamental difference between the sound intensity method and the classic two-room method resides in the principles employed in determining the transmitted power. The limitations and inflexibility of the classic method are inherent to the reverberation room method of sound power determination. The simplicity and versatility of the intensity method on the other hand, are effected by validation of Gauss' theorem in determining sound power by surface integration of the normal component of the sound intensity vector.

By using sound intensimetry, the principles of sound power determination by the intensity method take effect [7]. In regard to the determination of sound reduction indices and to sound transmission analysis, these principles have the following implications:

1. The sound power radiated from any source may be determined selectively by defining the measurement surface in such a way that it includes only the source under consideration. This means that the sound transmission characteristics of the test object, the flanking walls, or of any part of either, may be determined in reverberant environments.
2. Strictly speaking, no absorption should be allowed to take place within the volume contained by the measurement surface.
3. There are no restrictions to the shape of the measurement surface, provided the normal component of sound intensity is measured by directing the intensity probe perpendicularly to the measurement surface.
4. Measurements may be performed in the near field of the source.

The advantages implied by Gauss' theorem are applicable to the result obtained by surface integration; not to the sound intensity vector at discrete points on the surface. Examination of the sound intensity vector as a means of assessing the radiation characteristics of a test object should therefore be practised with caution. If the receiving room is not diffuse, the net contribution of the reverberant intensity will vary over the surface of the test object. The net sound intensity measured at specific points near the surface of the test object can therefore not be attributed exclusively to radiation from the test object. This does not detract much, however, from the value of sound intensimetry in performing diagnostic sound transmission analysis. Provided that small variations are ignored, examination of the general characteristics of radiation fields by inspection and mapping of the sound intensity vector is a very powerful method of detecting leaks and of evaluating the relative performance of various components of a composite test object. An effective technique in this regard is to measure the sound intensity vector at equally spaced points on a straight line extending across the regions of interest.

3.3.4 The measurement surface

In practice, the condition relating to the use of a closed integration surface is often violated in that the sound intensity is usually mea-

sured on a plane surface parallel to the surface of the test object. The implicit intention in doing this is to measure the sound intensity in the plane of the radiation surface. As a result of the finite minimum distance from the probe centre to the surface of the test object, the measurement surface is in reality always located some small distance from the radiation surface. Since the leakage gap created between the two surfaces almost invariably extends along physical boundaries, diffraction may generate a component of sound power entering the enclosed volume through the gap, yet leaving through the plane measurement surface. Depending on the design of the intensity probe and on the microphone spacing used, it may be necessary to perform sound intensity measurements on the leakage surface to prevent leakage error. It is for this reason that the areas A and A_2 in Eq. (3.42) were not taken to be identical as is usually assumed in the literature.

Consider the composition of the total direct power W_D and the total flanking power W_F in relation to the measured power W_m as depicted in Fig. 3.3. W_{F2} represents a fraction of W_F diffracted through the leakage gap towards the measurement surface. W_{FD} is another fraction of W_F reaching the measurement surface, in this case via the test object. W_{D2} represents a fraction of W_D transmitted through the leakage gap. W_{F1} represents the main portion of the flanking power, which is totally excluded by the measurement surface, while W_{D1} represents the main portion of the direct power which is transmitted through the plane measurement surface.

If sound intensity is integrated over a closed surface, the only component which is not eliminated from the measured result W_m is W_{FD} which has to be treated as part of W_D. If sound intensity measurement is only performed on a plane surface located at a distance r_m from the the test object as shown in Fig. 3.4, the sound reduction index of the test object R will be estimated with an error

$$Le = R_m - R = 10 \log \left[W_D/(W_D - W_{D2} + W_{F2}) \right] \quad dB. \qquad (3.47)$$

Equation (3.47) is based on the assumption that W_{FD} is regarded as a part of W_D. Assuming as a worst-case precaution that the average power

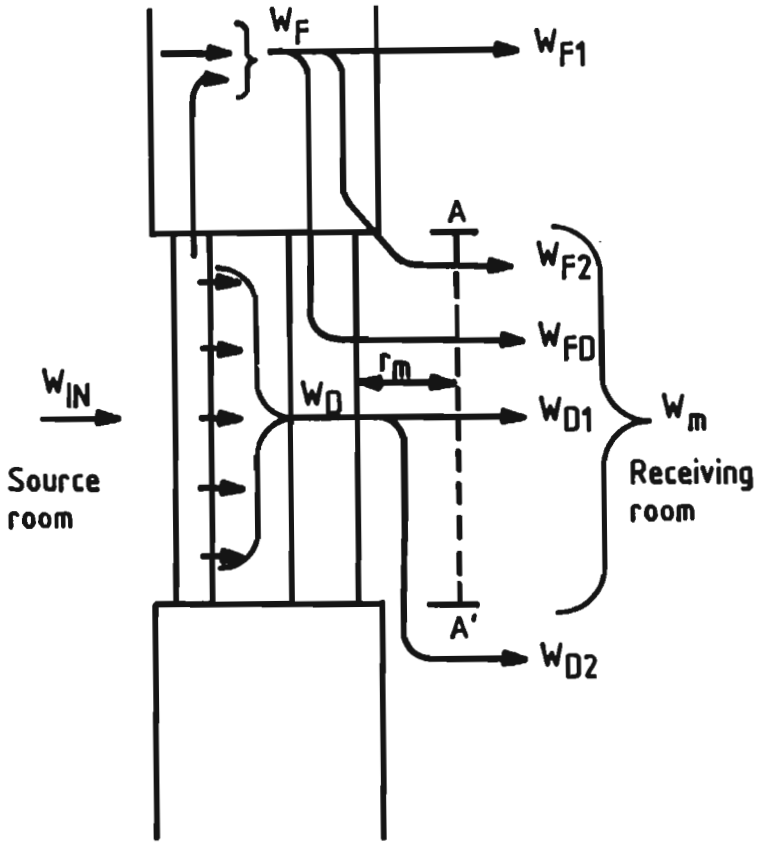

Figure 3.3

Composition of the direct power W_D and the flanking power W_F in relation to the measured power W_m

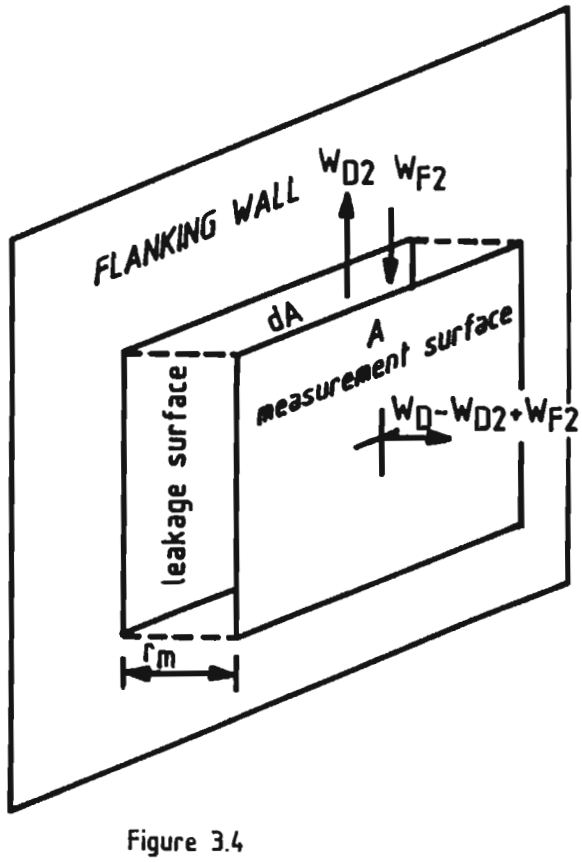

Figure 3.4

Sound power leakage due to finite distance r_m between the commonly used plane measurement surface and the test partition.

flow per unit area across the leakage surface dA is of the same magnitude as that across the plane measurement surface A, the leakage error becomes

$$Le = 10 \log [A/(A \pm dA)] \qquad dB \tag{3.48}$$

where dA and -dA respectively represent the cases $W_{F2} \gg W_{D2}$ and $W_{D2} \gg W_{F2}$ The latter case causes the largest error. If a maximum leakage error Lem dB is specified, the corresponding minimum distance r_m, assuming a square surface A = b x b, is found to be

$$r_m < \frac{b}{4}(1 - 10^{Lem/10}) \qquad (m). \tag{3.49}$$

Example 3.1. The maximum distance allowed between a plane measurement surface and a window of 1,4 m x 1,4 m if the leakage error is not to exceed - 1 dB, is r_m = 72 mm.

In practice, even for small microphone spacings, it is difficult to obtain r_m < 40 mm, especially if the sound intensity is averaged by a microphone-scanning procedure. Leakage error becomes particularly important if the sound radiation from small or narrow surfaces is determined. This occurs, for example, if the sound radiated by the frame of a window is to be isolated from the total radiation of the window and flanking walls. In such cases it is often not essential, however, to perform proper sound power measurements; sufficient information may be obtained by examination of the intensity vector along carefully chosen paths.

3.3.5 The effect of sound absorption by the test object.

One of the conditions for the elimination of background noise by Gauss' theorem is that the integration surface should not include any sinks as this would cause a net flow of background noise power to the enclosed volume. Sound absorption by the test object on the receiving room side constitutes such a sink. The flux of absorbed power substracts from the flux of power radiated by the test object, thus creating the impression that the test object is transmitting less than the actual pow-

er. The sound reduction index is therefore overestimated by the intensity method if sound absorption takes place at the surface of the test object.

Consider the estimation error due to sound absorption by the test object if the latter is surrounded by flanking surfaces as depicted in Fig. 3.5. If the average sound absorption coefficient of the surface A is α_A, the apparent sound reduction index of the test object obtained by the intensity method is

$$R' = 10 \log (W_{IN}/W') = 10 \log [W_{IN}/(I_D A - A\alpha_A I_R)] \qquad (3.50)$$

where W_{IN} = incident power, receiving room;
W' = apparent transmission power;
I_D = average direct intensity transmitted into receiving room;
I_R = average intensity incident on the test object from the reverberant field in the receiving room.

Although the formulation of the intensity method does not presume a diffuse receiving room, a reasonable estimate of the average intensity incident from the reverberant field is obtained by making use of the classic-room relationship

$$I_R = P_2^2/4\rho c \quad . \qquad (3.51)$$

The sound pressure in the receiving room P_2 depends upon the total power W transmitted into the room and upon the total sound absorption $S\alpha_A$ in the room, where

$$P_2^2 = 4W\rho c/S\alpha \quad . \qquad (3.52)$$

Since W is the sum of the direct power $W_D = hW$ and the flanking power $(1 - h)W$, Eq. (3.52) becomes

$$P_2^2 = 4I_D A\rho c/hS\alpha \quad . \qquad (3.53)$$

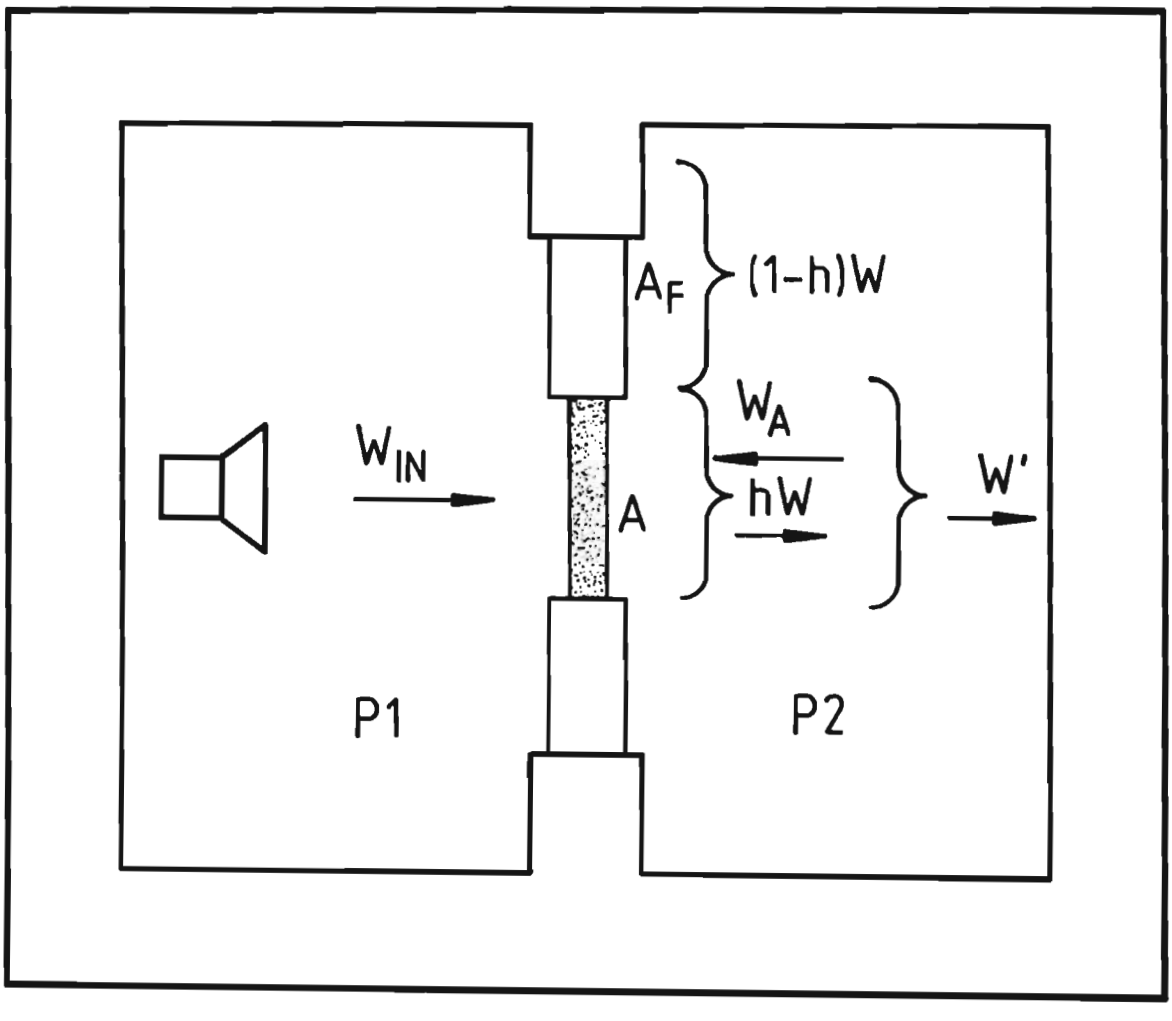

Figure 3.5

The effect of sound absorption at the surface of a test object surrounded by flanking walls.

By substitution of Eq. (3.53) into Eq. (3.51),

$$I_R = I_D A/hS\alpha \quad . \tag{3.54}$$

The apparent sound reduction index becomes

$$R' = 10 \log \left[W_{IN}/I_D A(1 - A\alpha_A/hS\alpha) \right] \quad . \tag{3.55}$$

The estimation error, obtained by inspection of Eqs. (3.32) and (3.55) and by using $A \approx A_2$, is

$$Le = R' - R = - 10 \log (1 - A\alpha_A/hS\alpha) \qquad dB. \tag{3.56}$$

By using the relationship given in Eq. (2.52), the estimation error due to sound absorption at the surface of the test object

$$Le = - 10 \log \left[1 - (1 + h_F)\frac{A\alpha_A}{S\alpha} \right] \qquad dB. \tag{3.57}$$

Equations (3.56) and (3.57) are plotted in Figs. 3.6(a) and (b), respectively. In the extreme case if all the sound absorption in the receiving room is located on the surface of the test object and if no flanking transmission is taking place (h = 1), Eq. (3.56) yield

$$Le = - 10 \log (1 - 1) \rightarrow \infty \tag{3.58}$$

which is the expected result, since all the power radiated into the receiving room is continually absorbed at the radiation surface.

Example 3.2. Consider the estimation error due to sound absorption by the test object if the sound reduction index of a 12 mm thick fibre panel is determined by the sound intensity method in a standard two-room test facility. The receiving room of volume 215 m^3 has a reverberation time of 5,5 s at 250 Hz. The panel of 9,0 m^2 is estimated to have an average sound absorption coefficient α_A = 0,15 at 250 Hz. Flanking transmission is assumed to be negligible (h = 1). The total sound absorption in the room, including that of the test panel is

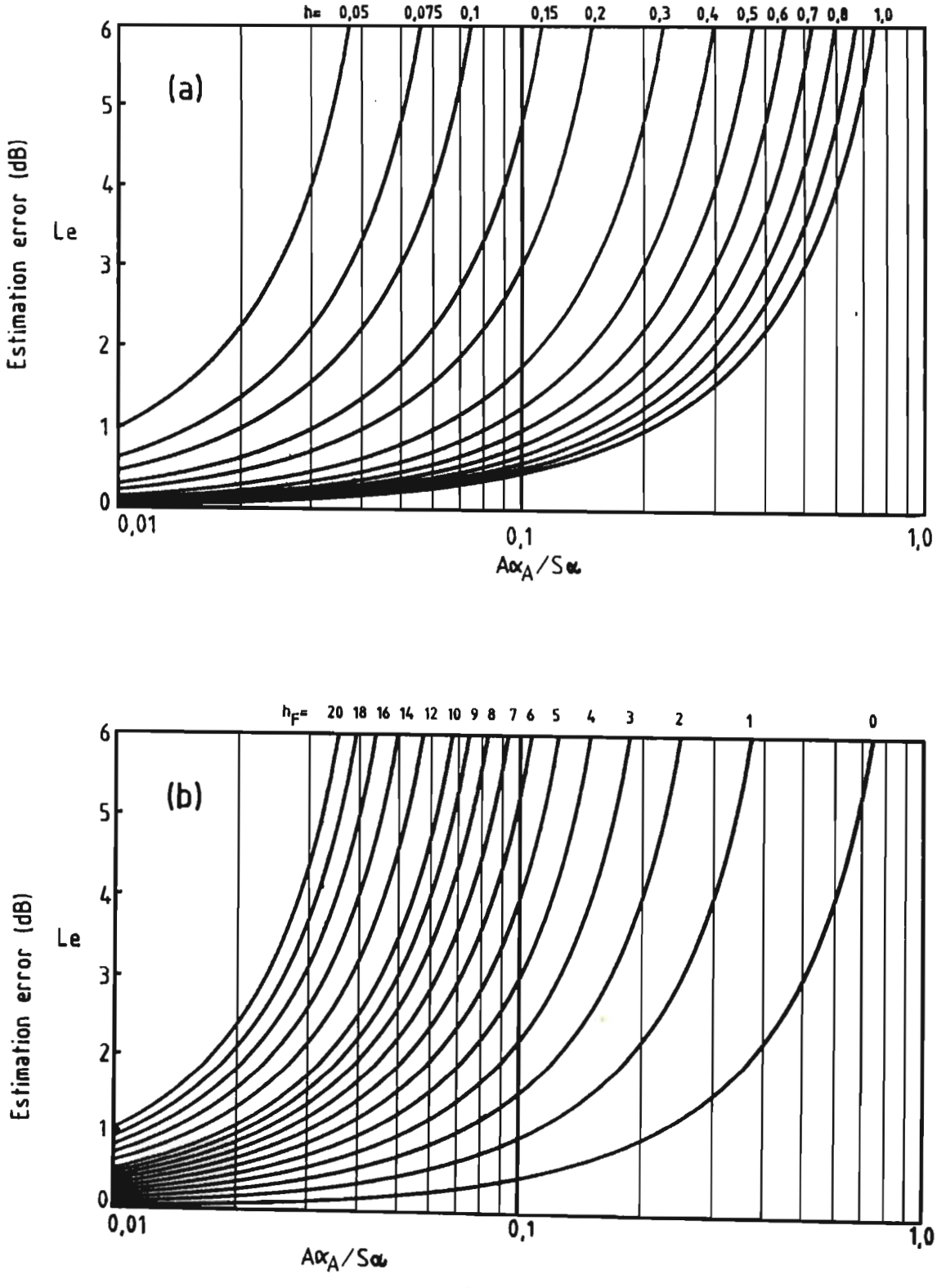

Figure 3.6

The error Le dB in the estimated value of sound reduction R if an amount $A\alpha_A$ m² of the total sound absorption $S\alpha$ in the receiving room is located on the surface of the test object.

(a) Parameter h=(direct power)/(total power)

(b) Parameter h_F=(flanking power)/(direct ower)

$$S\alpha = 0{,}16V/T + A\alpha_A = 6{,}25 + 1{,}35 \text{ m}^2 \quad . \tag{3.59}$$

The estimation error for $A\alpha_A/S\alpha = 0{,}18$, obtained from the graph in Fig. 3.6(a), is Le = 0,8 dB.

For most sound insulation tests in practice the error due to sound absorption by the test object is likely to be negligible; sound insulating panels usually have low absorption coefficients. But the problem needs further consideration to assess the risk of absorption error if the intensity method is used to measure the sound reduction indices of flanking walls such as the filler wall containing the test object during the primary test. Equations (3.56) and (3.57) may be applied to any part of the test structure by defining the area under consideration as A and by considering the power radiated by the remainder of the structure surrounding the test area as flanking power. In this context it is necessary to consider the broader meaning of h_F, namely h_F = (power radiated by surrounding structure)/(power radiated by component under test)

The point to be made is that the relatively high level of sound transmission through the test object in the primary test now constitutes a high flanking level which, according to Eq. (3.57), increases the risk of absorption error.

Example 3.3. Consider a test arrangement comprising a 6 mm single-glazed window with a surface area of 2,8 m^2 mounted in a brick filler wall in a test aperture of 10,0 m^2. The sound reduction index of the window is 29 dB at 500 Hz while the mass law predicts an index of 41 dB for the filler wall. The sound absorption coefficient of the plastered, yet unpainted filler wall is estimated at $\alpha = 0{,}03$. The receiving room has a volume of 210 m^3 and a reverberation time of 4,2 s at 500 Hz with the test object installed. The question is whether the sound reduction index of the filler wall can be determined by sound intensimetry in this test arrangement.

The expected estimation error due to sound absorption at the surface of the filler wall is calculated by assuming that the window is respons-

ible for all the flanking power.

From Eq. (2.51) : $h_F = (2,8/7,2)10^{-(29 - 41)/10} = 15,8$

Furthermore, $A\alpha_A/S\alpha = (7,2)(0,03)/\frac{(0,16)(210)}{4,2} = 0,027$

The estimation error predicted by Eq. (3.57) is Le = 2,6 dB. The sound reduction index of the filler wall would be overestimated by 2,6 dB. This example illustrates that a significant absorption error may occur if the sound intensity method is applied to the filler wall, notwithstanding the low values of sound absorption coefficient exhibited by typical filler wall constructions. The minimum amount of absorption $S\alpha$ normalized with respect to the absorption $A\alpha_A$ of the test surface, required to limit the absorption error to Le dB is obtained by solving Eq. (3.57) for $S\alpha/A\alpha_A$. The result is

$$S\alpha/A\alpha_A > (1 + h_F)/(1 - 10^{-Le/10}) \quad . \tag{3.60}$$

In the previous example Le < 1,5 dB would require $S\alpha > 12,4\ m^2$; reverberation time T < 2,7 s.

The effect of sound absorption considered in this section pertains to the result of the sound insulation test; an error is caused in the estimated value of the sound reduction index. This does not imply at all that the measured values of sound intensity are inaccurate or false. Sound transmission analyses by sound intensimetry gives an accurate account of the net energy field constituted by the total assembly of sources and sinks in the test arrangement*.

---

* It is assumed that the fundamental requirements in relation to the microphone spacing and phase matching are observed. The accuracy of sound transmission analysis in reactive fields is considered in Section 3.4.

3.4 SOUND TRANSMISSION ANALYSIS IN REACTIVE FIELDS

3.4.1 The measurement of sound intensity in reactive fields

Sound insulation tests and transmission analysis by intensimetry involve sound intensity measurement near the surface of the test object. If the receiving room is reverberant, the intensity level in this region may be much lower than the pressure level. Accurate measurement of sound intensity under such conditions imposes minimum requirements in regard to the dynamic range and accuracy of the sound intensity meter. Conversely, if optimum use is made of the capabilities of a given sound intensity meter, it is necessary to ensure that conditions at the surface of the test object are within reach of these capabilities. This section examines the relationship between intensity meter limitations and requirements relating to the acoustic properties of the receiving room.

The main purpose of sound intensity measurement is to detect energy flow in reactive fields. A suitable criterion for assessing the performance of practical intensity meters is the common mode rejection index LRm, defined as

$$LRm = LP - LIm \quad dB. \tag{3.61}$$

LIm is the residual intensity level indicated by the intensity meter if the probe is placed in a purely reactive field where the sound pressure level is LP dB. An expression for LRm is obtained by considering the derivation of sound intensity by means of the two-microphone technique. According to Euler's equation the particle velocity u_r in a direction r is related to the sound pressure p by

$$u_r = -\frac{1}{\rho}\int \frac{\partial p}{\partial r}\, dt \tag{3.62}$$

where ρ is the static density of air. Consider a field where the sound pressure at a radian frequency ω is

$$p = P(r)e^{j\,\theta(\omega,r)} \tag{3.63}$$

where P(r) is the rms value of the pressure at a distance r. The particle velocity

$$u_r = -\frac{1}{\rho}\int[P(r)\frac{\partial e^{j\theta(\omega,r)}}{\partial r} + \frac{\partial P(r)}{\partial r}e^{j\theta(\omega,r)}]dt. \qquad (3.64)$$

The result is

$$u_r = -[\frac{P(r)}{k\ \rho c}\frac{\partial\theta(\omega,r)}{\partial r}\ e^{j\theta(\omega,r)} - \frac{j}{k\ \rho c}\frac{\partial P(r)}{\partial r}\ e^{j\theta(\omega,r)}] \qquad (3.65)$$

where $k = \omega/c$ is the wave number and c is the velocity of sound in air. It is clear from Eq. (3.65) that the general expression for the complex sound intensity I will consist of two terms

$$I = pu_r^* = I_A + j\ I_R. \qquad (3.66)$$

The real part I_A, which is the desired active intensity, is given by

$$I_A = Re\{pu_r^*\} = -\frac{P^2(r)}{k\ \rho c}\frac{\partial\theta(\omega,r)}{\partial r}. \qquad (3.67)$$

The imaginary part I_R represents the reactive intensity which does not contribute to the average energy flow.

$$I_R = Im\{pu_r^*\} = \frac{P(r)\ \partial P(r)}{k\ \rho c\ \partial r}. \qquad (3.68)$$

It is observed from Eqs. (3.67) and (3.68) that

(a) there can only be a net active intensity component if the sound pressure has a finite phase gradient; a gradient in pressure amplitude does not contribute to active intensity flow;

(b) a gradient in the pressure amplitude constitutes a reactive component of sound intensity.

The following analysis of the effects of phase mismatch errors pertain to the direct method described in Section 3.2.2. For the purpose of this analysis, the measurement system is divided in two stages as shown

in Fig. 3.7. Stage I comprises the microphones, preamplifiers, filters and signal conditioning circuits leading to the inputs of the difference amplifier. The block diagram in Fig. 3.7 corresponds to the design of the Model A83 SIM analog sound intensity meter used in this investigation. The unconventional order of integration and differentiation gives a considerable improvement in the overall dynamic range of the measurement system in reactive fields [6]. Contrary to standard practice, the octave filters are located in Stage II, retaining only the bandlimiting and noise-rejection filters in Stage I. This configuration is used since it yields a better overall performance in reactive fields than the conventional configuration.

Stage I. If sound intensity is measured with an instrument which derives $\frac{\partial\theta}{\partial r}(\omega,r)$ from the phase difference $\Delta\theta$ between two pressure microphones spaced by a distance Δr, any phase mismatch error ε radians introduced in Stage I of the measurement system would cause an error in the measured intensity [6,67]

$$Le = 10 \log (1 + \varepsilon/\Delta\theta) \quad dB. \tag{3.69}$$

Since the acoustic phase difference $\Delta\theta$ detected by the measurement system is directly proportional to the microphone spacing, $\Delta\theta$ in a reactive field may be expressed as a fraction m of the phase difference $k\Delta r$ in a plane wave,

$$\Delta\theta = mk\Delta r \quad . \tag{3.70}$$

Using this expression,

$$Le = 10 \log (1 + \varepsilon/mk\Delta r) \quad dB. \tag{3.71}$$

At 25 °C and with ε in degrees, the intensity error

$$Le = 10 \log (1 + 0{,}96\ \varepsilon/mf\Delta r) \quad dB. \tag{3.72}$$

Le may therefore be controlled by adjustment of Δr. The microphone

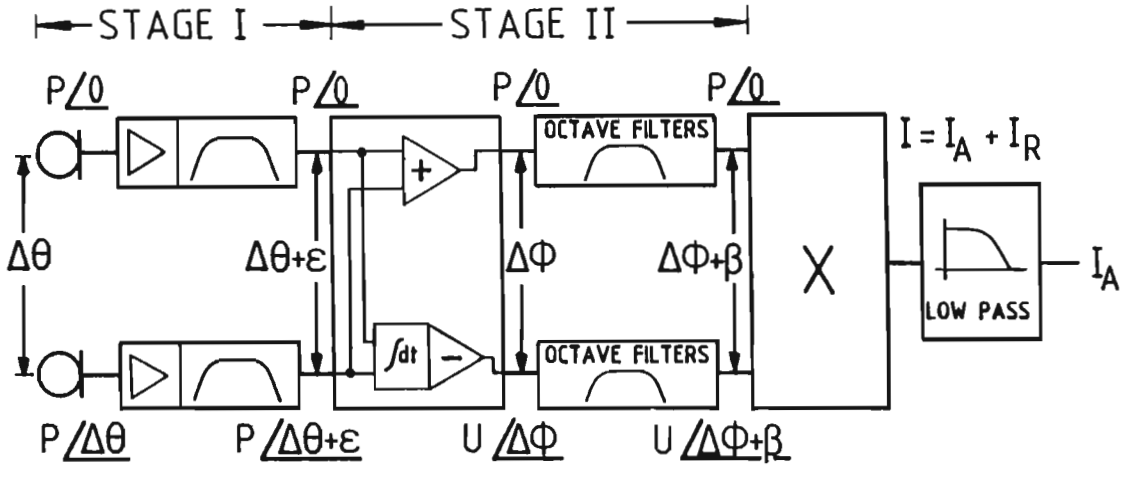

Figure 3.7

Phase mismatch errors in a sound intensity meter.
ε = phase mismatch error in Stage I
β = phase mismatch error in Stage II

spacing required to limit the intensity error in a reactive field to Le dB, obtained by solving Eq. (3.72) for Δr, is

$$\Delta r = (0{,}96\ \varepsilon/mf)/(10^{Le/10} - 1) = \Delta r_0/m \qquad (3.73)$$

where, according to Eq. (3.12), Δr_0 is the spacing required for the same error in a plane wave, with ε in degrees.

Gain mismatch, on the other hand, would not cause any principal errors in the measured intensity since the pressure amplitude gradient only relates to the reactive intensity. Equation (3.65) shows, however, that gain mismatch would directly affect the magnitude of the particle velocity signal. If gain matching is ignored, very large errors may be introduced in the particle velocity channel of the measurement system. Especially in the case of analog instruments this could result in a reduction of the dynamic range and hence also the common mode rejection index of the system.

In a purely reactive field an instrument with a phase error of ε radians would read

$$LIm = 10 \log \left[\frac{P^2(r)\varepsilon}{k\ \rho c \Delta r} / I_o\right] \quad dB. \qquad (3.74)$$

The common mode rejection index defined in Eq. (3.61) becomes

$$LRm = 10 \log \left[P^2(r)/Po^2\right] - 10 \log \left[\frac{P^2(r)\varepsilon}{k\ \rho c \Delta r} / I_o\right] \qquad (3.75)$$

where $Po = 20 \times 10^{-6}$ Pa and $Io = 10^{-12} W/m^2 = Po^2/400$. Assuming $\rho c \approx 400$, Eq. (3.75) reduces to

$$LRm = 10 \log (k\ \Delta r/\varepsilon) \quad dB. \qquad (3.76)$$

At 25 °C and with ε in degrees

$$LRm = 10 \log (1{,}04\ f\Delta r/\varepsilon) \quad dB. \qquad (3.77)$$

LRm may be determined by measuring the sound pressure and the sound in-

tensity levels LP and LIm in a rigidly terminated standing wave tube excited by broadband noise.

Stage II. The effect of phase mismatch on sound intensity meter performance is different for phase errors in Stages I and II in Fig. 3.7. The reason for this is that the phase error ε in Stage I affects the accuracy of the differential of two signals which is a function of the sine of the acoustic phase $\Delta\theta$, while a phase error β in Stage II affects the accuracy of the product of two signals which is a function of the cosine of the angle $\Delta\phi$ between sound pressure and particle velocity.

In terms of the rms sound pressure P and particle velocity U, the low-pass filtered multiplier output corresponding to the active sound intensity is

$$I_A = PV \cos \Delta\phi \quad . \tag{3.78}$$

In a reactive field an instrument with a phase error β in Stage II would indicate

$$LIm = 10 \log \left[PV \cos(\Delta\phi + \beta)/I_0\right] \quad \text{dB}. \tag{3.79}$$

instead of

$$LI = 10 \log \left[(PV \cos \Delta\phi)/I_0\right] \quad \text{dB}. \tag{3.80}$$

The measurement error

$$Le = 10 \log \left[\frac{\cos(\Delta\phi + \beta)}{\cos \Delta\phi}\right] \quad \text{dB}. \tag{3.81}$$

In contrast to the error due to phase mismatch in Stage I (Eq. 3.71)), the error due to phase mismatch in Stage II of the system in Fig. 3.7 depends on neither the frequency nor the microphone spacing Δr.

Hence, by shifting the octave filters from Stage I to Stage II, the major contributor to phase error, excepting the microphones, is removed from the critical input stage and placed in a section where phase mismatch is much less detrimental to overall system performance. This

not only lessens the risk of measurement error but simplifies the design of the filters as well.

The relationship between $\Delta\theta$ and $\Delta\phi$ is obtained by equating the active components of sound intensity given in Eqs. (3.67) and (3.78). For the purpose of the present consideration it is appropriate to use $P(r) = P$ and $\frac{\partial\theta}{\partial r}(\omega,r) = \frac{\Delta\theta}{\Delta r}$. Hence,

$$\frac{P^2\,\Delta\theta}{k\rho c\,\Delta r} = PV\cos\Delta\phi \quad . \tag{3.82}$$

Solving for $\cos\Delta\phi$ and substituting Z = specific acoustic impedance = P/V, gives

$$\cos\Delta\phi = \frac{Z}{\rho c}\,\frac{\Delta\theta}{k\Delta r} \tag{3.83}$$

Using the formulation of $\Delta\theta$ in Eq. (3.70),

$$\cos\Delta\phi = mZ/\rho c \quad . \tag{3.84}$$

The effect on Le of phase mismatch in Stages I and II of the system depicted in Fig. 3.7 may be examined for the type of reactive field prevailing at the surface of the test object by considering a reactive field ($\Delta\phi > 0$) in which $LP \approx LV$ ($Z \approx \rho c$). For the case considered, $\Delta\phi = \cos^{-1}(m)$. The intensity error due to a phase error β in Stage II, given by Eq. (3.81), becomes

$$Le = 10\log\left[\frac{\cos\{\cos^{-1}(m) + \beta\}}{m}\right] \quad dB. \tag{3.85}$$

The corresponding error due to a phase error ε degrees in Stage I is given by Eq. (3.72). Consider the case $\beta = \varepsilon = -1{,}0\,^{\circ}$ for Δr = 50 mm at f = 250 Hz in a reactive field of m = 0,1. Using these values, Eqs. (3.72) and (3.85) yield

Le (Stage I) = -6,3 dB

and Le (Stage II) = 0,7 dB.

The common mode rejection ratio defined in Eq. (3.61) becomes

$$LRm = 10 \log (P^2/P_0^2) - 10 \log [PV \cos(90 + \beta)/I_0] \quad \text{dB.} \quad (3.86)$$

If calibration complies with the set S_0 of Eq. (3.17) and if LP ≃ LV,

$$LRm = 10 \log [1/\cos(90 + \beta)] = - 10 \log \sin \beta \quad \text{dB.} \quad (3.87)$$

For the values used in the previous calculation of Le ($\beta = \varepsilon = -1{,}0\,^\circ$; Δr = 50 mm; f = 250 Hz), the common mode rejection indices given by Eqs. (3.77) and (3.87) for phase mismatch in Stages I and II, respectively, are

LRm (Stage I) = 11,1 dB

and LRm (Stage II) = 17,6 dB.

To attain LRm (Stage I) = 17,6 dB at 250 Hz for Δr = 50 mm, ε must be limited to $\varepsilon < 0{,}23\,^\circ$.

3.4.2 The concept of reactivity [142]

The reactivity in a sound field where the sound pressure and sound intensity levels are LP and LI, respectively, is defined as

$$LR = LP - LI \quad \text{dB.} \quad (3.88)$$

or equivalently,

$$LR = 10 \log \left(\frac{P^2}{P_0^2} \Big/ \frac{I_A}{I_0} \right) \quad \text{dB.} \quad (3.89)$$

A general expression for LR is obtained by substituting Eq. (3.67) into Eq. (3.89), using $\frac{\partial \theta}{\partial r}(\omega, r) = \frac{\Delta \theta}{\Delta r}$ and $\rho c \simeq 400$. The result is

$$LR = 10 \log \left(\frac{p^2}{P_0^2} \Big/ \frac{P^2}{I_0 k \rho c} \frac{\Delta \theta}{\Delta r} \right) = - 10 \log (\Delta \theta / k \Delta r) \quad \text{dB.} \quad (3.90)$$

At 25 °C, with $\Delta\theta$ in degrees,

$$LR = 10 \log (1{,}04\ f\ \Delta r/\Delta\theta) \quad \text{dB}. \tag{3.91}$$

Upon substituting Eq. (3.70) into Eq. (3.90), LR reduces to

$$LR = 10 \log (1/m) \quad \text{dB}. \tag{3.92}$$

Equations (3.84) and (3.92), assuming $Z \simeq \rho c$, yield

$$m = \cos \Delta\phi = 10^{-LR/10} \quad . \tag{3.93}$$

In persuance of the terminology used in electrical engineering, m is concluded to be the power factor of the sound intensity field. Substitution of Eq. (3.93) into Eqs. (3.72) and (3.85) and solving for ε and β, respectively, yield the phase mismatch errors which will cause an error Le dB in a field of reactivity LR dB. Hence,

$$\varepsilon = 1{,}04\ f\ \Delta r\ 10^{-LR/10}\ (10^{Le/10} - 1) \text{ (degrees)} \tag{3.94}$$

and

$$\beta = \cos^{-1}[10^{(Le - LR)/10}] - \cos^{-1}(10^{-LR/10}) \text{ (degrees)} \quad . \tag{3.95}$$

Eq. (3.94) is presented graphically in Fig. 3.8(a) - (f) for Δr = 9, 15, 60, 6, 12 and 50 mm respectively, for an intensity error Le = 2,0 dB. Equation (3.95) is plotted in Fig. 3.9.

3.4.3 Reactivity at the surface of the test object

If the sound power transmitted into the receiving room is determined by sound intensity measurement, it has to be ensured that LRm > LR at the surface of the test object. Of the total amount of acoustic power W radiated into the receiving room, only a fraction h is transmitted directly by the test object. The average direct intensity at the surface of a test object of area A is

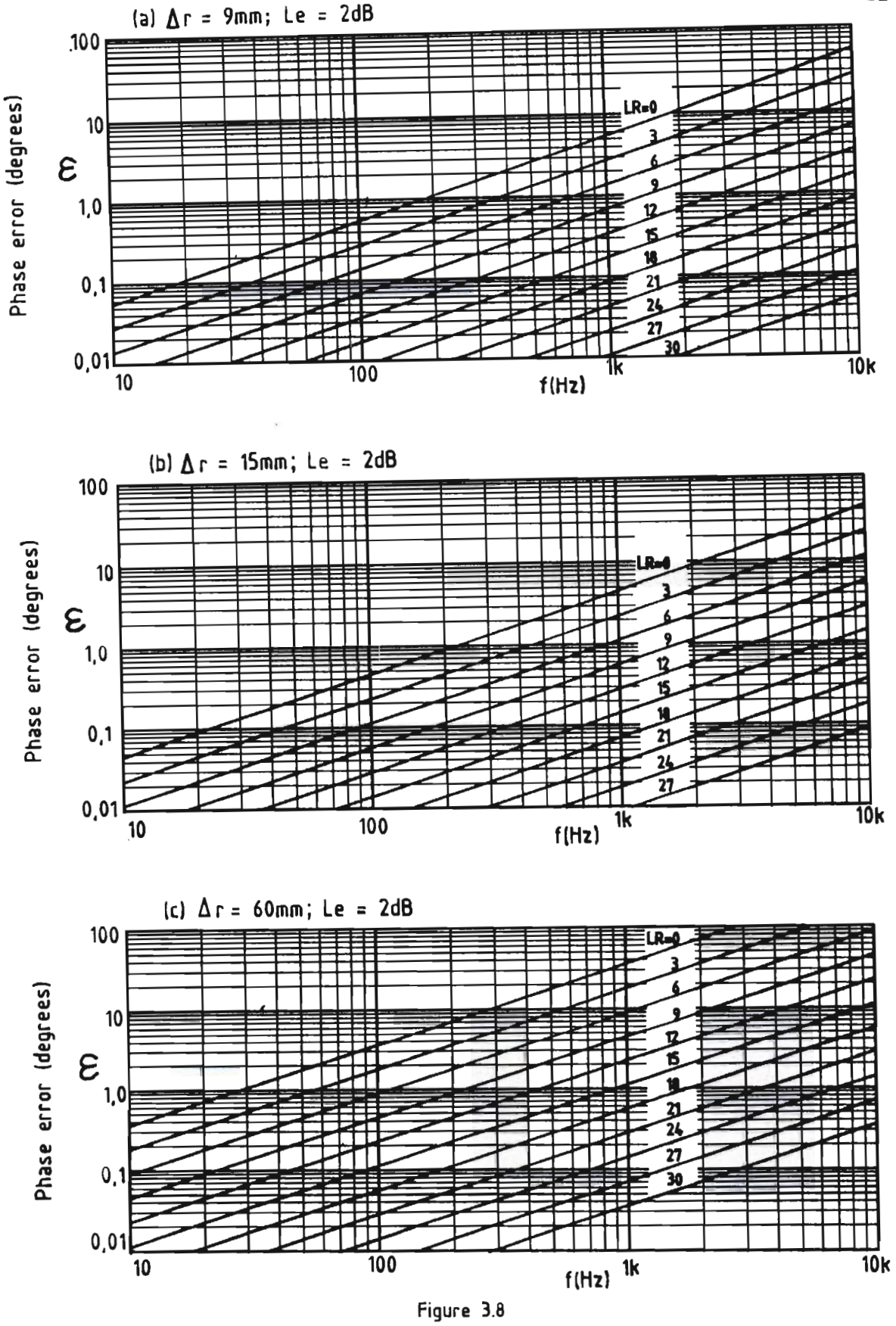

Figure 3.8

Phase match error $\varepsilon°$ in Stage I of the system depicted in figure 3.7 which will result in an intensity measurement error of 2dB for a mic-spacing Δr and a sound field reactivity LR dB.

(a) Δr=9mm (b) Δr=15mm (c) Δr=60mm

(Continued on next page).

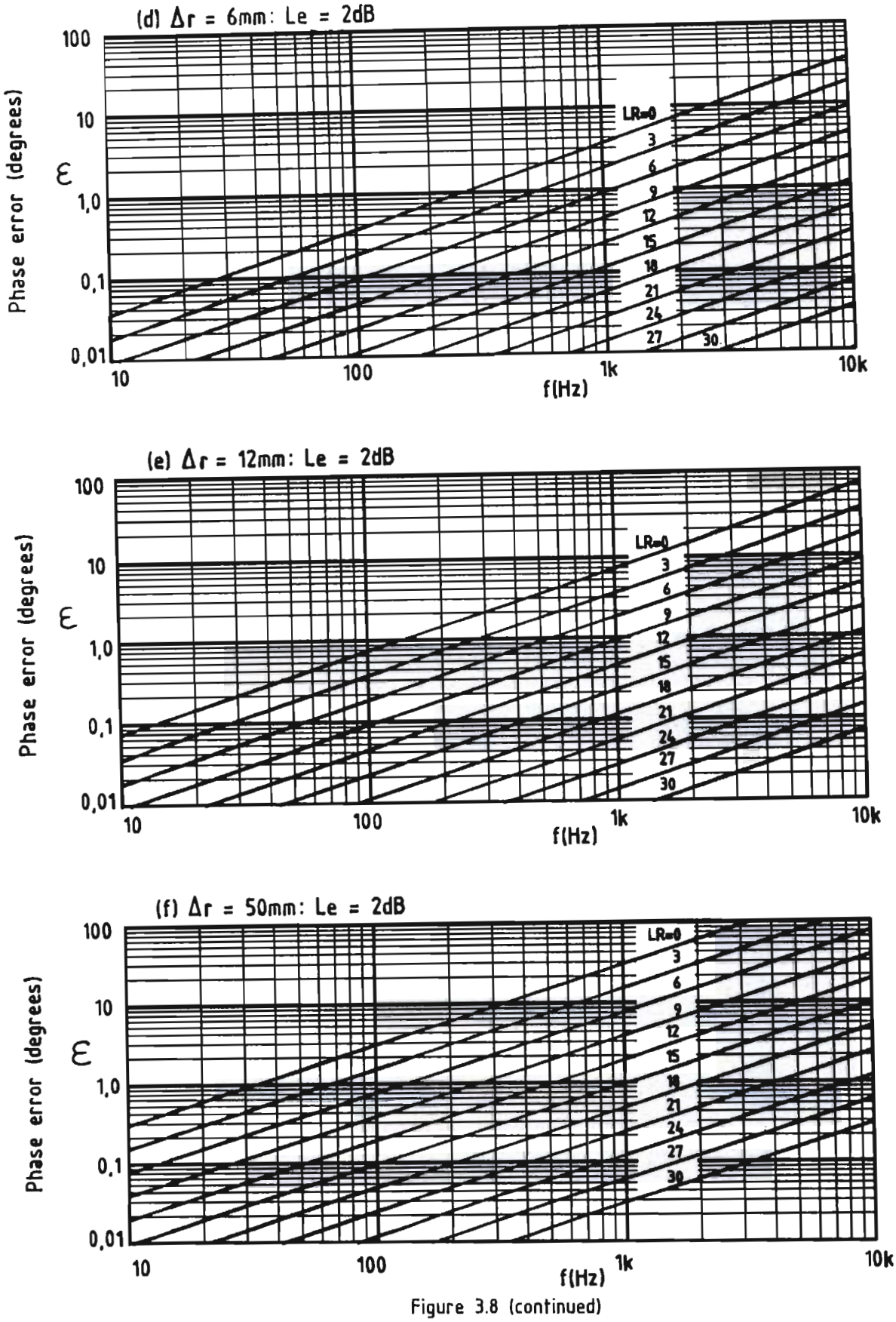

Figure 3.8 (continued)

Phase match error $\varepsilon°$ in Stage I of the system depicted in Figure 3.7 which will result in an intensity measurement error of 2dB for a mic-spacing Δr and a sound field reactivity LR dB.

(d) Δr=6mm (e) Δr=12mm (f) Δr=50mm

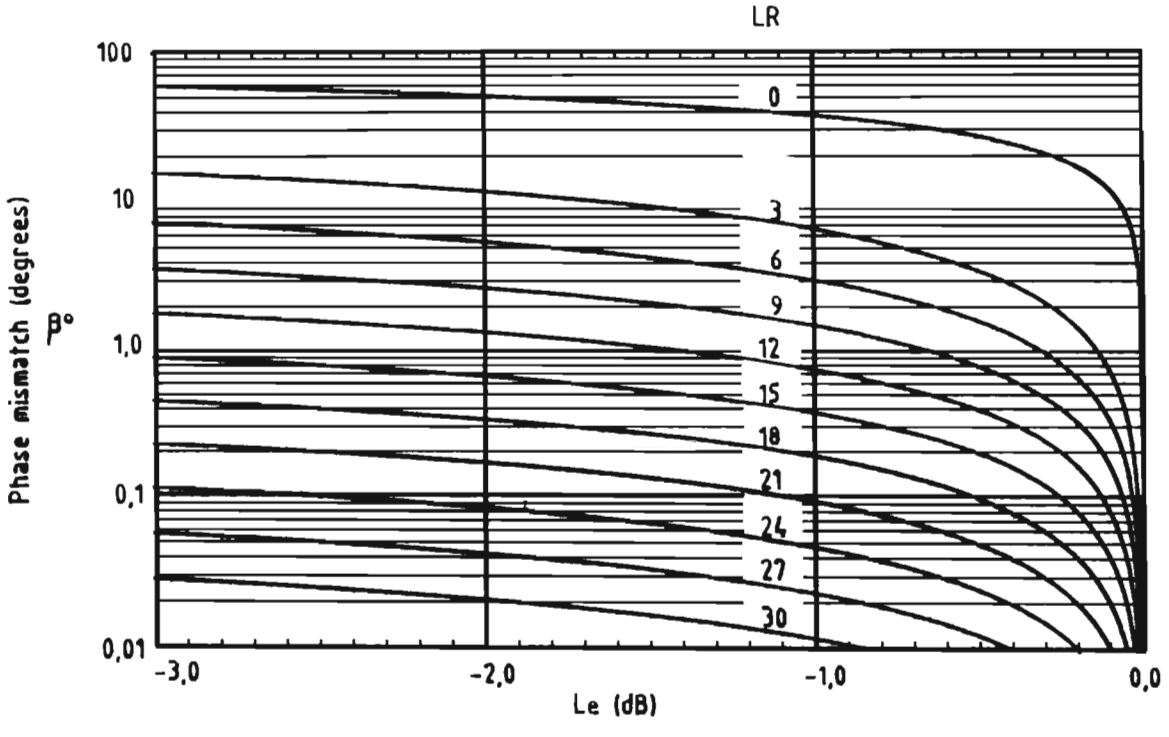

Figure 3.9

Phase match error in Stage II of the system depicted in Figure 3.7 which will result in an intensity measurement error Le dB if the reactivity in the sound field is LR dB.

$$I_D = hW/A. \tag{3.96}$$

The reactivity at the surface is

$$LR = 10 \log \left(\frac{P^2}{\rho c} / I_D\right). \tag{3.97}$$

The total sound pressure at the surface of the test object P results from the direct pressure P_D and the reverberant pressure P_R. In deriving an expression for P_D it will be assumed that plane wave radiation is taking place. This is a reasonable assumption as the sound intensity is measured very close to the relatively large surface of the test object. For plane wave radiation

$$P_D^2 = hW\rho c/A \quad . \tag{3.98}$$

The receiving room, although not necessarily diffuse, is assumed to be reverberant. The reverberant pressure at the centre of the room

$$P_{Ro}^2 = 4W(1 - \alpha)\rho c/S\alpha \tag{3.99}$$

where α is the average sound absorption coefficient of the total internal surface area S of the receiving room. As a result of interference patterns the reverberant pressure at the surface of the test object will exceed that at the centre of the room by 3 dB. Hence, assuming uncorrelated random noise,

$$P^2 = P_D^2 + 2\, P_{Ro}^2. \tag{3.100}$$

If Eqs. (3.98) and (3.99) are substituted into Eq. (3.100) and if it is assumed that $\alpha \ll 1$, the total pressure becomes

$$P^2 = (h/A + 8/S\alpha)W\, \rho c \quad . \tag{3.101}$$

Upon substitution of Eqs. (3.96) and (3.101) into Eq. (3.97), the reactivity at the surface of the test object is found to be

$$LR = 10 \log (1 + 8A/hS\alpha) \quad . \tag{3.102}$$

In terms of the flanking ratio h_F = (flanking power)/(direct power) = (1 - h)/h, and using the approximation: room constant $R_\alpha \simeq S\alpha$,

$$LR = 10 \log \left[1 + 8 (h_F + 1)A/S\alpha\right] \quad dB. \tag{3.103}$$

This relationship is plotted in Fig. 3.10. By examination of Eqs. (3.70), (3.92) and (3.103) it is concluded that the power factor of the intensity field at the surface of the test object is given by

$$m = \frac{\Delta\theta}{k\Delta r} = 1/\left[1 + 8(h_F + 1)\frac{A}{S\alpha}\right] \quad . \tag{3.104}$$

3.4.4 Minimum requirements for sound transmission analysis in reactive fields

Consider the control of sound intensity error in a reactive field. If the error is not to exceed a specified value Lem dB, then

$$10 \log \left[1 \pm 10^{(LR - LRm)/10}\right] < \left|Lem\right| \tag{3.105}$$

where Lem > 0 if ε adds to the acoustic phase $\Delta\theta$ and Lem < 0 if ε subtracts from $\Delta\theta$. The condition in Eq. (3.105) will be met if the common mode rejection index of the measurement system exceeds the reactivity at the measurement point by at least ΔL dB:

$$LRm - LR > \Delta L \quad dB. \tag{3.106}$$

Eqs. (3.105) and (3.106) yield

$$\Delta L > - 10 \log (10^{Lem/10} - 1); \quad Lem > 0 \tag{3.107}$$

and $$\Delta L > - 10 \log (1 - 10^{Lem/10}); \quad Lem < 0. \tag{3.108}$$

Equation (3.108) gives the more unfavourable result of the previous two equations for numerically equal values of Lem. When performing sound transmission analysis it is important to check whether the condition

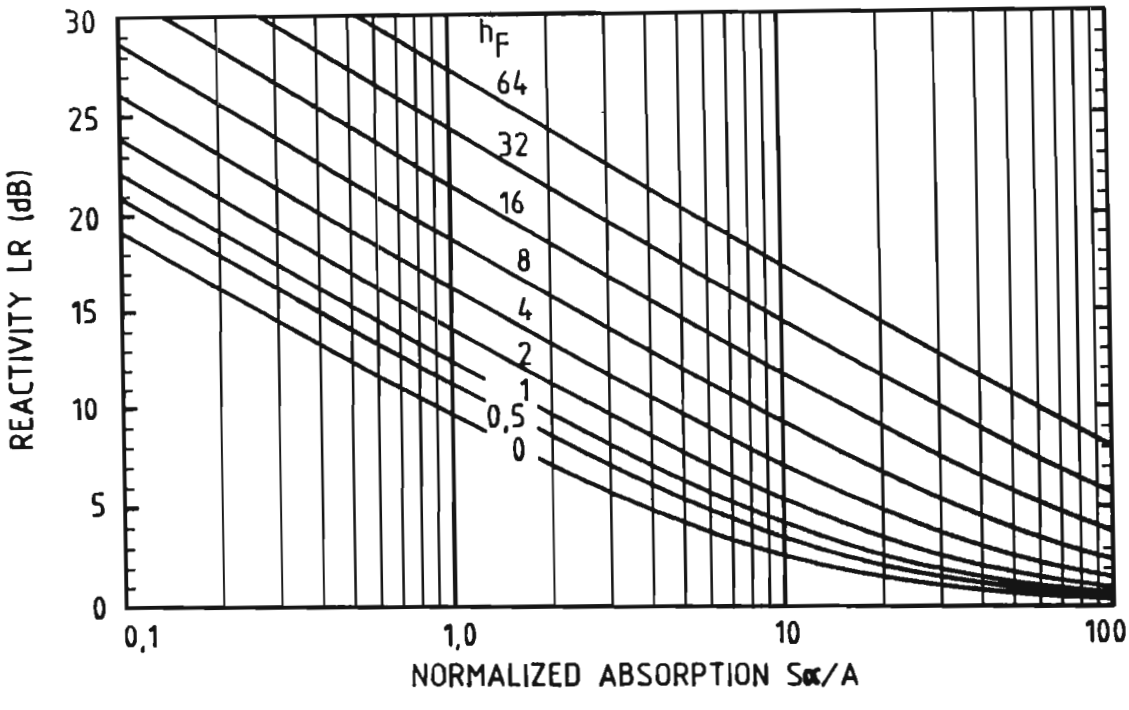

Figure 3,10

Reactivity at the surface of a test object in a receiving room containing $S\alpha$ m^2 sound absorption.

A = surface area of test object

h_F = (flanking power)/(direct power)

stated in Eq. (3.106) is true at the surface of the test object. If necessary, LRm may be increased by using a larger spacing Δr, or LR may be reduced by adding sound absorption to the receiving room. The minimum value required for Δr, using the former approach, is obtained by substituting Eqs. (3.76) and (3.103) into Eq. (3.106). At 25 °C, with ε in degrees

$$\Delta r > \left(\frac{0.96\varepsilon 10^{\Delta L/10}}{f}\right)[1 + 8\,(h_F + 1)A/S\alpha] \quad . \tag{3.109}$$

If it is decided to reduce LR in order to meet the requirement in Eq. (3.106), a minimum number of absorption units $S\alpha$ will be required in the receiving room. Substitution of Eq. (3.103) into Eq. (3.106) and solving for $S\alpha/A$ gives

$$S\alpha/A > 8(h_F + 1)/(10^{LR/10} - 1) = 8(h_F + 1)/(10^{(LRm - \Delta L)/10} - 1). \tag{3.110}$$

The minimum number of absorption units normalized with respect to the surface of the test object is plotted in Fig. 3.11 as a function of the intended reactivity LR = LRm - ΔL. At 25 °C, with ε in degrees

$$S\alpha/A > 8\,(h_F + 1)/\left(\frac{1{,}04\ f\Delta r}{\varepsilon}\ 10^{-\Delta L/10} - 1\right) \quad . \tag{3.111}$$

Example 3.4. Consider a sound insulation test performed on a door ($A = 2m^2$) contained in a filler wall with a surface area $A_F = 6m^2$. The wall is known to have a sound reduction index R_F of 34 dB at 125 Hz and 41 dB at 500 Hz, while the door is expected to yield approximate sound reduction indices R of respectively 33 and 36 dB. The power transmitted into a reverberation room of volume 210 m^3 is to be determined with a sound intensity meter which has phase mismatch errors of 0,10 and 0,25 degrees at 125 Hz and 500 Hz, respectively. A maximum error of 2,0 dB is allowed. The question is whether a microphone spacing of 12 mm could be used in this application if the receiving room has reverberation times of approximately 7,0 s. Analysis of the problem leads to the result summarized in Table 3.1.

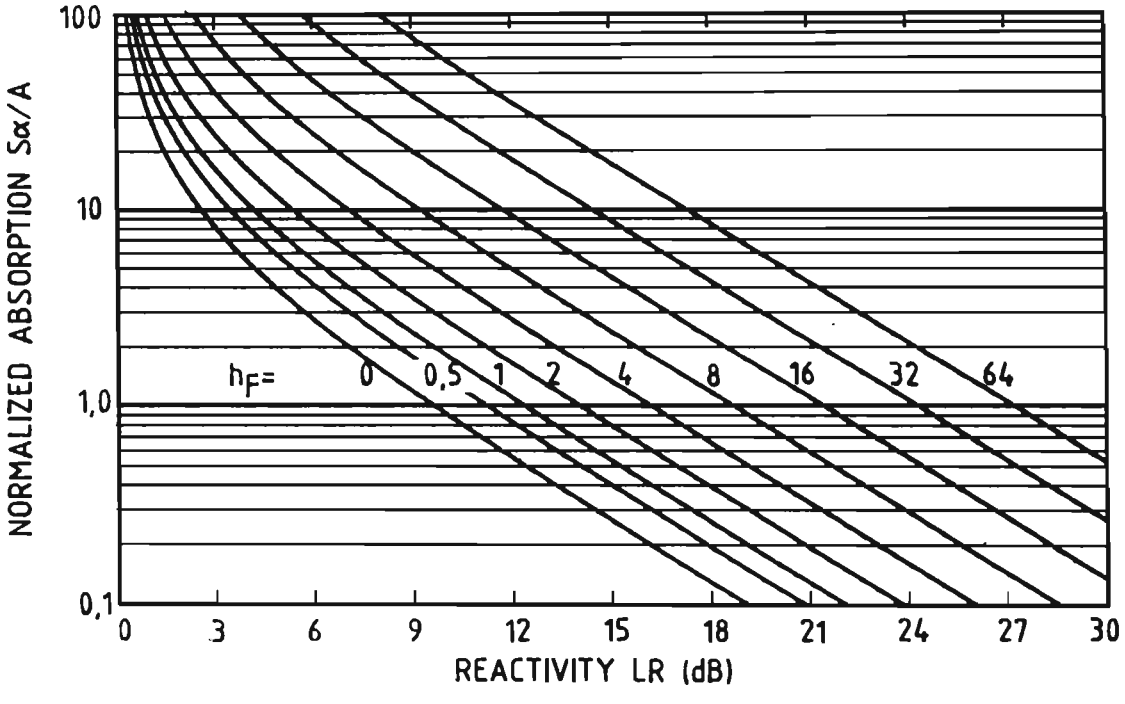

Figure 3.11

Number of absorption units (normalized with respect to surface area of test object A) required in receiving room to maintain a reactivity LR at the surface of the test object. A safety margin LR = LRm - ΔL should be maintained to limit the intensity error to Lem dB. ΔL is calculated from Eqs. (3.107) and (3.108).

h_F = (flanking power)/(direct power)

Table 3.1

Analysis of the problem in Example 3.4

A_F = 6,0 m^2; A = 2,0 m^2; V = 210 m^3; T = 7,0 s; Lem = 2,0 dB; ΔL = 4,3 dB.						
Frequency (Hz)			125		500	
Sound reduction:	Flanking wall R_F		34		41	
	door R		33		36	
Flanking ratio	h_F	Eq. (2.51)	2,4		1,0	
Predicted reactivity	LR	Eq. (3.103)	10,9		8,8	
Microphone spacing	Δr		12 mm	50 mm	12 mm	50 mm
Intensity meter	LRm	Eq. (3.76)	11,9	18,1	14,0	20,2
Minimum absorption	$S\alpha$	Eq. (3.110)	11,3	2,3	3,8	0,8
Maximum reverberation time	T		3,0	14,4	8,9	40,6

The flanking ratio, assuming that the filler wall is the predominating radiator of flanking power, is given by Eq. (2.51).

It is clear that a microphone spacing Δr = 12 mm would be insufficient at 125 Hz, unless the amount of absorption in the reverberation room is increased. Obviously, it would be more sensible to use a larger microphone spacing, leaving the room as it is. By using Δr = 50 mm the absorption requirement is relaxed to $S\alpha > 2,3\ m^2$ ($T < 14,4$ s) at 125 Hz and $S\alpha > 0,8\ m^2$ ($T < 40,6$ s) at 500 Hz, respectively.

3.4.5 Sound transmission analysis at flanking surfaces

The criteria which have been developed here could just as well be applied to the measurement of flanking transmission. The only difference is that the flanking surface would then be regarded as the test object and vice versa as shown in Fig. 3.12.

Example 3.5. Consider the feasibility of sound transmission analysis by sound intensimetry applied to the flanking wall in the sound insulation test described in Example 3.4. Analysis of the problem leads to the result summarized in Table 3.2.

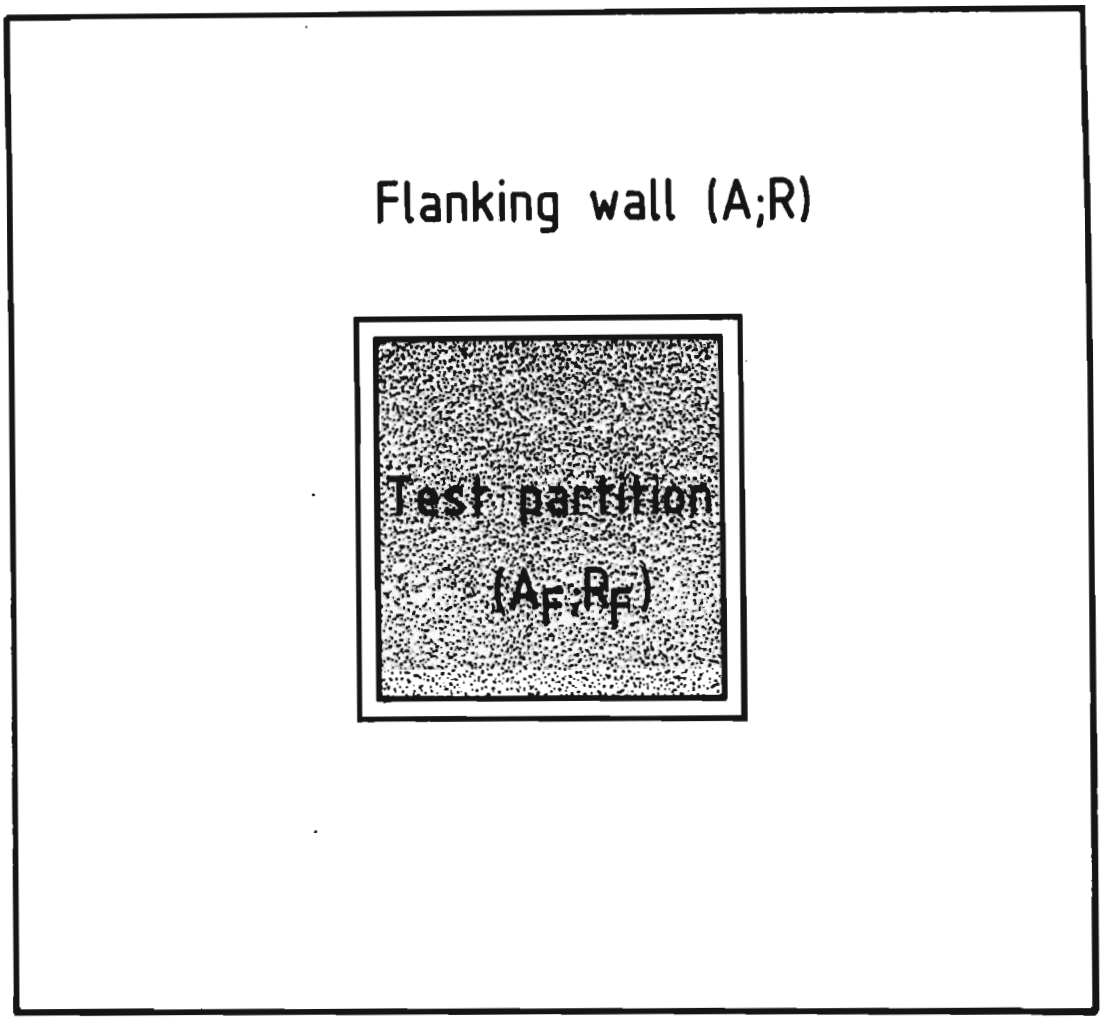

Figure 3.12

Designation of A, A_F, R and R_F for sound transmission analysis at flanking surfaces.

Table 3.2

Analysis of the problem in Example 3.5

A_F = 2,0 m^2; A = 6,0 m^2; V = 210 m^3; T = 7,0 s; Lem = 2,0 dB; ΔL = 4,3 dB.						
Frequency (Hz)			125		500	
Sound reduction:	Filler wall R door R_F		34 33		41 36	
Flanking ratio Predicted reactivity	h_F LR	Eq. (2.51) Eq. (3.103)	0,4 11,8		1,1 13,3	
Microphone spacing	Δr		12 mm	50 mm	12 mm	50 mm
Intensity meter Minimum absorption Maximum reverberation time	LRm Sα T	Eq. (3.76) Eq. (3.110)	11,9 14,2 2,4	18,1 2,9 11,4	14,0 11,9 2,8	20,2 2,6 12,8

For the room as given, a microphone spacing Δr = 12 mm would be inadequate at 125 Hz as well as 500 Hz. By using Δr = 50 mm, it would not be necessary to add absorption to the receiving room in order to perform sound transmission analysis on the filler wall.

It should be emphasized that this thesis is primarily concerned with sound transmission analysis in **reactive fields,** hence the consistent use of the approximation $R_\alpha \approx S\alpha$. For situations where the receiving room has an average boundary absorption coefficient $\alpha > 0{,}2$, $S\alpha$ should be replaced by R_α in the equations derived in this Chapter.

3.4.6 Estimation of the total amount of flanking power transmitted into the receiving room by sound transmission analysis

For most sound insulation tests the flanking power transmitted by the permanent structure of the test facility may be assumed negligible compared to the direct power transmitted by the test object and the flanking power transmitted by the filler wall. The situation is different, however, if high-performance sound insulating elements are tested. Although this poses no problem to the sound intensity method, it may be

of interest to know the total amount of flanking power, especially if comparative tests are conducted by the intensity method and the classic two-room method.

The total amount of flanking power radiated into the receiving room may be determined by selective determination and by addition of the sound powers radiated by each of the flanking elements constituting the total flanking surface. In most cases this would require a large number of measurements. A much simpler method may be derived by taking cognizance of the relationship between the reactivity at the surface of the test object LR and the flanking factor h_F as formulated in Eq. (3.103). If the test object is mounted in a filler wall, it may be presumed as in the examples considered in the preceeding sections, that the filler wall is responsible for practically all the flanking power transmitted into the receiving room. Strictly speaking, however, the flanking power implied in the definition of h_F in Eqs. (2.50) and (2.51), and in subsequent formulae containing h_F, is the total power radiated by all flanking surfaces. Solving Eq. (3.103) for h_F yields the ratio (flanking power)/(direct power),

$$h_F = \frac{S\alpha}{8A}(10^{LR/10} - 1) - 1 \quad . \tag{3.112}$$

The ratio h = (direct power)/(total power), obtained by substituting Eq. (3.112) into Eq. (2.52), is

$$h = \frac{8A}{S\alpha} /(10^{LR/10} - 1) \quad . \tag{3.113}$$

It is concluded that an estimate of h_F or h may be obtained by measuring LR at the surface of the test object as well as the reverberation times of the receiving room. Equations (3.112) and (3.113) are depicted graphically in Figs. 3.13(a) and (b), respectively.

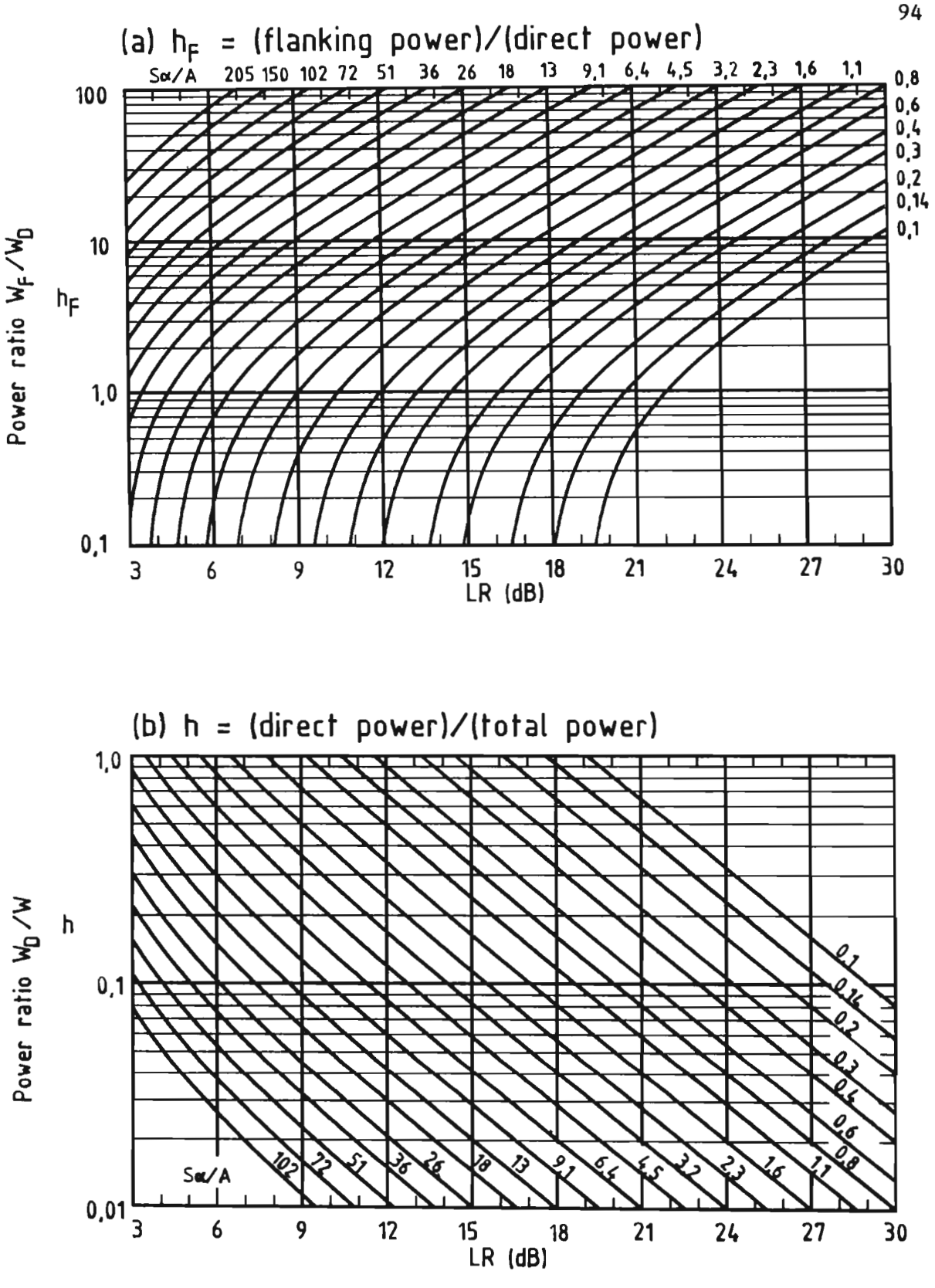

Figure 3.13

Assessment of flanking conditions by measurement of the reactivity LR at the surface of the test object
Sα = the total absorption in receiving room; A = area of test object.
(a) h_F = (flanking power)/(direct power)
(b) h = (direct power)/(total ppwer)

3.5 DIFFUSION

3.5.1 Sound pressure and sound intensity in diffuse fields

Consider a simple sound source which radiates continuous broadband random noise into a room which has the following properties:

1. The room is large and irregularly shaped so that the number of normal modes is practically infinite.
2. The inner surface of the room is homogeneous with respect to sound absorption and the absorption coefficient is small but finite.

It is clear that the total sound field is constituted by the simultaneous presence of the direct and reverberant fields. The direct field results from an undisturbed, continuous flow of sound energy from the source towards the boundaries. (A boundary is any surface at which acoustic energy is reflected and may for instance be a diffuser.) The reverberant field is constituted by that part of the radiated energy which is continuously traversing the space between boundaries. This results in a constant average amount of stored or reverberant energy which, at any point inside the room, appears to be dispersing radially in all directions.

The total mean-squared pressure in the farfield of the source is given by the sum of the direct and the reverberant pressure fields. Thus

$$P^2 = W\rho c/4\pi r^2 + [4W\rho c(1 - \alpha)]/S\alpha] \quad , \tag{3.114}$$

where r is the radial distance from the source, which has a sound power output W. The direct intensity is

$$I_D = W/4\pi r^2 \quad . \tag{3.115}$$

In a large irregularly shaped room, assuming homogeneous boundary absorption, the rate at which reverberant energy arrives at any internal point will be the same from all directions; there can be no net flow

of reverberant energy through such a point. By closed surface integration of the incident reverberant intensity vector $\overline{I}_r$,

$$I_r = (1/A) \iint_A \overline{I}_r \cdot \overline{dA} = 0 \quad , \tag{3.116}$$

and the total net sound intensity I_n at any internal point

$$I_n = W/4\pi r^2 \quad . \tag{3.117}$$

3.5.2 Descriptive model of the sound intensity field in reverberant rooms

Consider the sound field in the vicinity of a simple source when placed in various acoustic environments, ranging from a free field on the one extreme to a diffuse room on the other. In a free field the mean-squared pressure, as well as the intensity, will vary in accordance with the inverse square law as shown in Fig. 3.14(a). If reflecting surfaces are added, departure from the free-field behaviour will be observed and the sound intensity is expected to behave differently from the sound pressure due to the following considerations:

1. Since energy density is a measure of the total energy per unit volume, regardless of the directions in which reflected waves are travelling, an increase of reflected energy will result in an increase of the mean-squared pressure.

2. Sound intensity on the other hand, is a vector quantity and the net intensity is determined by the magnitudes, as well as the directions of the incident energies. Since reflections will in some regions add to and in other regions subtract from the inverse square law characteristic of the direct field, the sound intensity in a semi-reverberant field is expected to fluctuate around the free-field curve as shown in Fig. 3.14(b).

If the reflectivity of the environment is progressively increased, the sound pressure will increase and tend to become independent of dis-

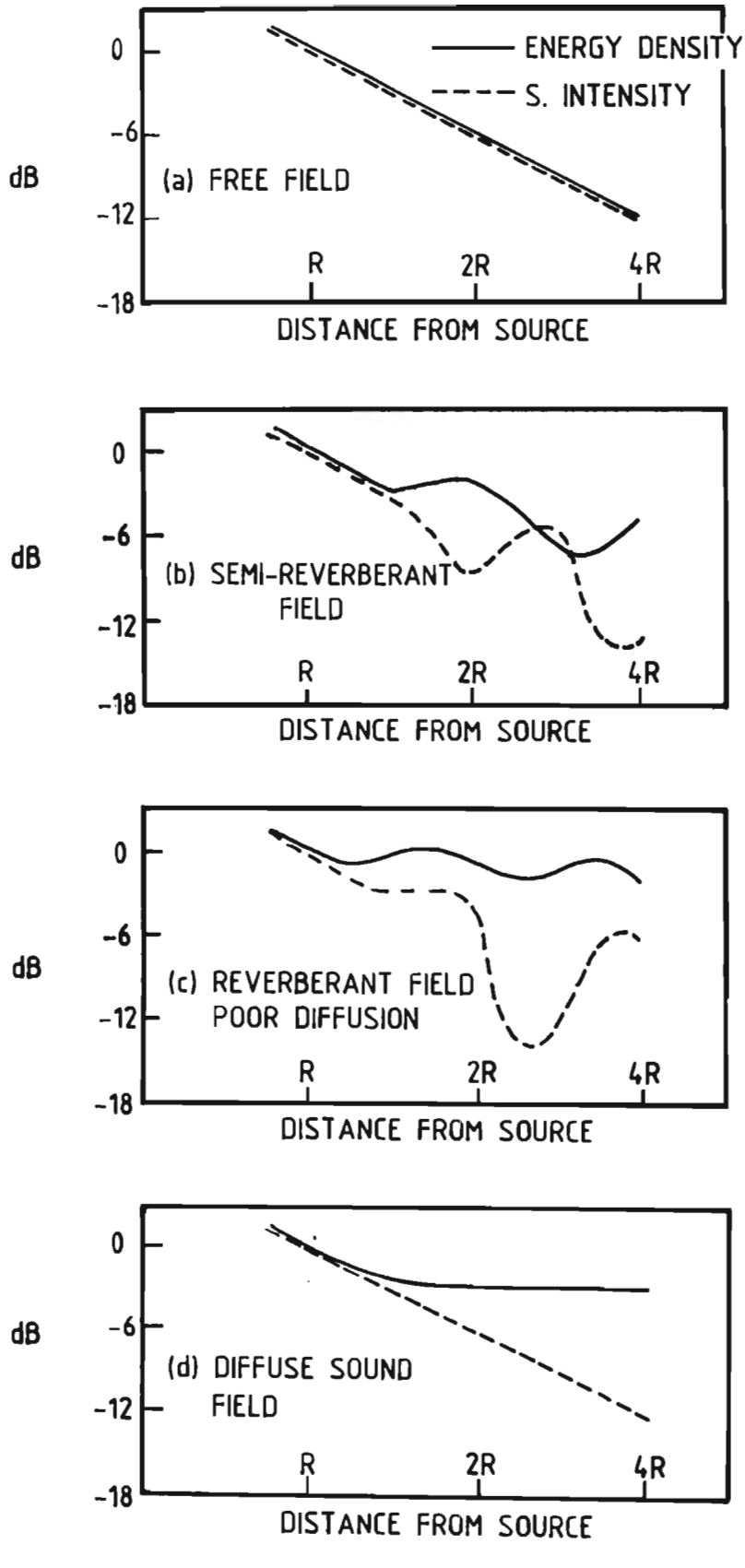

Figure 3.14

General properties of the sound intensity and energy density fields in the farfield of a simple source located in different acoustic environments.

tance. The sound intensity will oscillate around the inverse square law curve because of specular reflection or uneven scattering taking place at the boundaries as depicted in Fig. 3.14(c). A special case arises if, in addition to providing for a high degree of reflectivity, care is also taken to ensure that all directions of sound propagation are equally probable, namely, that the net sound intensity will again take on the free-field inverse square law characteristic as shown in Fig. 3.14(d). This condition is achieved in a reverberation room conforming to the classic room model in that the reverberant part of the sound field is directionally diffuse.

Since the reverberant part of the total sound field does not contribute to the net acoustic energy flow in the room, it becomes "translucent" to the sound intensity meter which only observes the net energy flow due to the direct field. It is concluded that the total net sound intensity field in the vicinity of a source in a diffuse room is identical to that in a free field.

3.5.3 Formulation of diffusivity in terms of sound intensity

The net sound intensity at a point in a room could serve as an indicator of the state of directional diffusion at that point; for perfect directional diffusion the incident intensities would balance out to give zero net intensity flow through the point. A lack of directional diffusion is manifested as an imbalance in the directional distribution of the incident intensity, which can be detected by sound intensity measurement. The difference between the reverberant sound pressure level LP and the net sound intensity level LI, defined by Eq. (3.88) as the reactivity LR, would depend upon the energy balance and could therefore serve as a measure of the degree of directional diffusivity.

The formulation of a criterion by which the degree of directional diffusivity can be expressed as a percentage deserves some consideration. In developing such a criterion, the following must be borne in mind:

1. There is no absolute definition of the degree of directional diffusivity.

2. There is no direct correspondence between the net sound intensity and the quantity measured by the directivity method of Thiele and Meyer discussed in Section 2.6.1. The parameter I' implied in Eq. (2.39) is the incident intensity, whereas a sound intensity meter measures the net result of all components present. Moreover, the quantity measured with a highly directional microphone is not unconditionally equivalent to the real incident intensity. The microphone is essentially sensitive to pressure rather than intensity. It is therefore impossible to attain perfect conformity between the sound intensity method derived here and the directivity method. Notwithstanding this, the formulation of the intensity method will be aimed at attaining maximum agreement between the two methods.
3. Since the correlation method discussed in Section 2.6.2 gives a qualitative assessment of the state of diffusion in a sound field, it cannot be compared directly to either of the aforementioned methods. The three methods are based on different principles altogether.

The degree of directional diffusivity d may be defined in terms of the reactivity LR by

$$d = (1 - f\{ LR \}) \times 100\ \% \quad . \tag{3.118}$$

In order to arrive at a suitable formulation of $f\{ LR \}$ it is expedient to consider the cases for which conformity between the sound intensity method and the directivity method is desirable. These cases are

(1) A plane wave in a free-field.
(2) Diffuse incidence on a perfect absorbing plane (open window).
(3) A perfectly diffuse field.

The results obtained by the directivity method depend upon the directional characteristics of the microphone. In the following examination of the directivity method the microphone is assumed to have a pencil-beam directivity

$$\left\{ \begin{array}{l} H(\gamma) = 1 \; ; \; \gamma = 0 \\ H(\gamma) = 0 \; ; \; \gamma \neq 0 \end{array} \right\} \quad , \tag{3.119}$$

where γ is the angle of incidence with respect to the direction of maximum microphone sensitivity.

(a) General case. Consider the result of the directivity method in the general case depicted in Fig. 3.15(a). The distribution of the incident intensity I' is uniform and confined to the solid angle $\Omega = \Omega_0$ sr,

$$\left\{ \begin{array}{l} I' = I \; ; \; \Omega = \Omega_0 \\ I' = 0 \; ; \; \Omega \neq \Omega_0 \end{array} \right\} \quad . \tag{3.120}$$

The average incident intensity in the solid angle $\Omega = 4\pi$ sr is

$$\langle I' \rangle_{4\pi} = \frac{\Omega_0}{4\pi} I \quad . \tag{3.121}$$

By Eq. (2.39) the average absolute deviation of the incident intensity from $\langle I' \rangle_{4\pi}$ is

$$M = (4\pi / I \; \Omega_0)(1/4\pi)\left[\Omega_0 \left| I - \frac{I \; \Omega_0}{4\pi} \right| + (4\pi - \Omega_0) \left| (0) - \frac{I \; \Omega_0}{4\pi} \right| \right] . \tag{3.122}$$

Upon simplification,

$$M = 2\left[1 - \frac{\Omega_0}{4\pi}\right] \quad . \tag{3.123}$$

The normalization factor M_0 is obtained by letting $\Omega_0 \to 0$ in Eq. (3.123). Hence, $M_0 = 2$. The general expression for the degree of directional diffusion, defined in Eq. (2.38), becomes

$$d = 100\left(1 - 2\left[1 - \frac{\Omega_0}{4\pi}\right]/2\right) = 100\left(\frac{\Omega_0}{4\pi}\right) \% \quad . \tag{3.124}$$

(b) Plane wave in a free field. This case, depicted in Fig. 3.15(b), occurs if $\Omega_0 \to 0$ in Eqs. (3.121) - (3.124). The result is

$$\left\{ \langle I' \rangle_{4\pi} = 0 \; ; \; M = M_0 = 2 \; ; \; d = 0 \; \%. \right\} \quad . \tag{3.125}$$

(c) Uniform distribution at an open window. This case, depicted in Fig. 3.15(c), occurs if $\Omega_0 = 2\pi$ in Eqs. (3.121) - (3.124). The result is

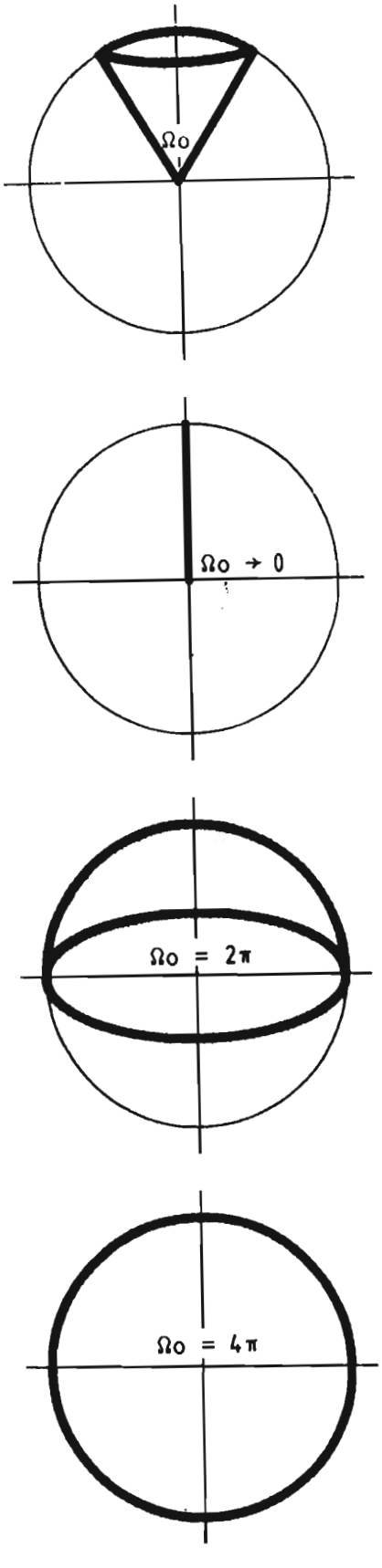

(a) General case

$\langle I' \rangle_{4\pi} = (\Omega_0/4\pi)I$

$M = 2\left[1 - \frac{\Omega_0}{4\pi}\right]$

$d = 100\left(\frac{\Omega_0}{4\pi}\right)$ %

(b) Plane wave; free field

$\langle I' \rangle_{4\pi} \rightarrow 0$

$M_0 = 2$

$d = 0$ %

(c) Uniform distribution; open window

$\langle I' \rangle_{4\pi} = I/2$

$M = 1$

$d = 50$ %

(d) Uniform distribution: no absorption

$\langle I' \rangle_{4\pi} = I$

$M = 0$

$d = 100$ %

Figure 3,15

Assessment of diffusivity by the directivity method

$$\{ \langle I' \rangle_{4\pi} = I/2 \; ; \; M = 1 \; ; \; d = 50 \; \% \} \quad . \tag{3.126}$$

(d) **Uniform distribution; no absorption.** This case, depicted in Fig. 3.15(d), occurs if $\Omega_0 = 4\pi$ in Eqs. (3.121) - (3.124). The result is

$$\{ \langle I' \rangle_{4\pi} = I \; ; \; M = 0 \; ; \; d = 100\% \} \quad . \tag{3.127}$$

If the degree of directional diffusivity for the intensity method is defined as

$$d = 100(1 - 10^{-LR/20}) \quad \% \quad , \tag{3.128}$$

the following result is obtained:

Plane wave in a free field: $\{ LR = 0 \text{ dB}; \; d = 0 \; \% \}$. (3.129)

Uniform distribution at open window: $\{ LR = 6 \text{ dB}; \; d = 50 \; \% \}$. (3.130)

Uniform distribution; no absorption: $\{LR = -\infty \text{ dB}; \; d = 100 \; \%\}$ (3.131)

It is therefore suggested that either of the following measures be employed in the assessment of the degree of directional diffusivity:

(1) Assessment of directional diffusivity in terms of the intrinsic reactivity of the sound field

$$LRd = LP - LId \quad \text{dB} \tag{3.132}$$

at the point under consideration when the room is expected to be diffuse. LRd is determined by measuring the pressure level LP and the intrinsic intensity level LId with the room excited with a random noise source in the absence of any direct field, such as transmitted by the test object during the sound transmission test. The residual intensity level may be determined by searching for the maximum intensity level LId in a solid angle $\Omega = 4\pi$, or by measuring the components of sound intensity LId_x, LId_y and LId_z along mutually perpendicular x, y and z coordinates. The total intensity level is given by

$$LId = 5 \log (10^{LId_x/5} + 10^{LId_y/5} + 10^{LId_z/5}) \quad dB. \qquad (3.133)$$

(2) The percentage directional diffusivity d defined as

$$d = 100(1 - 10^{-LRd/20}) \ \% \quad . \qquad (3.134)$$

Equation (3.134) is plotted in Fig. 3.16.

3.5.4 The effect of a lack of directional diffusion on the accuracy of sound transmission analysis in reactive fields

Consider the intensity error due to a lack of directional diffusion in the type of sound fields encountered in sound transmission analysis. The reactivity in a particular field

$$LR = LP - LI \quad dB \qquad (3.135)$$

where the intensity level LI represents the flow of sound energy constituted by the sound transmission process being investigated. If the field has an intrinsic reactivity LRd dB, an error component will be added to LI. The measured intensity would become

$$LIm = 10 \log \left[10^{(LP - LR)/10} + 10^{(LP - LRd - \Delta LP)/10} \right] \quad dB. \qquad (3.136)$$

where $\Delta LP = LP - LPr$ is the difference between the total pressure level LP in the field and the reverberant pressure level LPr. (Note that $LId = LPr - LRd$). Equation (3.136) may also be written as

$$LIm = LI + 10 \log \left[1 + 10^{(LR - LRd - \Delta LP)/10} \right] \quad dB. \qquad (3.137)$$

Equations (3.136) and (3.137) are based on the worst-case assumption that LId and LI have the same direction. The intensity error

$$Le = 10 \log \left[1 + 10^{(LR - LRd - \Delta LP)/10} \right] \quad dB. \qquad (3.138)$$

If a maximum error Le dB is allowed, the minimum requirements for directional diffusion are obtained by solving Eq. (3.138) for LRd, giving

$$LRd = LR - \Delta LP + 10 \log \left[1/(10^{Le/10} - 1) \right] \quad dB. \qquad (3.139)$$

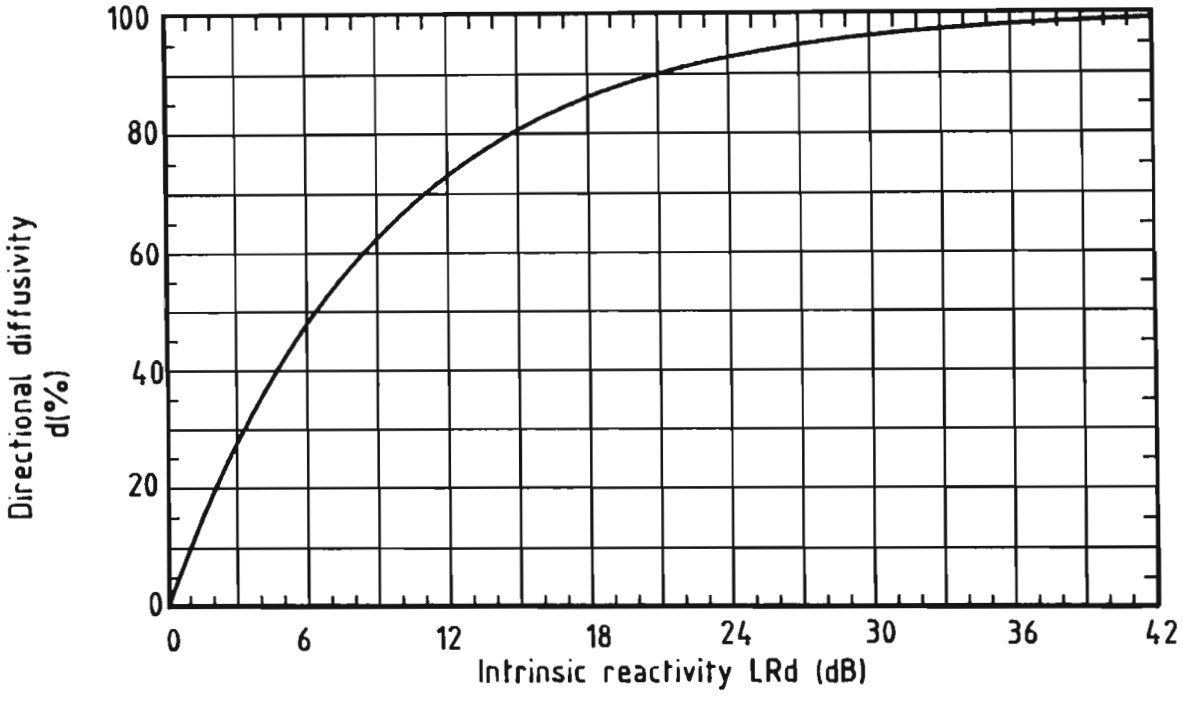

Figure 3.16

Degree of directional diffusivity as a function of the intrinsic reactivity LRd in a sound field.

And, by substituting Eq. (3.139) into Eq. (3.134)

$$d = 100\left[1 - (10^{-\{LR - \Delta LP\}/20})(10^{Le/10} - 1)^{0,5}\right] \quad \% \quad . \qquad (3.140)$$

Consider the diffusivity requirements in the source and receiving rooms for sound transmission analysis by sound intensimetry.

(a) Diffusivity in the source room. Determination of sound reduction indices by sound intensimetry requires a diffuse field in the source room. The average intensity incident on the surface of the test object from the reverberant field

$$LI = LP - 6 \qquad dB. \qquad (3.141)$$

The incident portion of the diffuse field has a reactivity LR = 6 dB. Inasmuch as the direct intensity flux absorbed by the test object is comparatively small in relation to LI, the difference ΔLP in the source room may be disregarded. The minimum requirements for directional diffusivity in the source room are therefore given by

$$LRd > 6 + 10 \log \left[1/(10^{Le/10} - 1)\right] \qquad (3.142)$$

and

$$d > 100\left[1 - 0,5(10^{Le/10} - 1)^{0,5}\right] \% \quad . \qquad (3.143)$$

For a maximum error Le ≤ 1,0 dB, Eqs. (3.142) and (3.143) yield

$$\{\ Lrd > 12\ dB\ ;\ d > 75\ \%\ \} \quad . \qquad (3.144)$$

(b) Diffusivity requirements in the receiving room. First, consider the difference ΔLP = LP - LPr at the surface of the test object. It follows by inspection of Eqs. (3.98) - (3.100) that

$$\Delta LP = 10 \log \left[\frac{8Wρc}{Sα} + \frac{hWρc}{A} \Big/ \frac{8Wρc}{Sα} \right] \qquad dB. \qquad (3.145)$$

Upon simplification and using h = 1/(h_F + 1), Eq. (3.145) becomes

$$\Delta LP = 10 \log \left[1 + \frac{S\alpha}{8A(h_F + 1)}\right] \quad dB. \tag{3.146}$$

Subtraction of Eq. (3.146) from (3.103) yields

$$LR - \Delta LP = 10 \log \left[8(h_F + 1)\frac{A}{S\alpha}\right] \quad dB. \tag{3.147}$$

The diffusivity requirement at the surface of the test object in the receiving room follows by substituting Eq. (3.147) into Eq. (3.139). Hence, the minimum intrinsic reactivity

$$LRd \geq 10 \log \left[8(h_F + 1)\frac{A}{S\alpha} / (10^{Le/10} - 1)\right] \quad dB. \tag{3.148}$$

By substituting Eq. (3.147) into Eq. (3.140) the minimum degree of directional diffusivity is given by

$$d \geq 100\left[1 - \left(\{ 10^{Le/10} - 1 \}/8\{ h_F + 1 \}\frac{A}{S\alpha}\right)^{0,5}\right] \quad \% \quad . \tag{3.149}$$

The requirements derived here do not apply to the determination of sound reduction indices by sound intensimetry; the sound intensity method does not require a diffuse field in the receiving room. For the purpose of diagnostic analysis an error of 2,5 dB is usually tolerable. For Le = 2,5 dB, Eqs. (3.148) and (3.149) become

$$LRd \geq 10 \log \left[10,28(h_F + 1)\frac{A}{S\alpha}\right] \quad dB. \tag{3.150}$$

and

$$d \geq 100\left[1 - \left(0,1/\{ h_F + 1 \}\frac{A}{S\alpha}\right)^{0,5}\right] \quad \% \quad . \tag{3.151}$$

Example 3.6. Consider the diffusivity requirements for sound transmission analysis for the case examined in Example 3.4, if

(a) the error in estimating the sound reduction index of the door, due to a lack of directional diffusion, is not to exceed 2,0 dB;
(b) the intensity radiation field at the surface of the test door has to be mapped with a maximum error Le = 2,5 dB;

(c) the intensity radiation field at the surface of the filler wall containing the door has to be mapped with a maximum error Le = 2,5 dB.

The results, summarized in Table 3.3, give an indication of the quantitive significance of the criteria developed in this section in regard to diffusivity requirements for sound transmission analysis in reactive fields by sound intensimetry. The sound intensity method for assessing diffusivity and for specifying diffusivity requirements is seen to offer the following advantages over the directivity method and the correlation method discussed in Sections 2.6.1 and 2.6.2, respectively:

(1) The intensity method is far more simple and quicker in providing an estimate of the degree of directional diffusivity at a point, than any of the other two methods. The principle parameter, namely the net sound intensity vector at the point, is determined by taking only three measurements, rather than a whole series as required by the other two methods.

(2) Only by the sound intensity method is it possible to derive simple and quantifiable criteria for minimum requirements of directional diffusivity in practical situations. It is not possible, for example, to specify the minimum degree of directional diffusivity required for sound transmission analysis in reactive fields, in terms of either the mean absolute deviation defined in Eq. (2.39), or the cross-correlation function of Eq. (2.40).

Table 3.3

Analysis of the problem in Example 3.6

$V = 210\ m^3$; $T = 7{,}0$ s.				
Frequency (Hz)			125	500
(a) **Source room; diffusivity requirements for sound insulation test; Le < 2,0 dB**				
Reactivity, incident portion	LR		6,0 dB	6,0 dB
Minimum intrinsic reactivity	LRd	Eq. (3.142)	8,3 dB	8,3 dB
Minimum directional diffusivity	d	Eq. (3.143)	62 %	62 %
(b) **Receiving room; diffusivity requirements for mapping of radiation field at surface of test door; Le < 2,5 dB ($A = 2{,}0\ m^2$; $A_F = 6{,}0\ m^2$)**				
Flanking ratio	h_F	Table 3.1	2,4	1,0
Absorption	$A/S\alpha$		0,42	0,42
Reactivity; door surface	LR	Table 3.1	10,9 dB	8,8 dB
Minimum intrinsic reactivity	LRd	Eq. (3.150)	11,7 dB	9,4 dB
Minimum directional diffusivity	d	Eq. (3.151)	74 %	65 %
(c) **Receiving room; diffusivity requirements for mapping of radiation field at surface of filler wall; Le < 2,5 dB ($A = 6{,}0\ m^2$; $A_F = 2{,}0\ m^2$)**				
Flanking ratio	h_F	Table 3.2	0,4	1,1
Absorption	$A/S\alpha$		1,25	1,25
Reactivity at filler wall surface	LR	Table 3.2	11,8 dB	13,3 dB
Minimum intrinsic reactivity	LRd	Eq. (3.150)	12,6 dB	14.3 dB
Minimum directional diffusivity	d	Eq. (3.151)	76 %	80 %

3.5.5 A direct-reading diffusivity meter

The degree of directional diffusivity defined in Eq. (3.134) may be computed from the spatially-averaged sound pressure level in the room and the net sound intensity level at the point of interest. To simplify this determination, a direct-reading diffusivity meter has been developed. The instrument, shown block diagramatically in Fig. 3.17, is used in conjunction with a Model A83 SIM portable sound intensity meter.

The spatial average of the sound pressure level is first determined by linear averaging while the microphone is moved through the room. The result is stored for all octave bands in the diffusivity meter, which is then ready to give a direct indication of the degree of directional diffusivity at the point where the intensity probe is placed. The diffusivity is taken to be the minimum reading obtainable at the point under consideration.

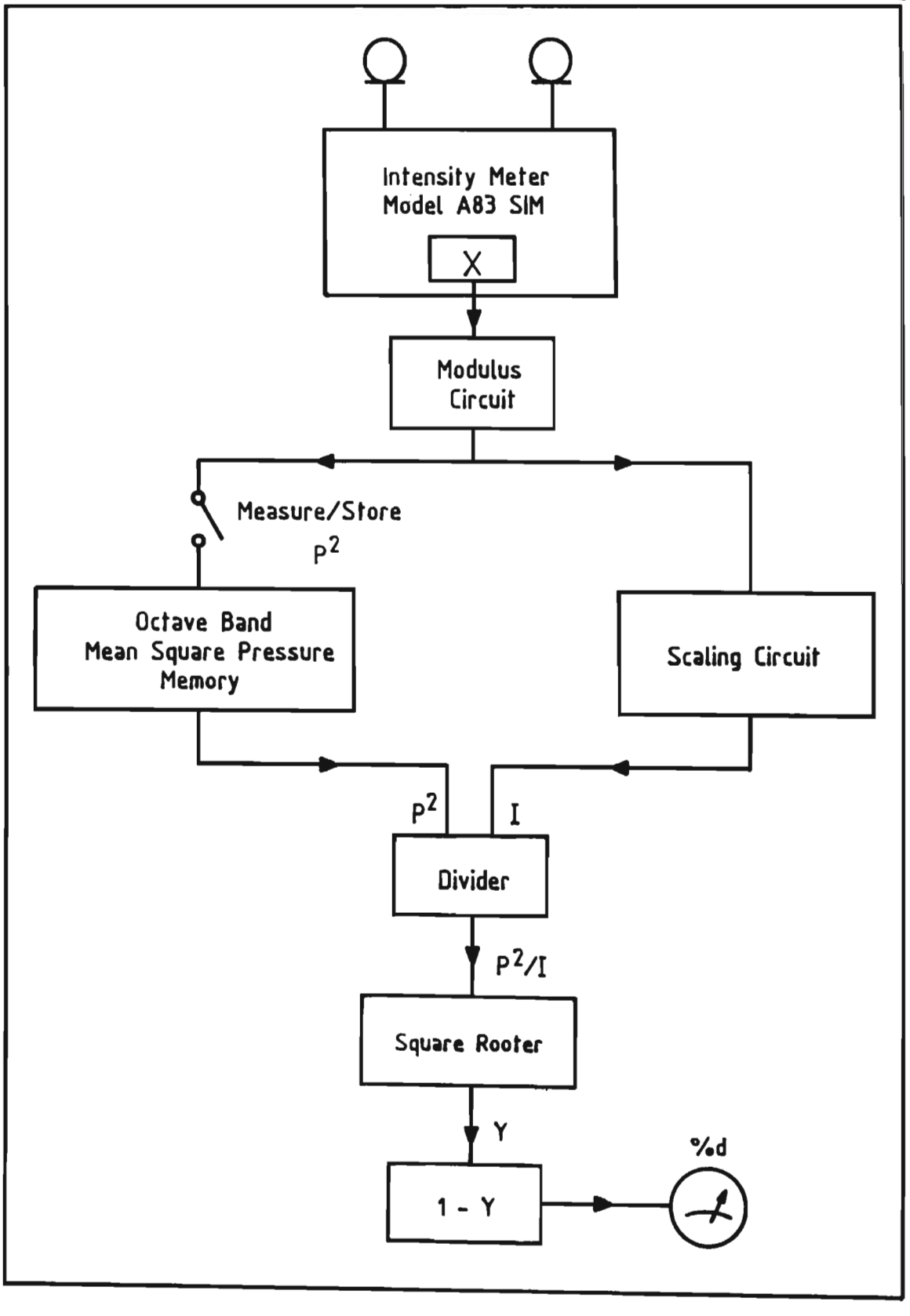

Figure 3.17

Blockdiagram of a direct-reading diffusivity meter based on sound intensity

CHAPTER 4

EXPERIMENTAL WORK

4.1 INTRODUCTION

4.1.1 Background

This chapter presents the results of case studies and laboratory investigations designed to apply and evaluate the principles and theory of sound transmission analysis developed in Chapter 3. The majority of investigations evolved from authentic sound insulation tests conducted on industrial products at the NPRL.

Difficulties encountered in assessing the sound insulation characteristics of high-performance acoustic building elements by employment of the classic two-room method presented a golden opportunity to apply and to evaluate the sound intensity method on a comparative basis with the classic method. For purposes of product development it was required to obtain selective estimates of the sound reduction indices of certain test objects which, owing to their small size, had to be mounted in comparatively large filler walls in the test aperture. Since the creation of a niche was considered to be undesirable, the maximum filler wall thickness was limited in each case to the thickness of the test object. The unfavourable surface ratio A_F/A and the thickness constraint in conjunction with the outstanding efficiencies of the test objects made it practically impossible to reduce flanking transmission to negligible levels as required by ISO 140. Hence, the sound reduction indices had to be determined by sequential testing of the filler wall and the filler wall-test object combination. This technique, however, failed completely, despite painstaking efforts to optimize measurement accuracy and precision.

In view of these difficulties it was decided to perform selective sound transmission analysis by employment of the sound intensity method. This proved to be successful in more than one way: not only were the problems associated with flanking transmission solved, but it had now

become possible to analyze the behaviour and performance of test objects by diagnostic sound transmission analysis as well.

A further opportunity to apply the concepts of sound transmission analysis and the assessment of diffusion by sound intensimetry, arose when the NPRL was requested to undertake the commissioning of the new acoustic laboratories of the South African Bureau of Standards (SABS) in Groenkloof, Pretoria in 1985. Diffusivity was examined by employment of the sound intensity approach developed in Section 3.5, using a digital sound intensity analyzer as well as a direct-reading diffusivity meter developed by the candidate. Sound transmission analysis was used to assess the efficiency of the acoustic doors used in the test facility. One of these doors fortuitously happened to be a production unit from a series of prototypes which had previously been tested at the NPRL. Since this unit served as an entrance door between a reverberation room and a highly absorbent lobby, the sound intensity method could be applied under conditions less stringent than those which had prevailed in the highly reverberant receiving room of the NPRL when the prototypes were tested.

4.1.2 Test room properties

Except for the field tests, all experimental work was conducted in the sound transmission test rooms of the NPRL. Test objects were installed in a test aperture between a reverberation room containing a large number of stationary diffusers and an irregularly shaped highly reflective transmission room. Although most of the results reported here have been obtained by using the transmission room as the source room, the roles of the two rooms were frequently reversed, using different sets of measuring equipment as a measure of detecting and eliminating systematic errors. The physical and acoustical properties of the NPRL test rooms are summarized in Table 4.1

4.1.3 Description of the test objects

The greater part of the experimental work reported here is based on

Table 4.1

Physical and acoustical properties of the NPRL test rooms
T = reverberation times; Sα = total absorption, rooms empty.

	REVERBERATION ROOM		TRANSMISSION ROOM	
Frequency (Hz)	T (s)	S α (m^2)	T (s)	S α (m^2)
100	5,9	11,2	3,1	4,2
125	6,9	9,6	3,3	3,9
160	5,5	12,0	3,4	3,8
200	5,6	11,8	3,8	3,4
250	5,1	13,0	2,4	5,4
315	5,1	13,0	2,7	4,8
400	5,2	12,7	2,7	4,8
500	5,1	13,0	2,7	4,8
630	5,4	12,3	2,5	5,2
800	5,5	12,0	2,4	5,4
1 000	5,6	11,8	2,2	5,9
1 250	5,5	12,0	2,1	6,2
1 600	5,1	13,0	2,0	6,5
2 000	4,7	14,1	1,9	6,8
2 500	4,0	16,6	1,8	7,2
3 150	3,2	20,7	1,6	8,1
4 000	2,6	25,5	1,5	8,6
Volume (m^3)	414		81	
Internal surface area (m^2)	340			
Test aperture size = 8,8 m^2.				

sound insulation tests conducted on a number of high-quality acoustical doors and windows and on brick filler walls which contained the test objects in the test aperture between the two test rooms. For the sake of brevity, alpha-numeric codes are used to describe window and filler-wall constructions. The numbers in the codes represent cross-sectional dimensions in mm, while the letters and brackets have the following meanings:

S = solid
L = laminated
A = absorptive treatment
P = plastered
( ) = air cavity

Sound insulation tests and sound transmission analyses were performed on the following elements:

(a) Experimental door (Door A). A steel door filled with sound damping material and hinged in a steel frame. The threshold was sealed with a soft rubber seal extending around the perimeter of the door. The door, including the metal frame with a total surface area of 2,0 m^2 was installed in a 220 mm brick filler wall as shown in Plate 4.1.

(b) Windows and filler walls. The windows and the filler walls which contained them, are specified in Table 4.2. The same set of steel

Table 4.2

Window and corresponding filler-wall construction

WINDOW CONSTRUCTION	BRICK FILLER WALL
9,5 L (200 A) 10 S 9,5 L (500 A) 10 S 12 S (500 A) 10 S	220 P 220 P (150A) 110 P P 220 P (150A) 110 P

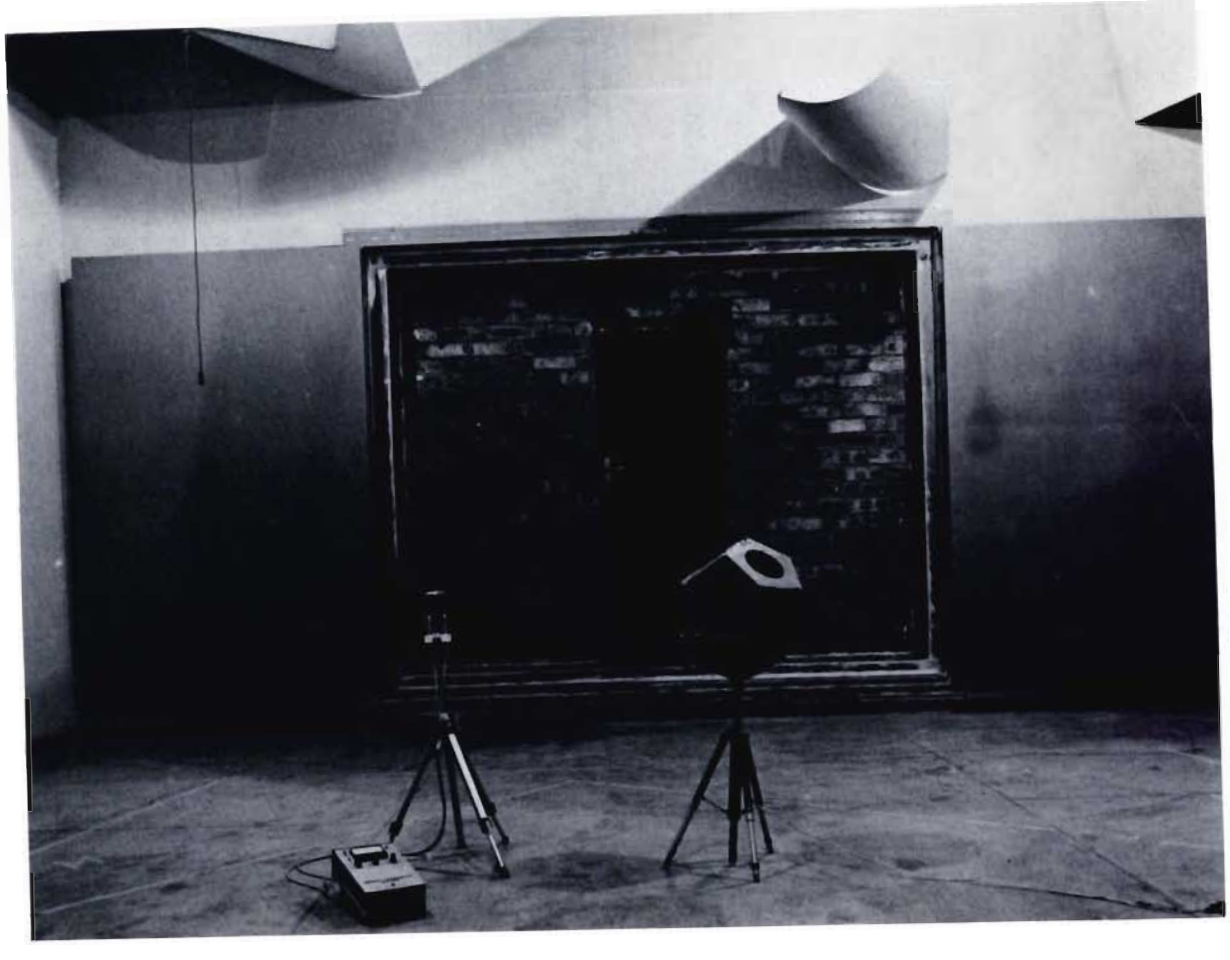

Plate 4.1

Test arrangement for sound transmission analysis on a door mounted in a brick filler wall.

frames and seals were used in all three cases. Frame dimensions are shown in Fig. 4.1, while the construction and mounting of the windows are illustrated in Fig. 4.2. The window surface area, including the frame, was 2,13 m^2.

(c) Panels. These will be described when referred to in the text.

4.1.4 Instrumentation

(a) Sound source. The door and the filler wall which contained it were tested with the source room being excited with two sound sources, each comprising a loudspeaker driven by a power amplifier. The two power amplifiers, fed with third-octave band filtered random noise, each delivered 15 W rms electrical power to the loudspeaker connected to it.

In order to cope with the exceptionally high sound insulation of the windows at high frequencies, a third sound source was added. Also driven with third-octave band filtered random noise, this source served the purpose of boosting the sound pressure level in the frequency range from 3,15 kHz upwards.

(b) Sound pressure analysis. Sound pressure levels were analyzed with the aid of a Brüel & Kjaer type 4417 Building Acoustics Analyzer using two sets of Brüel & Kjaer type 4165 condenser microphones in conjunction with B & K type 2619 preamplifiers. Sound pressure level averaging was accomplished by means of the B & K 4417 analyzer, taking at least 6 spatial averages with a rotating microphone (360 ° rotation with a radius of 1,5 m). Microphone calibration was performed with the aid of a B & K 4220 pistonphone and a B & K 4230 sound level calibrator. Spot checks were regularly made of the sound pressure levels, using hand-held sound level meters.

(c) Reverberation times and room absorption. Reverberation times and equivalent absorption areas were determined with the aid of a B & K 4417 analyzer. Tests were repeated whenever a change in the test ar-

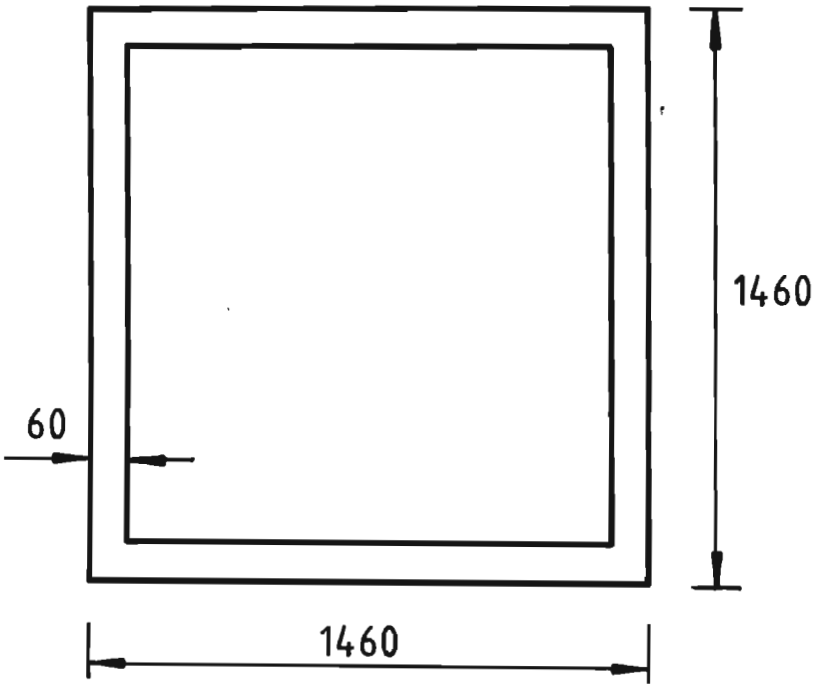

Figure 4.1

Window frame dimensions in mm.

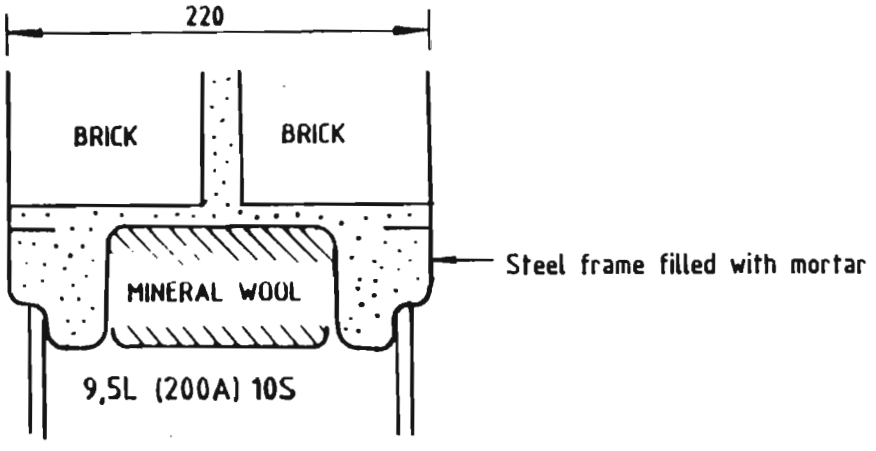

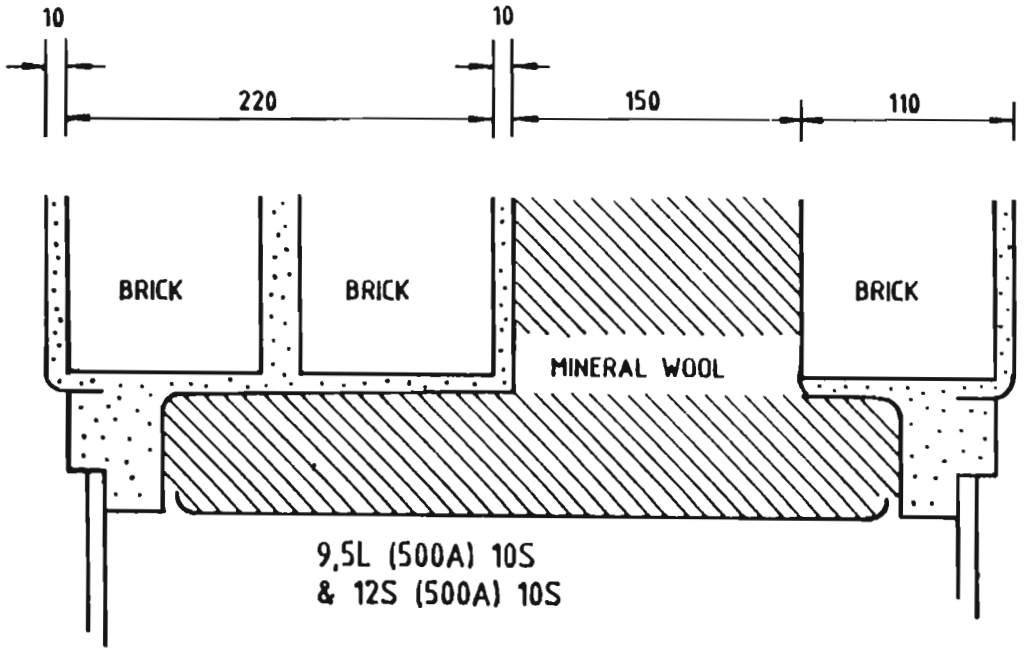

Figure 4.2

Window mounting and filler-wall construction.
Dimensions are given in mm.

rangement had been made, but also at regular intervals during prolonged testing.

(e) Sound intensity analysis. Sound intensity analysis was performed with the aid of two sound intensity meters.

(1) A Model A83 SIM portable analog sound intensity meter developed by the candidate at the NPRL. A microphone spacing of 15 mm was used in all measurements. Low-frequency results (100 Hz - 500 Hz) were checked and corrected if necessary, by using a 60 mm-spacer.

(2) A Brüel & Kjaer 3360 digital sound intensity analyzer. A microphone spacing of 12 mm was used in all measurements. Low-frequency results were checked and corrected if necessary, by using a 50mm-spacer.

Whereas the B & K 3360 analyzer only became available after completion of the first part of this investigation, sound intensity measurements performed on Door A and the 220 mm brick wall were made with the NPRL-instrument only. The measurements involving the windows and their corresponding filler walls were made by using the two instruments simultaneously.

(f) X-Y measurement frame. The sound intensity probes were mounted in a computer-controlled X - Y measurement frame shown in Plate 4.2 which facilitated accurate and repeatable positioning of the sound intensity probe. The frame was also used in diagnostic sound transmission analysis to scan the microphone along predetermined measurement paths.

4.1.5 Test procedures for determining sound reduction indices

(a) The classic two-room method Implementation of the classic two-room method was accomplished by measuring sound reduction indices in accordance with ISO 140 and recommendation R717, 1968(E), except that flanking transmission was accounted for by correcting the apparent transmission for the effect of flanking transmission through the filler wall. This involved two sound insulation tests in each case, namely one on the filler wall and one on the filler wall whilst containing the test object.

Plate 4.2

Computer-controlled frame used to position the sound intensity probe in sound transmission analysis.

(b) Intensity method In the case of Door A, sound reduction indices were determined by taking sound intensity measurements at 20 equally spaced microphone positions on a plane measurement surface situated at a distance of 80 mm from the surface of the door in the receiving room. A total of 37 and six measurement points were used for the windows and for the filler walls, respectively.

4.2 DETERMINATION OF SOUND REDUCTION INDICES IN THE PRESENCE OF FLANKING TRANSMISSION

4.2.1 Sound insulation tests on Door A mounted in 220 mm brick filler wall

A 220 mm unplastered brick wall was first built into the 8,8 m^2 test aperture and the sound reduction indices R_F determined by the classic two-room method, using Eq. (2.19). An opening was made in the wall and the door installed in it. The sound insulation test was repeated to determine the apparent sound reduction indices R' of the door, using Eq. (2.19) again. Finally, using Eq. (2.56), the true sound reduction indices R(clas) were computed by correcting R' for the contribution of the flanking wall.

Great care was taken to minimize measurement errors and to achieve the highest possible degree of accuracy and precision. The final results reported here are the averages obtained from 12 estimates, six of which were made with the reverberation room acting as source room and the transmission room as receiving room. The other six estimates were obtained with the roles of the two rooms reversed.

Sound reduction indices were also determined by the sound intensity method and calculated by using Eq. (3.38). (The effect of the differences between Eqs. (3.38) and (3.42) will be examined in subsequent sections.) The results are listed in Table 4.3 and shown graphically in Fig. 4.3. The flanking factor h_F was calculated by Eq. (2.51) using $A = 2,0\ m^2$ and $A_F = 6,8\ m^2$ and by substituting the indices R(int) obtained by the intensity method for R.

The discrepancies between the indices given by the methods are ascribed to the following factors:

(1) Classic method failure to distinguish between direct and flanking transmission by means of sequential testing.
(2) Possible changes in filler wall properties due to installation of the door.

In Table 4.4 the measurement error $Le_F = - Le_{R'} = Le$ dB which is likely to have caused the observed discrepancy R(clas) - R(int) was calculated by Eq. (2.70), using R = R(int). Inspection of the Le values shows that the large discrepancies R(clas) - R(int) in the frequency range 200 - 500 Hz seem to have occurred despite the attainment of good accuracy in determining R' and R_F by the classic method. These results are in agreement with the findings which emanated from the theoretical analysis in Section 2.8, namely that the classic method is not suited to selective determination of sound reduction indices in the presence of flanking transmission, even if sequential tests are performed to account for the flanking portion.

The flanking problem in this case is further illustrated by considering the minimum requirements imposed on the sound insulation of the filler wall in order to enable distinction between direct and flanking power by sequential testing of the filler wall and the filler wall - test object combination. The minimum sound reduction indices R_F(min) required for the filler wall in order to limit the overall error to $|Le_{RT}| < 1{,}5$ dB for a measurement accuracy $|Le| < 1{,}0$ dB, were computed by Eqs. (2.71) - (2.73) and listed in Table 4.4. It is seen that in the case under consideration, the sound insulation of the 220 mm brick wall was inadequate for the purpose of assessing the sound transmission loss of the door by the classic method. The sound intensity method appears not to be affected by the flanking transmission.

Table 4.3

Sound reduction indices for Door A, mounted in a 220 mm brick wall.

R_F = brick wall index (classic method);

R' = apparent index, Door A;

$R(clas)$ = index Door A, corrected for flanking;

$R(int)$ = index Door A, intensity method;

h_F = (flanking power)/(direct power)

Third-octave	Classic method			Intensity method	Flanking factor
f_c (Hz)	R_F	R'	$R(clas)$	$R(int)$	h_F
100	36,3	30,5	40,3	23,5	0,2
125	40,2	29,4	30,8	30,8	0,4
160	42,3	34,6	38,3	37,7	1,2
200	41,3	35,7	47,7	37,3	1,4
250	43,5	36,3	40,8	39,0	1,2
315	46,0	40,6	57,7	41,2	1,1
400	47,8	40,8	45,7	42,2	0,9
500	51,5	44,2	48,6	44,0	0,6
630	53,5	45,4	48,6	48,6	1,1
800	55,2	47,5	51,2	49,0	0,8
1 000	58,5	49,0	51,1	49,0	0,4
1 250	60,2	48,5	49,6	47,2	0,2
1 600	61,1	51,0	52,8	50,3	0,3
2 000	63,7	53,0	54,5	50,0	0,1
2 500	65,7	54,0	55,1	53,7	0,2
3 150	65,6	51,4	52,0	53,5	0,2
4 000	64,3	52,8	54,0	-	-
Ia (dB)	54	47	50	47	

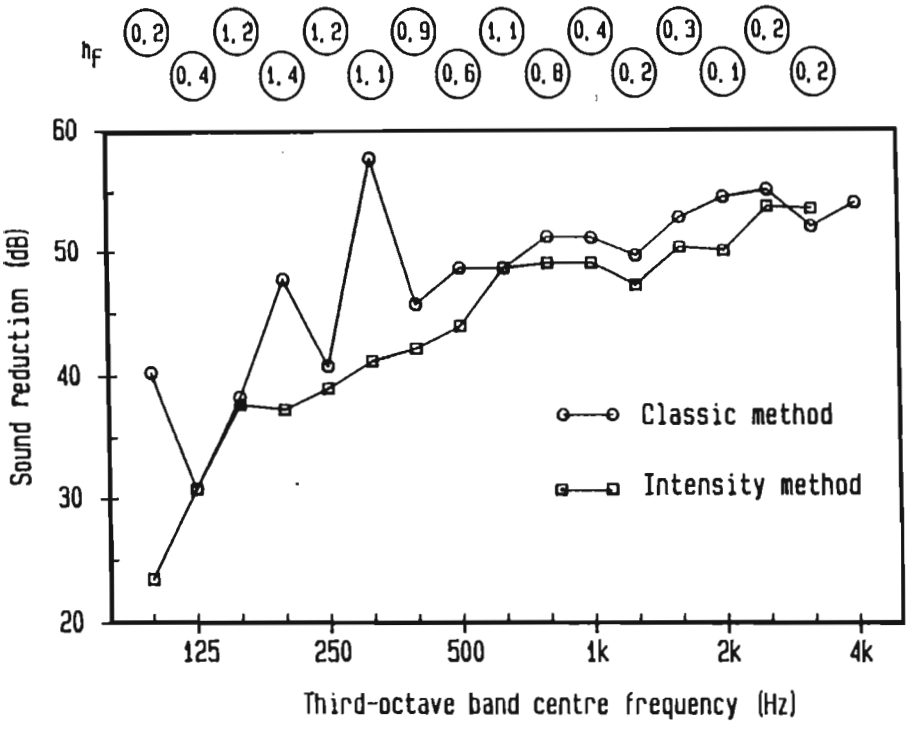

Figure 4.3

Sound reduction R of Door A.

○ Classic method

□ Intensity method

h_F = (flanking power)/(direct power)

Table 4.4

Error analysis of sound insulation test on Door A; classic method.

h_F = flanking ratio, Eq. (2.51);

Le_{RT} = total error = R(clas) - R, using R = R(int);

$|Le|$ = error in R_F and R' estimates which would have caused Le_{RT}, according to Eq. (2.70);

$R_F(min)$ = R_F required for filler wall to guarantee $|Le_{RT}| < 1,5$ dB if the measurement error $|Le| < 1,0$ dB.

R_F = sound reduction indices of 220 mm brick wall.

Third-octave	Analysis of measured results			Filler wall	
				Required index	220 mm brick
f_c (Hz)	h_F	Le_{RT} (dB)	$\|Le\|$ (dB)	$R_F(min)$ (dB)	R_F (dB)
100	0,2	16,8	-3,8	36,1	36,3
125	0,4	0,0	0,0	43,4	40,2
160	1,2	0,6	0,2	50,3	42,3
200	1,4	10,4	1,1	49,9	41,3
250	1,2	1,8	0,4	51,6	43,5
315	1,1	16,5	1,4	53,8	46,0
400	0,9	3,5	0,9	54,8	47,8
500	0,6	4,6	1,4	56,6	51,5
630	1,1	0,0	0,0	61,2	53,5
800	0,8	2,2	0,7	61,6	55,2
1 000	0,4	2,1	1,0	61,6	58,5
1 250	0,2	2,4	1,5	59,8	60,2
1 600	0,3	2,5	1,3	62,9	61,1
2 000	0,1	4,5	3,0	62,6	63,7
2 500	0,2	1,4	0,9	66,3	65,7
3 150	0,2	-1,5	1,2	66,1	65,6

4.2.2 Window 9,5 L (200A)10S in 220 mm brick filler wall

The window was installed in an unplastered 220 mm brick filler wall. Sound reduction indices were determined by the classic method, correcting the apparent transmission of the window for the flanking transmission through the filler wall, and by the sound intensity method. The sound reduction indices R_F of the filler wall were determined in the test described in the previous section.

The sound reduction indices obtained by the two methods are given in Table 4.5 and shown graphically in Fig. 4.4. In this case the flanking ratios are considerably higher than those obtained for the door in the previous test. As expected, the discrepancies between the two methods have increased accordingly. The classic method result is evidently unreliable; at 100 and 400 Hz the sound reduction indices of the window appear to be infinitely high. Analysis by the approach used in the previous section yield the results given in Table 4.6.

As in the previous case, the errors in the individual estimates of R' and R_F obtained with the classic method seem to be well under control; the large errors in the eventual estimates of R are inevitable, considering the requirements implicitly involved in this method. In order to limit the total error to $|Le_{RT}| < 1,5$ dB for $|Le| < 1,0$ dB, the filler wall requirements (see Table 4.6), became totally unrealistic. Conversely, if the 220 mm brick wall with its comparatively inferior performance is used, the accuracy requirements imposed on the individual R' and R_F determinations for $|Le_{RT}| < 1,5$ dB become practically unattainable. For example, the required accuracies in the case under consideration at 250, 315, 400 and 500 Hz, computed by Eq. (2.70), are $|Le| < 0,10$, 0,09 , 0,04 and 0,07 dB, respectively.

At this stage there is no proof of the validity of the results obtained by the intensity method except for the observation that the sound insulation curve is well-behaved. The local minimum observed at 1,6 kHz is in agreement with the theoretical coincidence frequency for glass of 10 mm thickness. The validity of the results will be assessed later in this chapter on basis of the criteria developed in Chapter 3.

Table 4.5

Sound reduction indices for Window 9,5 L (200A) 10S mounted in a 220 mm brick wall.

R_F = brick wall index (classic method);
R' = apparent index, window;
R(clas) = window index, corrected for flanking;
R(int) = window index, intensity method;
h_F = (flanking power)/(direct power)

Third-octave f_c (Hz)	Classic method R_F	R'	R(clas)	Intensity method R(int)	Flanking factor h_F
100	36,3	35,0	∞*	40,4	8,1
125	40,2	30,3	32,0	42,9	5,9
160	42,3	36,9	47,2	43,8	4,4
200	41,3	36,2	51,7	41,2	3,1
250	43,5	37,8	45,9	46,2	5,9
315	46,0	38,8	42,8	49,2	6,6
400	47,8	43,6	∞*	54,8	15,8
500	51,5	46,2	57,6	55,9	8,7
630	53,5	47,6	54,8	60,2	14,7
800	55,2	48,2	52,5	58,3	6,4
1 000	58,5	49,4	51,5	58,0	2,8
1 250	60,2	50,0	51,6	54,2	0,8
1 600	61,1	51,1	52,7	53,2	0,5
2 000	63,7	52,1	53,2	54,8	0,4
2 500	65,7	52,9	53,7	58,4	0,6
3 150	65,6	54,2	55,3	62,4	1,5
4 000	64,3	55,6	58,0	64,9	3,6
Ia (dB)	54	48	-	54	

* R incalculable; measured values R_F and R' result in logarithm of a negative number in (Eq. 2.56).

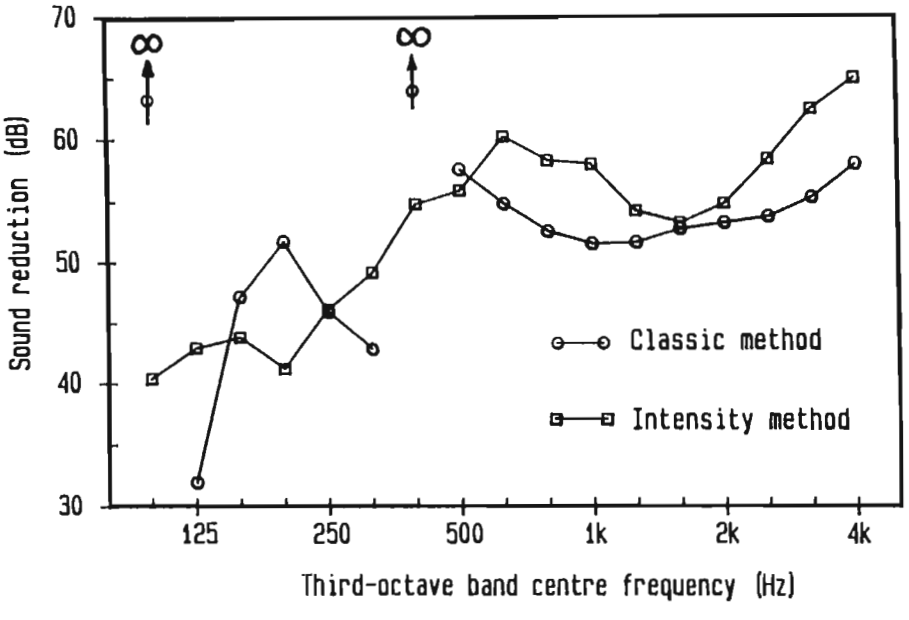

Figure 4.4

Sound reduction R of window 9,5L(200A)10S mounted in 220mm brick wall

- o Classic method
- □ Intensity method

h_F = (flanking power)/(direct power)

Table 4.6

Error analysis of sound insulation test on Window 9,5L(200A)10S; classic method

h_F = flanking ratio, Eq. (2.51);

Le_{RT} = total error = R(clas) - R, using R = R(int);

$|Le|$ = error in R_F and R' estimates which would have caused Le_{RT}, according to Eq. (2.70);

$R_F(min)$ = R_F required for filler wall to guarantee $|Le_{RT}| < 1,5$ dB if the measurement error $|Le| < 1,0$ dB.

R_F = sound reduction indices of 220 mm brick wall.

Third-octave	Analysis of measured results			Filler wall	
				Required index	220 mm brick
f_c (Hz)	h_F	Le_{RT} (dB)	$\|Le\|$ (dB)	$R_F(min)$ (dB)	R_F (dB)
100	8,1	∞	0,3	52,7	36,3
125	5,9	-10,9	3,4	55,2	40,2
160	4,4	3,4	0,2	56,1	42,3
200	3,1	10,5	0,6	53,5	41,3
250	5,9	-0,3	0,0	58,5	43,5
315	6,6	-6,4	1,0	61,5	46,0
400	15,8	∞	0,1	67,1	47,8
500	8,7	1,7	0,1	68,2	51,5
630	14,7	-5,4	0,4	72,5	53,5
800	6,4	-5,8	0,9	70,6	55,2
1 000	2,8	-6,5	2,1	70,3	58,5
1 250	0,8	-2,6	1,3	66,5	60,2
1 600	0,5	-0,5	0,3	65,5	61,1
2 000	0,4	-1,6	1,0	67,1	63,7
2 500	0,6	-4,7	3,1	70,7	65,7
3 150	1,5	-7,1	3,6	74,7	65,6

4.2.3 Window 9,5L(500A)10S in P220P(150A)110P brick filler wall

The 220 mm brick filler wall used in the previous two tests was plastered on both sides and the frame containing the 10 mm solid pane removed, leaving the 9,5 mm laminated pane in position. A 110 mm brick wall, plastered on one side, was erected 150 mm from the existing one and the dismantled frame installed in this second wall. The cavity between the walls was filled with mineral wool. With the 10 mm solid pane in the new position the interpane distance now became 500 mm, as shown in Fig. 4.2.

Since the test object was only available for a limited period of time, it was decided to determine R_F by sound intensity measurement rather than by the classic method, which would have involved complete dismantling of the test object and bricking up of the opening, before measurements could have been resumed.

Sound reduction indices obtained by the classic method as well as the sound intensity method are listed in Table 4.7 and shown graphically in Fig. 4.5. The flanking ratios were calculated by Eq. (2.51), using $R = R(int)$, $A = 2,13\ m^2$ and $A_F = 6,7\ m^2$.

These results and the analysis given in Table 4.8 are consistent with the general conclusions which emanated from the previous two investigations. It would appear that selective determination of sound reduction indices by the classic method becomes unreliable when the flanking factor h_F approaches or exceeds unity. The cavity brick-wall construction with an Ia value of 66 dB is totally inadequate for the purpose of assessing the window insulation by sequential application of the classic method.

Table 4.7

Sound reduction indices for Window 9,5 L (500A) 10S mounted in a P220P(150A)110P brick wall.

R_F = brick wall index (intensity method);
R' = apparent index, window;
R(clas) = window index, corrected for flanking;
R(int) = window index, intensity method;
h_F = (flanking power)/(direct power)

Third-octave f_c (Hz)	Intensity method R_F	Classic method R'	Classic method R(clas)	Intensity method R(int)	Flanking factor h_F
100	50,6	40,7	42,4	44,8	0,7
125	48,8	43,0	50,6	45,8	1,6
160	55,3	48,5	53,1	53,7	2,2
200	51,7	46,3	56,6	52,5	3,8
250	54,1	50,4	∞*	56,4	5,3
315	58,0	52,7	64,1	58,2	3,3
400	59,3	55,6	∞*	61,3	5,0
500	65,0	60,3	∞*	66,2	4,1
630	69,6	64,1	73,6	72,2	5,7
800	73,5	66,8	71,6	73,5	3,1
1 000	73,9	67,3	72,4	72,9	2,5
1 250	72,6	66,9	75,0	69,8	1,7
1 600	76,0	66,8	68,9	69,8	0,8
2 000	77,0	68,6	71,2	70,9	0,8
2 500	**	71,0	**	74,6	-
3 150	**	74,6	**	80,6	-
4 000	**	77,5	**	85,6	-
Ia (dB)	-	61	-	66	

* R incalculable; measured values R_F and R' result in logarithm of a negative number (Eq. 2.56).

** Sound source power rating inadequate to achieve measurable receiving room levels.

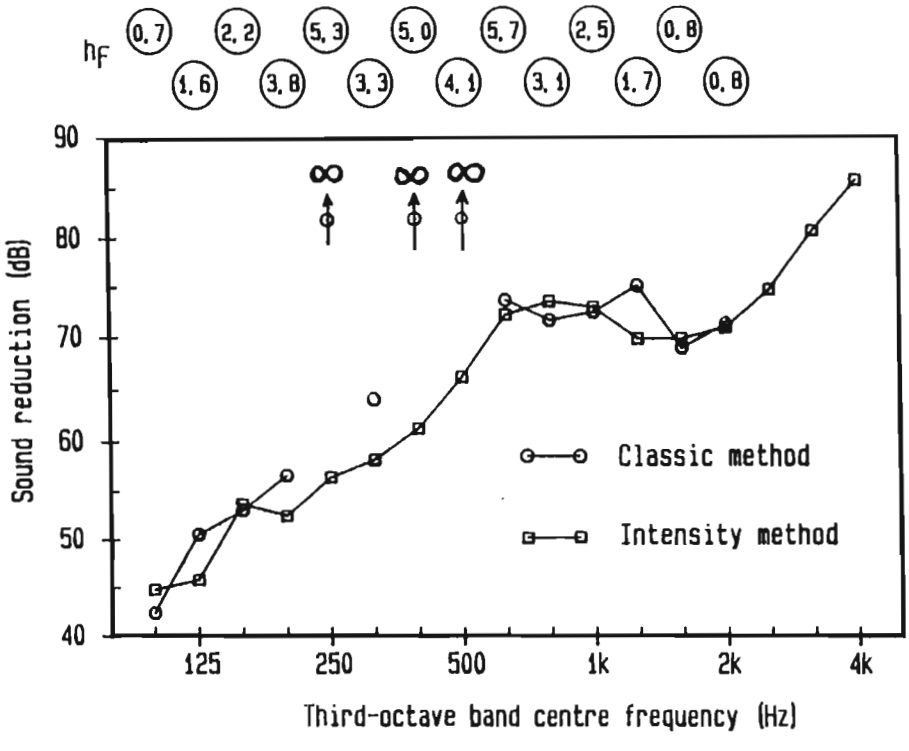

Figure 4.5

Sound reduction indices of Window 9,5L(500A)10S mounted in a P220P(150A)110P brick filler wall

o Classic method

□ Intensity method

h_F = (flanking power)/(direct power).

Table 4.8

Error analysis of sound insulation test on Window 9,5 L(500A)10S; classic method

h_F = flanking ratio, Eq. (2.51);

Le_{RT} = total error = R(clas) - R, using R = R(int);

$|Le|$ = error in R_F and R' estimates which would have caused Le_{RT}, according to Eq. (2.70);

$R_F(min)$ = R_F required for filler wall to guarantee $|Le_{RT}| \leq$ 1,5 dB if the measurement error $|Le| \leq$ 1,0 dB;

R_F = sound reduction indices of P220P(150A)110P brick wall.

Third-octave	Analysis of measured results			Filler wall	
				Required index	Practical wall
f_c (Hz)	h_F	Le_{RT} (dB)	$\|Le\|$ (dB)	$R_F(min)$ (dB)	R_F (dB)
100	0,7	-2,4	1,2	57,1	50,6
125	1,6	4,8	0,7	58,1	48,8
160	2,2	-0,6	0,1	66,0	55,3
200	3,8	4,1	0,3	64,8	51,7
250	5,3	∞	0,4	68,7	54,1
315	3,3	5,9	0,4	70,5	58,0
400	5,0	∞	0,4	73,6	59,3
500	4,1	∞	0,5	78,5	65,0
630	5,7	1,4	0,1	84,5	69,6
800	3,1	-1,9	0,3	85,8	73,5
1 000	2,5	-0,5	0,1	85,2	73,9
1 250	1,7	5,2	0,2	82,1	72,5
1 600	0,8	-0,9	0,4	82,1	76,0
2 000	0,8	0,3	0,1	83,2	77,0

4.2.4 Hardboard panel of 6 mm thickness mounted in a 220 mm brick filler wall

A comparison between the classic two-room method and the sound intensity method for low levels of flanking transmission was made by conducting a test on a 0,5 m^2 hardboard panel of 6,0 mm thickness mounted in a metal frame in the 220 mm brick filler wall used in the previous tests.

The results given in Table 4.9 and plotted in Fig. (4.6) show good agreement between the two methods, owing to the comparatively low levels of flanking power. Considering the small effect (R' - R(clas)) of the flanking correction, it is evident that selective assessment of the panel insulation was in this case effected by suppression of flanking transmission rather than by distinguishing between direct and flanking transmission.

It is interesting to note that the causative error $|Le|$ obtained by the analysis given in Table 4.10 is small and very similar in magnitude to those obtained in the previous cases. This indicates that good accuracy can be attained by the classic method, provided flanking is well-supressed. Yet the method is not suited to selective determination of the sound reduction indices of relatively efficient panels.

Table 4.9

Sound reduction indices of a 6 mm hardboard panel mounted in a 220 mm brick wall.

R_F = brick wall index (classic method);
R' = apparent index of hardboard panel;
R(clas) = index, hardboard panel, classic method;
R(int) = index, hardboard panel, intensity method;
h_F = (flanking power)/(direct power)

Third-octave f_c (Hz)	Classic method R_F	R'	R(clas)	Intensity method R(int)	Flanking factor h_F
100	36,3	17,6	18,7	18,1	0,29
125	40,2	16,1	16,4	14,5	0,07
160	42,3	18,6	18,9	17,3	0,08
200	41,3	21,1	21,8	20,5	0,19
250	43,5	18,8	19,1	18,9	0,06
315	46,0	22,8	23,2	22,4	0,09
400	47,8	22,4	22,6	21,7	0,05
500	51,5	24,7	24,9	25,2	0,04
630	53,5	26,4	26,5	26,0	0,03
800	55,2	27,4	27,5	27,4	0,03
1 000	58,5	29,3	29,4	30,3	0,02
1 250	60,2	30,3	30,4	29,9	0,02
1 600	61,1	32,2	32,3	32,7	0,02
2 000	63,7	32,8	32,9	33,7	0,01
2 500	65,7	33,5	33,5	33,9	0,01
3 150	65,6	31,8	31,8	32,2	0,01
4 000	64,3	28,7	28,7	29,2	0,00

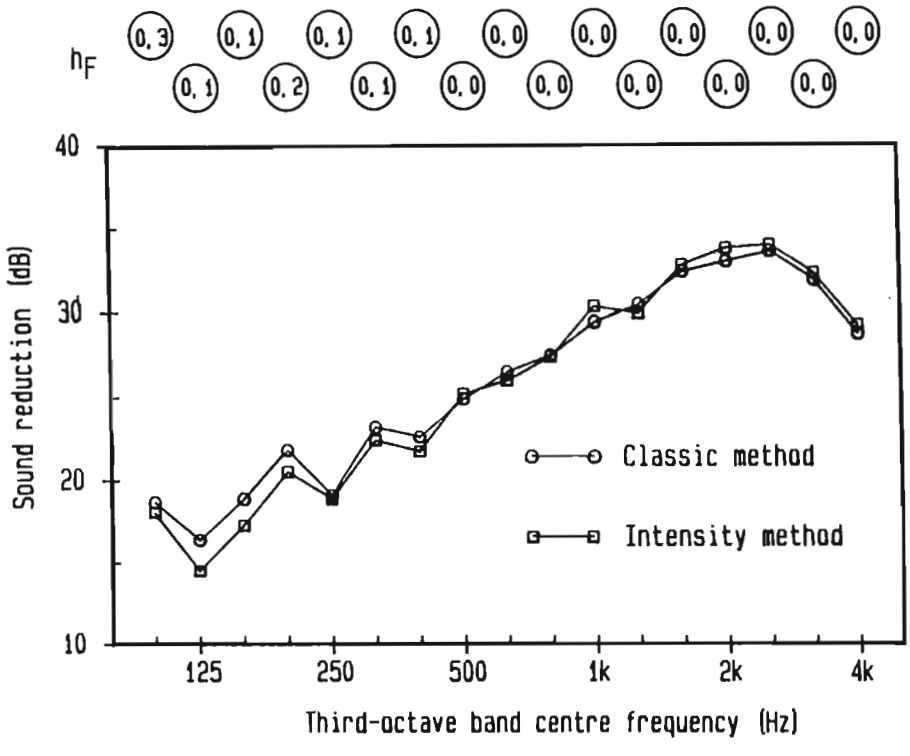

Figure 4.6

Sound reduction indices of 6mm hardboard panel mounted in a 220mm brick filler wall.

○ Classic method

□ Intensity method

h_F = (flanking power)/(direct power).

Table 4.10

Error analysis of sound insulation test on 6 mm hardboard panel; clasic method

h_F = flanking ratio, Eq. (2.51);

Le_{RT} = total error = R(clas) - R, using R = R(int);

$|Le|$ = error in R_F and R' estimates which would have caused Le_{RT}, according to Eq. (2.70);

$R_F(min)$ = R_F required for filler wall to guarantee $|Le_{RT}| \leq$ 1,5 dB if the measurement error $|Le| \leq$ 1,0 dB.

R_F = sound reduction indices of 220 mm brick wall.

Third-octave	Analysis of measured results			Filler wall	
				Required index	220 mm brick
f_c (Hz)	h_F	Le_{RT} (dB)	$\|Le\|$ (dB)	$R_F(min)$ (dB)	R_F (dB)
100	0,29	0,6	0,4	37,6	36,3
125	0,07	1,9	1,6	34,0	40,2
160	0,08	1,6	1,3	36,8	42,3
200	0,19	1,3	0,9	40,0	41,3
250	0,06	0,2	0,2	38,4	43,5
315	0,09	0,8	0,7	41,9	46,0
400	0,05	0,9	0,8	41,2	47,8
500	0,04	-0,3	0,3	44,7	51,5
630	0,03	0,5	0,5	45,5	53,5
800	0,03	0,1	0,1	46,9	55,2
1 000	0,02	-0,9	0,9	49,8	58,5
1 250	0,02	0,5	0,5	49,4	60,2
1 600	0,02	-0,4	0,4	52,2	61,1
2 000	0,01	-0,8	0,8	53,2	63,7
2 500	0,01	-0,4	0,4	53,4	65,7
3 150	0,01	-0,4	0,4	51,7	65,5
4 000	0,00	-0,5	0,5	48,7	64,3

4.2.5 Sound insulation test on an open window

The previous tests covered a range of conditions extending from extremely unfavourable flanking conditions to normal applications. To complete the range, comparative sound insulation tests were performed on an open window. This consisted of a 2,05 x 0,89 m opening cut into the 220 mm brick filler wall used in the previous tests. Measurements were performed in octave bands with centre frequencies from 125 to 4 kHz.

(a) Classic method The classic method was applied in the usual way, using Eq. (2.19), but the room absorption was determined in two ways.

(1) In the first experiment, reverberation times measured with the open window in position, were used directly in Eq. (2.19) to compute the sound reduction indices R1 listed in Table 4.11.

Table 4.11

Sound reduction indices of an open window, determined by the classic method (R1 and R2) and by the intensity method (R3). Reverberation times used in calculating R1 were subject to source - receiving room interaction; those for R2 not.

Octave band centre f (Hz)	Classic method		Intensity method
	R1	R2	R3
125	6,4	4,1	3,0
250	4,3	1,5	2,1
500	2,5	-0,7	0,6
1 000	3,0	-0,5	1,4
2 000	3,3	0,5	0,5
4 000	2,9	1,0	2,0

It can be assumed that failure to obtain 0 dB transmission loss was caused by acoustic coupling between the two test rooms due to the presence of the open window in the dividing wall. This presumably caused the sound decay-process in the source room to interact with that in the receiving room, which resulted in false reverberation times.

(2) In the second experiment the test aperture containing the brick wall with the open window was shut off with steel doors. This allowed determination of receiving room reverberation times in the absence of source room interference. Since equivalent absorption areas calculated from these reverberation times did not account for absorption by the open widow, the measured reverberation times Tm were corrected as follows:

Receiving room absorption, excluding the area of the open window, is

$$S\alpha m = 0{,}16\ V/Tm \quad . \tag{4.1}$$

The total absorption, including that of the 1,8 m^2 open window, is

$$S\alpha = 0{,}16\ V/Tm + 1{,}8 \quad , \tag{4.2}$$

which corresponds to an equivalent reverberation time

$$T = 0{,}16\ V/S\alpha = 0{,}16\ VTm/(0{,}16\ V + 1{,}8\ Tm) \quad . \tag{4.3}$$

Sound reduction indices R2 in Table 4.11 were calculated by substituting Eq. (4.3) into Eq. (2.19). The indices obtained in this way are in agreement with the expectations for an open window. Owing to its finite size, the opening tested here did not exhibit perfect open-window behaviour at low frequencies.

(b) Sound intensity method The sound intensity method was applied in the usual way without any corrections. Sound reduction indices R3 in Table 4.11, calculated by using Eq. (3.38), are in good agreement

with R2 obtained by the classic method. The theory developed in Section 3.3.5 indicates that the intensity method is expected to overestimate the sound insulation of an open window as a result of the sound absorbed by the latter from the reverberant field in the receiving room. This effect will be examined in Section 4.6.

4.3 SELECTIVE DETERMINATION OF FLANKING TRANSMISSION BY SOUND INTENSIMETRY

4.3.1 Brick filler wall containing Door A

The sound reduction indices of the 220 mm brick filler wall used in the sound insulation test on Door A (Section 4.2.1), were determined by the following two methods:

(a) Classic method; before installation of the door The brick wall was built into the test aperture and tested by the classic two-room method according to ISO 140.

(b) Sound intensity method; after installation of the door A 2,0 m^2 opening was cut into the wall and Door A installed in it. Sound reduction indices for the wall were determined selectively by application of the sound intensity method, using six microphone positions to determine the average intensity transmitted through the wall.

The results given in Table 4.12 and Fig. 4.7 show fair agreement between the two methods. The differences can be ascribed to the following two factors:

(1) The wall is likely to have sustained small cracks during installation of the test object, causing a slight deterioration of sound insulation at high frequencies.
(2) The natural frequencies and the stiffness of the original square wall had presumably changed as a result of the reduction in wall area.

The relatively small number of measurement positions used in this case was justified by the uniformity in sound radiation exhibited by the brick wall, a phenomenon which is characteristic of well-damped materials. Partitions having low internal damping are characterized by non-uniform radiation patterns caused by reactive acoustic power exchange between surface elements vibrating in anti-phase.

Table 4.12

Selective determination of sound reduction indices of a 220 mm brick wall by sound intensimetry.
R1 : Classic method; 8,8 m^2 test aperture containing wall only.
R2 : Intensity method; test aperture containing wall, including 2,0 m^2 test object.

Third-octave f_c (Hz)	Classic method R1	Intensity method R2
100	36,3	37,0
125	40,2	39,8
160	42,3	37,5
200	41,3	44,4
250	43,5	44,9
315	46,0	48,5
400	47,8	50,1
500	51,5	51,9
630	53,5	55,5
800	55,2	58,6
1 000	58,5	57,3
1 250	60,2	58,1
1 600	61,1	60,6
2 000	63,7	60,0
2 500	65,7	63,5
3 150	65,6	62,3
4 000	64,3	64,6
Ia	54	55

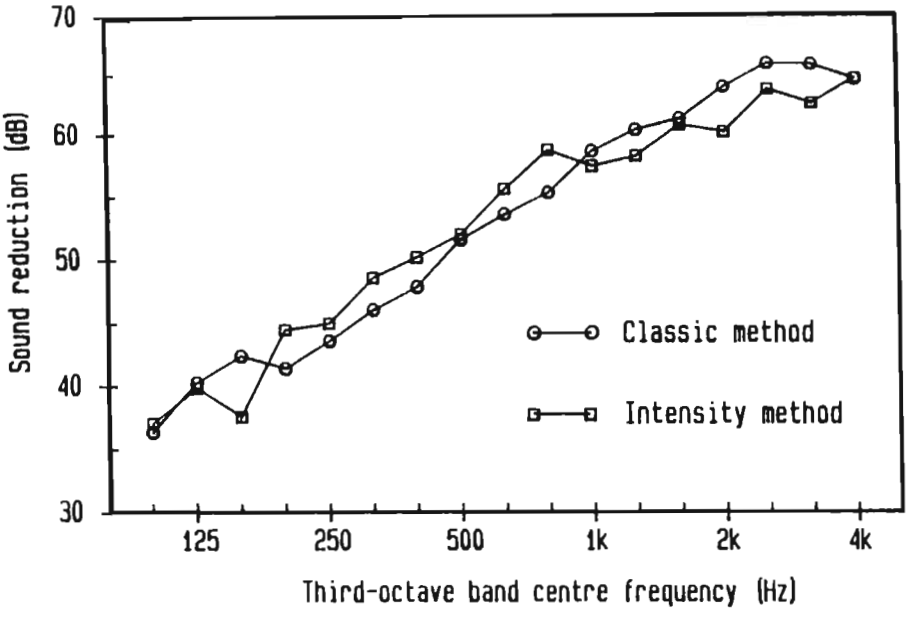

Figure 4.7

Sound insulation test on 220mm brick wall.

- o Classic method; 8,8m2 test opening containing wall only.
- □ Intensity method; selective measurement of wall insulation after installation of a 2,0m2 door.

4.4 THE EFFECT OF INTERFERENCE PATTERNS

In the foregoing evaluation of the sound intensity method the standard formula, Eq. (3.38), was consistently used in calculating the sound reduction index. The effect of interference patterns at the source room boundaries, accounted for in Eq. (3.42), have thus been ignored. The Waterhouse correction

$$L_{Wc1} = 10 \log (1 + \lambda S_1/8V_1) \quad \text{dB}, \tag{4.4}$$

which should be added to indices obtained by Eq. (3.38), is given as a function of frequency in Table 4.13. As for the classic method, the source room correction L_{Wc1} is partially cancelled by the receiving room correction L_{Wc2} as a result of the difference LP1 - LP2 taken in Eq. (2.19). The net correction

$$L_{Wc1} - L_{Wc2} = 10 \log [(1 + \lambda S_1/8V_1)/(1 + \lambda S_2/8V_2)] \quad \text{dB} \tag{4.5}$$

which is generally disregarded, is also given in Table 4.13. The significance of these corrections is illustrated in Fig. 4.8 for the sound insulation test on the 6 mm hardboard panel which was considered in Section 4.2.4. Introduction of the Waterhouse correction terms is seen to yield a general improvement in the agreement between the two methods, a result which is also obtained for the open window test. In fact, the author suspects that the slight low-frequency discrepancy generally observed in respect of comparative results presented in the literature [134,137,138,141], can be ascribed to this factor.

Table 4.13

Waterhouse corrections for NPRL test rooms.

L_{Wc1} = source room correction, applicable to the intensity method;

$L_{Wc1} - L_{Wc2}$ = net effect of source and receiving room corrections, applicable to the classic method.

Third-octave f_c (Hz)	Classic method L_{Wc1} (dB)	Intensity method $L_{Wc1} - L_{Wc2}$ (dB)
100	2,5	1,3
125	2,1	1,1
160	1,8	0,9
200	1,5	0,8
250	1,2	0,6
315	1,0	0,5
400	0,8	0,4
500	0,6	0,4
630	0,5	0,3
800	0,4	0,2
1 000	0,3	0,2
1 250	0,3	0,2
1 600	0,2	0,1
2 000	0,2	0,1
2 500	0,1	0,1
3 150	0,1	0,1
4 000	0,1	0,1

(a) Without correction for interferece field energy

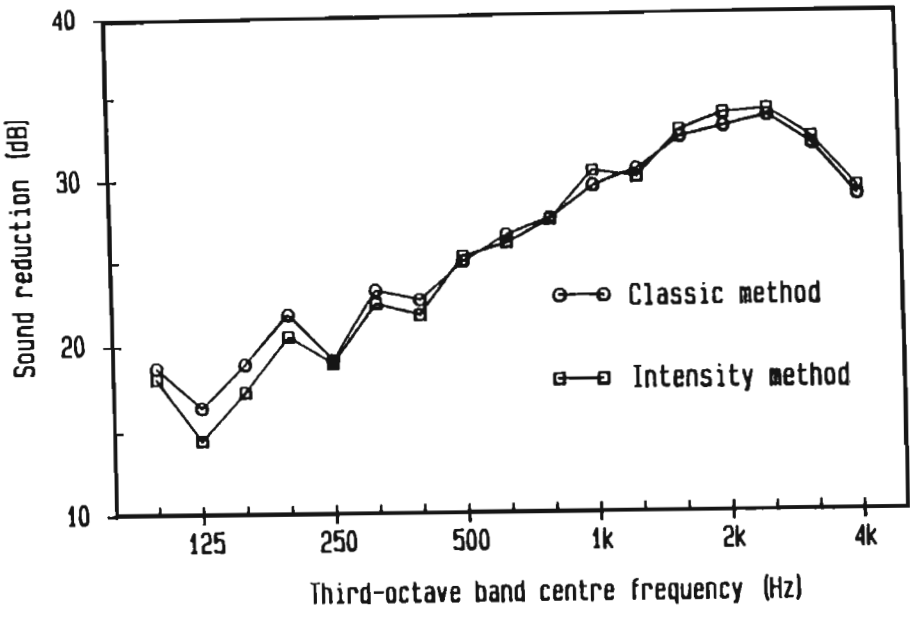

(b) With correction for interference field energy

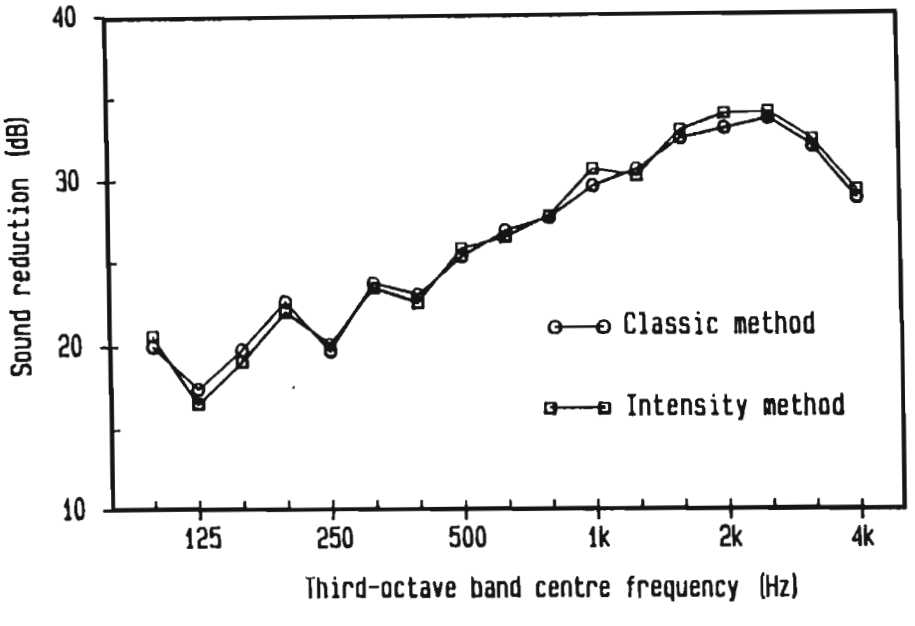

Figure 4.8

The effect of interference pattern errors on the results given by the classic two-room method (o——o) and the sound intensity method (□——□) for the 6mm hardboard panel of Section 4.2.4
(a) Sound reduction indices without Waterhouse corrections.
(b) Sound reduction indices corrected for interference effects by application of Waterhouse corrections

4.5 LEAKAGE ERROR

4.5.1 Window 12S(500A)10S mounted in P220P(150A)110P filler wall

The sound insulation of Window 12S(500A)10S was determined by the intensity method using a plane measurement surface situated at a distance of 40 mm from the window. The sound reduction R1 was first determined without taking leakage into account, using

$$R1 = 10 \log (W_{IN}/I_A A) \quad , \tag{4.6}$$

where I_A is the average intensity normal to the plane measurement surface of area A equal to that of the window under test.The sound power transmitted through the leakage gap along the perimeter of the plane surface was then determined by measuring the intensity I_{dA} normal to the leakage surface dA. The sound reduction index R, accounting for the total transmission through the window was calculated as

$$R = 10 \log [W_{IN}/(I_A A + I_{dA} dA)] \quad . \tag{4.7}$$

The leakage error Le = R1 - R in Table 4.14 emphasizes the point that the intention to measure "in the plane" of the radiating surface is foiled in practice by the physical construction of the intensity probe, the surface profile of the test object and by requirements of microphone mobility. The usage of a plane measurement surface thus results in a leakage gap which in some cases may cause a significant leakage error.

Table 4.14

Leakage error due to the use of a plane measurement surface situated at a distance of 40 mm from Window 12S(500A)10S.

Third-octave f_c (Hz)	R (dB)	Le (dB)
125	40,0	0,6
250	50,2	0,7
500	60,5	0,7
1 000	59,2	0,8
2 000	66,1	0,2
4 000	79,2	0,1

4.6 THE EFFECT OF SOUND ABSORPTION BY THE TEST OBJECT

4.6.1 Comparative measurements on a brick wall with and without absorptive cladding

The effect of sound absorption by the test object on the result of the sound intensity method was examined by measuring the sound reduction indices of a 220 mm brick filler wall containing a panel. In this experiment the wall was defined as the test object with the panel acting as a source of flanking power. The flanking panel consisted of 12 mm wood, 180 mm air cavity and 6 mm hardboard, i.e. 12W(180)6H. The sound absorption of the wall was controlled by cladding it with 75 mm thick glass-wool panels. The effect of sound absorption on the estimated sound insulation of the wall is shown in Table 4.15 which compares the error predicted in Eq. (3.57) and the actual error, taken as the difference between the indices measured with, and without absorptive cladding on the wall. The amount of absorption added was determined by the reverberation room method. The effect on the sound insulation curve is shown in Fig. 4.9.

The effect of sound absorption by the test object is to cause an overestimation of the sound reduction index, exaggerated in this case by the use of excessive amounts of absorption. The accuracy of the predicted error is limited by the accuracy of the experimentally determined estimate of the amount of absorption added to the surface of the test object and by the sensitivity of the error function when large errors are induced (see Fig. 3.6). The accuracy of the measured error Lem was presumably affected by the high levels of reactivity at the wall surface.

Table 4.15

The effect of sound absorption by the test object on the estimated value of the sound reduction index.

Test object: 8,3 m^2 brick wall containing 0,5 m^2 flanking panel.

$S\alpha$ = receiving room absorption, including additional amount $A\alpha_A$ attached to the wall.

Le = predicted error, Eq. (3.57);

Lem = measured error.

Octave f_c (Hz)	$S\alpha$ (m^2)	$A\alpha_A$ (m^2)	h_F	LR (dB)	Le (dB)	Lem (dB)
250	17,4	7,8	0,06	9,3	2,8	2,4
500	23,2	10,2	0,12	14,7	3,0	8,2
1 000	21,8	10,0	0,51	23,3	5,1	8,4
2 000	24,0	9,9	3,2	24,0	$I_A > I_D$	$I_A > I_D$
4 000	35,9	10,4	2,4	27,6	18,2	20,9

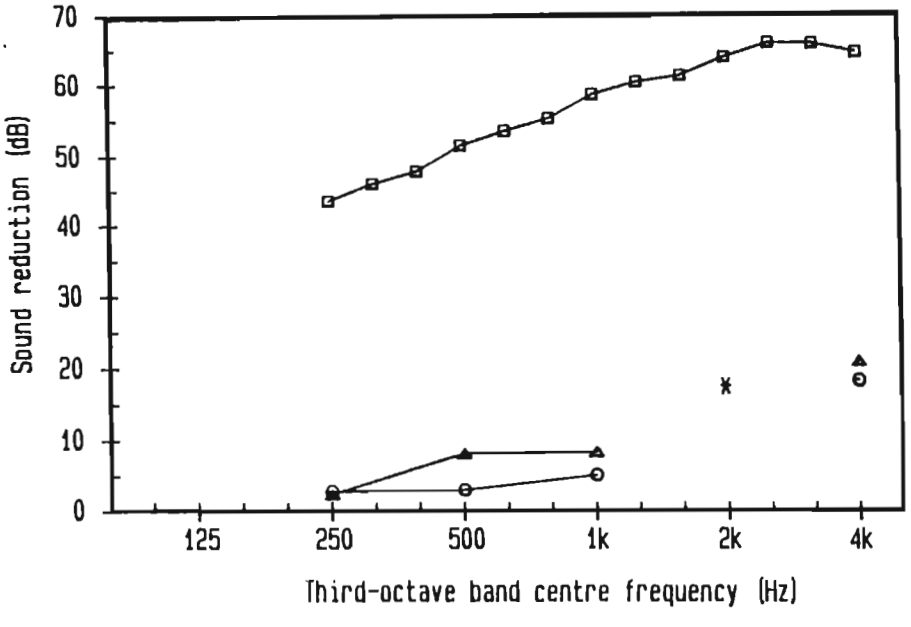

Figure 4.9

The effect of sound absorption by the test object on the sound reduction index of a 220mm brick wall determined by the intensity method.

- □ 8,3m2 wall uncladded
- o wall cladded with 8,3m2 glass wool of 75mm thickness (predicted)
- △ wall cladded with 8,3m2 glass wool of 75mm thickness (measured)
- * absorbed intensity I_A > transmitted intensity I_D

4.6.2 Absorption error : open window

The effect of sound absorption by the test object is further illustrated by considering the sound insulation test on an open window, described in Section 4.2.5. Ideally, an open window has zero sound reduction, while all the sound incident on it from the reverberant field in the receiving room is absorbed. In the case under consideration (A_F = 1,82 m^2; A = 7,0 m^2; $R_F \simeq 0$ dB; R > 30 dB), flanking may be regarded as negligible.

The predicted error Le in Table 4.16 was calculated by Eq. (3.57), using $h_F = 0$ and $\alpha_A = 1{,}0$ for all frequencies. The values used for $S\alpha$ are those determined in the experiment described in Section 4.2.5(a)(2). Correction of the sound reduction indices R3 of Table 4.11 for the effect of sound absorption by the open window results in the indices R4 listed in Table 4.14. These corrected values,

$$R4 = R3 - Le \quad \text{dB}, \tag{4.8}$$

are seen to be closer to the theoretical value R = 0 dB and are in good agreement with the values R2 of Table 4.11 obtained by the classic two-room method. Note that in the experiment under consideration, the transmission room was used as receiving room, hence the small values of $S\alpha$.

Table 4.16

The effect of sound absorption by the test object on the sound reduction index of an open window, determined by the sound intensity method.
Test object: 1,82 m^2 open window in 220 mm brick wall.

$S\alpha$ = receiving room absorption, including $A\alpha_A$ = 1,8 m^2 of the open window.

Le = predicted error, Eq. (3.57);

h_F = 0.

Octave f_c (Hz)	$S\alpha$ (m^2)	Le (dB)	R3 Table 4.10	R4 Eq.(4.8)	R2 Table 4.10
125	5,6	1,7	3,0	1,3	4,1
250	6,8	1,4	2,1	0,7	1,5
500	7,0	1,3	0,6	-0,7	-0,7
1 000	6,8	1,4	1,4	0,0	-0,5
2 000	7,6	1,2	0,5	-0,7	0,5
4 000	10,1	0,9	2,0	1,1	1,0

4.6.3 Absorption error: windows and filler walls

In practice the sound absorption coefficients of test objects and flanking walls are generally very low. This, however, does not completely eliminate the absorption error, since the latter also depends upon the flanking factor. Hence, no matter how low the absorption coefficient (as long as it is finite), Eq. (3.57) shows that a flanking factor can be found for which the sound intensity result would become unreliable. It is therefore of interest to consider the risk of absorption error for the sound insulation tests conducted on some of the test objects and filler walls described in Sections 4.2 and 4.3.

(a) Window 9,5L(200A)10S and 220 mm brick filler wall The sound intensity method was used to determine the sound insulation of Window 9,5L(200A)10S (Section 4.2.2) as well as the filler wall (Section 4.3.1). The question is whether the absorption error was negligible. Using Eq. (3.57), the predicted error is found to be well below 1,0 dB, as shown in Table 4.17. The values used for α_A were obtained from tables in the literature [105, 143].

Table 4.17

Predicted absorption error for Window 9,5L(200A)10S and 220 mm brick wall.

Window area = 2,1 m^2; wall area = 6,7 m^2.

$S\alpha$ = receiving room absorption, including $A\alpha_A$ of the test object;

Le = predicted error, Eq. (3.57);

h_F = (flanking power)/(direct power).

Octave f_c (Hz)	Window 9,5L(200A)10S				220 mm brick filler wall			
	$S\alpha$ (m^2)	$A\alpha_A$ (m^2)	h_F	Le (dB)	$S\alpha$ (m^2)	$A\alpha_A$ (m^2)	h_F	Le (dB)
125	9,9	0,09	5,86	0,3	9,9	0,13	0,17	0,1
250	9,7	0,09	5,86	0,3	9,7	0,13	0,17	0,1
500	13,1	0,06	8,66	0,2	13,2	0,20	0,12	0,1
1 000	11,9	0,06	2,80	0,1	12,1	0,27	0,36	0,1
2 000	14,1	0,04	0,28	0,0	14,4	0,34	3,57	0,5
4 000	25,5	0,04	0,74	0,0	25,8	0,34	1,36	0,1

(b) Window 9,5L(500A)10S and P220P(150A)110P filler wall As in the previous case, the absorption error in Table 4.18 is seen to be well below 1,0 dB. Consider the conditions which would cause an absorption error Le > 1,5 dB in the estimated sound reduction index of the wall at 1 kHz, if the sizes and absorption properties of the window and the wall remain unchanged. Solving Eq. (3.57) for h_F yields

$$h_F < \frac{S\alpha}{A\alpha_A} (1 - 10^{-Le/10}) - 1 \quad . \tag{4.9}$$

For the window test ($S\alpha/A\alpha_A$ = 188), this requirement becomes h_F < 54. The requirement for testing the wall whilst containing the window is h_F < 12.

Table 4.18

Predicted absorption error for Window 9,5L(500A)10S and P220P(150A)110P filler wall.

Window area = 2,1 m^2; wall area = 6,7 m^2.

$S\alpha$ = receiving room absorption, including $A\alpha_A$ of the test object;

Le = predicted error, Eq. (3.57);

h_F = (flanking power)/(direct power).

Octave	Window 9,5L(500A)10S				Brick filler wall			
f_c (Hz)	$S\alpha$ (m^2)	$A\alpha_A$ (m^2)	h_F	Le (dB)	$S\alpha$ (m^2)	$A\alpha_A$ (m^2)	h_F	Le (dB)
125	9,9	0,09	1,58	0,1	9,9	0,13	0,63	0,1
250	9,7	0,09	5,34	0,3	9,7	0,13	0,19	0,1
500	13,1	0,06	4,15	0,1	13,2	0,20	0,24	0,1
1 000	11,9	0,06	2,50	0,1	12,1	0,27	0,40	0,1
2 000	14,1	0,04	0,77	0,0	14,4	0,34	1,30	0,2

4.7 REACTIVITY AT THE SURFACE OF THE TEST OBJECT

The validity of the formula derived for the reactivity at the surface of the test object in Section 3.4.3, was examined by comparing the reactivity levels measured at the surface of test objects to those predicted by Eq. (3.103). Predicted and measured values of LR for Window 9,5L(200A)10S mounted in a 220 mm brick filler wall and for Window 9,5L(500A)10S mounted in wall P220P(150A)110P, are presented in Table 4.19. The results are in support of the theory developed in Section 3.4.3.

Table 4.19

Predicted and measured reactivity levels LR at the surface of two test objects.

Case 1: Window 9,5L (200A)10S mounted in 220 mm brick filler wall.

Case 2: Window 9,5L(500A)10S mounted in P220P(150A)110P brick filler wall.

T = reverberation times of receiving room;

h_F = ratio: (power through filler wall)/(power through test object)

Third-octave f_c (Hz)	T	Case 1			Case 2		
		h_F	LR(dB) predicted	LR(dB) measured	h_F	LR(dB) predicted	LR(dB) measured
100	5,9	8,1	11,7	10,2	0,7	5,6	10,3
125	6,9	5,9	11,3	11,7	1,6	7,5	7,4
160	5,5	4,4	9,4	11,4	2,2	7,5	10,3
200	5,6	3,1	8,4	8,4	3,8	9,0	8,4
250	5,1	5,9	10,1	10,5	5,3	9,7	8,9
315	5,1	6,6	10,4	8,3	3,3	8,3	7,2
400	5,2	15,8	13,7	11,4	5,0	9,6	9,6
500	5,1	8,7	11,4	8,5	4,1	8,9	9,3
630	5,4	14,7	13,6	10,5	5,7	10,2	10,3
800	5,5	6,4	10,6	9,0	3,1	8,4	10,3
1 000	5,6	2,8	8,2	8,9	2,5	7,9	9,3
1 250	5,5	0,8	5,5	6,8	1,7	6,9	6,7
1 600	5,1	0,5	4,8	5,6	0,8	5,3	5,7
2 000	4,7	0,4	4,3	4,5	0,8	5,1	5,5
2 500	4,0	0,6	4,3	4,8	-	-	-
3 150	3,2	1,5	4,9	4,5	-	-	-
4 000	2,6	3,6	6,1	6,0	-	-	-

4.8 ASSESSMENT OF THE VALIDITY OF SOUND INSULATION TESTS BY THE INTENSITY METHOD BY EMPLOYMENT OF THE CRITERIA FOR MINIMUM RECEIVING ROOM REQUIREMENTS

4.8.1 General

It has been shown in Section 3.4.4 that for a given measurement system the receiving room should contain a certain minimum amount of sound absorption. This is to ensure that the reactivity LR at the measurement surface is kept within the dynamic range (common mode rejection index LRm) of the measurement system. Since the latter figure depends on the ratio (microphone spacing Δr)/(phase mismatch error ε), the minimum amount of absorption $S\alpha$ required in the receiving room can be reduced by using a larger microphone spacing. Practical sound intensity meters usually provide three fixed gain settings corresponding to microphone spacings of approximately 6 mm, 12 mm and 50 mm. The use of a 100 mm spacer for sound insulation tests is not considered to be practical, as it would set an upper frequency limit of only 250 Hz. Hence, to cover the frequency range from 100 Hz to 4 kHz, measurements would have to be repeated for three different microphone spacings, rather than two.

The practical implications of the criteria developed in Section 3.4.4 in respect of minimum receiving room absorption in relation to the performance of the measurement system, will now be examined by analysis of various test cases presented in the foregoing sections. The validity of results obtained by the intensity method will be examined for each test by calculating the minimum amount of sound absorption $S\alpha$ (maximum reverberation time T) required in the receiving room, assuming that the sound insulation test is conducted with the aid of a Model A83 SIM portable intensity meter, using microphone spacings of 15 mm and 60 mm. The analysis is performed in each case for selective determination of sound reduction indices of the test object as well as the filler wall containing it.

The results given in Tables 4.20 to 4.27 were obtained as follows:

Reverberation time T : Average reverberation times measured in the receiving room.

Sound reduction R_F : The sound reduction index of the flanking structure; the filler wall index if the panel is under test and vice versa.

Sound reduction R : The sound reduction index of the component under test.

Flanking ratio h_F : (Flanking power)/(direct power); Eq. (2.51)

Reactivity predicted LR : Reactivity near the surface under investigation predicted by Eq. (3.103).

Reactivity measured LR : Reactivity measured near the surface under investigation.

Phase mismatch ε : The phase error introduced by the measurement system, including the microphones; measured with the microphones placed in a rigidly terminated standing-wave tube excited with random noise.

CMRI LRm : The common mode rejection index of the measurement system; Eq. (3.77).

Minimum absorption $S\alpha$: The minimum receiving room absorption (m^2) required to reduce the intensity error for a given set of instrument performance figures (CMRI) to 2,0 dB; Eq. (3.110), ΔL = 4,3 dB.

Maximum reverberation T : The maximum reverberation times allowed in the receiving room to reduce the intensity error for a given instrument to 2,0 dB; T = 0,16 V/(minimum $S\alpha$).

4.8.2 Case 1: sound insulation test on Door A mounted in 220 mm brick wall

The analysis in Table 4.20 shows that the reverberation times which prevailed during the test were well below the maximum values required for an error of less than 2,0 dB, even if the low-frequency measurements (125 - 500 Hz) were performed with a spacing Δr = 15 mm instead of 60 mm, which is normally used in reactive fields. For the test under consideration the intensity method could be used with very little sound absorption in the receiving room. Note that the common mode rejection index of the intensity meter amply exceeds the reactivity level expected at the surface of the test object.

4.8.3 Case 2: sound insulation test on 220 mm brick wall containing Door A

This test, applied selectively to the filler wall containing the door of the previous test, is described in Section 4.3.1. The analysis given in Table 4.21 shows that the minimum requirements for the filler wall test are more stringent than that for the door; the reactivity at the surface of the wall is considerably higher than at the door. In this case it is imperative to use the 60 mm spacer at 125 Hz, since Δr = 15 mm would require a reverberation time $T < 1,9$ s. In the 2 kHz third-octave band, for which Δr = 60 mm is too large (finite distance approximation error > 2 dB), Eq. (3.110) calls for a maximum reverberation time $T < 4,6$ s, while the receiving room actually had a reverberation time $T = 4,7$ s. Strictly speaking, a small amount of absorption should have been added to the reverberation room to reduce its reverberation time. The 3,7 dB difference at 2 kHz between the results given by the classic two-room method and the intensity method (Fig. 4.7) is believed to be partly due to intensity meter error in the highly reactive field.

Table 4.20

Validity of intensity method results according to the criteria for minimum receiving room absorption (maximum reverberation time) of Section 3.4.4. Case 1: sound insulation test on Door A mounted in 220 mm brick wall.

Constants: A_F = 6,8 m^2; A = 2,0 m^2; V = 414 m^3

Analysis based on requirement Lem < 2,0 dB; ΔL > 4,3 dB

Third-octave centre frequency (Hz)			125	250	500	1000	2000
Test conditions							
Reverberation times		T	6,9	5,1	5,1	5,6	4,7
Sound reduction:	Wall	R_F	40,2	43,5	51,5	58,5	63,7
	Door	R	30,8	39,0	44,0	49,0	50,0
Flanking ratio		h_F	0,4	1,2	0,6	0,4	0,1
Reactivity:	predicted	LR	5,2	5,7	4,7	4,6	3,6
Instrumentation							
Phase mismatch (degrees)		ε	0,11	0,06	0,10	0,31	0,49
CMRI (Δr = 15 mm)		LRm	12,5	18,1	18,9	17,0	18,0
CMRI (Δr = 60 mm)		LRm	18,5	24,1	24,9	-	-
Minimum requirements							
Minimum Sα (Δr = 15 mm)			4,0	1,5	0,9	1,2	0,8
Minimum Sα (Δr = 60 mm)			0,9	0,4	0,2	-	-
Maximum T (Δr = 15 mm)			16,6	43,4	72,2	53,0	81,9
Maximum T (Δr = 60 mm)			75,5	179,4	296,0	-	-

Table 4.21

Validity of intensity method results according to the criteria for minimum receiving room absorption (maximum reverberation time) of Section 3.4.4. Case 2: sound insulation test on 220 m brick wall containing Door A.

Constants: A_F = 2,0 m^2; A = 6,8 m^2; V = 414 m^3

Analysis based on requirement Lem < 2,0 dB; ΔL > 4,3 dB

Third-octave centre frequency (Hz)			125	250	500	1000	2000
Test conditions							
Reverberation times		T	6,9	5,1	5,1	5,6	4,7
Sound reduction:	Door	R_F	30,8	39,0	44,0	49,0	50,0
	Wall	R	40,2	43,5	51,5	58,5	63,7
Flanking ratio		h_F	2,6	0,8	1,7	2,6	6,9
Reactivity:	predicted	LR	13,3	9,4	10,8	12,5	15,0
Instrumentation							
Phase mismatch (degrees)		ε	0,11	0,06	0,10	0,31	0,49
CMRI (Δr = 15 mm)		LRm	12,5	18,1	18,9	17,0	18,0
CMRI (Δr = 60 mm)		LRm	18,5	24,1	24,9	-	-
Minimum requirements							
Minimum Sα (Δr = 15 mm)			34,7	4,3	5,2	11,1	19,0
Minimum Sα (Δr = 60 mm)			7,6	1,0	1,3	-	-
Maximum T (Δr = 15 mm)			1,9	15,4	12,8	6,0	4,6
Maximum T (Δr = 60 mm)			8,7	63,6	52,7	-	-

4.8.4 Case 3: sound insulation test on Window 9,5L(200A)10S mounted in 220 mm brick wall

It has been shown in this thesis that the classic two-room method is not suited to selective determination of sound reduction indices if the flanking factor exceeds a value of approximately 1,0. This was practically demonstrated by the result of the sound insulation test on Window 9,5L(200A)10S (See Fig. 4.4). The validity of the intensity method in this case may be assessed by the analysis presented in Table 4.22. Except for the 125 Hz third-octave band for which the 60 mm spacer is needed, the 15 mm spacer could safely be used in this highly reverberant receiving room.

Unlike the classic two-room method, the validity of the intensity method does not depend essentially upon the flanking factor h_f, but rather on the reactivity at the measurement surface. As stated in Eq. (3.103), LR is determined by h_f as well as the ratio $A/S\alpha$. Hence, although h_f in the test under consideration is generally larger than that in Case 2 of Section 4.8.3, the present case is handled with greater ease and with a smaller risk of error, owing to the relatively low levels of reactivity prevailing at the window surface.

4.8.6 Case 4: sound insulation test on 220 mm brick wall containing Window 9,5L(200A)10S

This test has not actually been performed but the analysis in Table 4.23 shows that no difficulties should arise provided the 60 mm spacer is used in the 125 Hz third-octave band.

Table 4.22

Validity of intensity method results according to the criteria for minimum receiving room absorption (maximum reverberation time) of Section 3.4.4. Case 3: sound insulation test on window 9,5L(200A)10S mounted in 220 mm brick wall.

Constants: A_F = 6,67 m^2; A = 2,13 m^2; V = 414 m^3

Analysis based on requirement Lem < 2,0 dB; ΔL > 4,3 dB

Third-octave centre frequency (Hz)			125	250	500	1000	2000
Test conditions							
Reverberation times		T	6,9	5,1	5,1	5,6	4,7
Sound reduction:	Wall	R_F	40,2	43,5	51,5	58,5	63,7
	Window	R	42,9	46,2	55,9	58,0	54,8
Flanking ratio		h_F	5,9	5,9	8,7	2,8	0,4
Reactivity:	predicted	LR	11,3	10,1	11,4	8,2	4,3
	measured	LR	11,7	10,5	8,5	8,9	4,5
Instrumentation							
Phase mismatch (degrees)		ε	0,11	0,06	0,10	0,31	0,49
CMRI (Δr = 15 mm)		LRm	12,5	18,1	18,9	17,0	18,0
CMRI (Δr = 60 mm)		LRm	18,5	24,1	24,9	-	-
Minimum requirements							
Minimum Sα (Δr = 15 mm)			20,8	5,0	5,9	3,7	1,1
Minimum Sα (Δr = 60 mm)			4,6	1,2	1,4	-	-
Maximum T (Δr = 15 mm)			3,2	13,2	11,3	18,1	62,8
Maximum T (Δr = 60 mm)			14,4	54,4	46,4	-	-

Table 4.23

Validity of intensity method results according to the criteria for minimum receiving room absorption (maximum reverberation time) of Section 3.4.4. Case 4: sound insulation test on 220 mm brick wall containing Window 9,5L(200A)10S.

Constants: A_F = 2,13 m^2; A = 6,67 m^2; V = 414 m^3
Analysis based on requirement Lem < 2,0 dB; ΔL > 4,3 dB

Third-octave centre frequency (Hz)			125	250	500	1000	2000
Test conditions							
Reverberation times		T	6,9	5,1	5,1	5,6	4,7
Sound reduction:	Window	R_F	42,9	46,2	55,9	58,0	54,8
	Wall	R	40,2	43,5	51,5	58,5	63,7
Flanking ratio		h_F	0,2	0,2	0,1	0,4	2,5
Reactivity:	predicted	LR	8,8	7,6	7,5	8,5	11,5
Instrumentation							
Phase mismatch (degrees)		ε	0,11	0,06	0,10	0,31	0,49
CMRI (Δr = 15 mm)		LRm	12,5	18,1	18,9	17,0	18,0
CMRI (Δr = 60 mm)		LRm	18,5	24,1	24,9	-	-
Minimum requirements							
Minimum Sα (Δr = 15 mm)			11,2	2,7	2,1	4,1	8,2
Minimum Sα (Δr = 60 mm)			2,5	0,7	0,5	-	-
Maximum T (Δr = 15 mm)			5,9	24,5	31,1	16,2	8,1
Maximum T (Δr = 60 mm)			26,9	101,3	128,0	-	-

4.8.6 Case 5: sound insulation test on Window 9,5L(500A)10S mounted in P220P(150A)110P brick wall

In contrast with the complete failure of the classic two-room method (Fig. 4.5) due to unfavourable flanking conditions ($h_F > 1$), the analysis in Table 4.24 shows that the situation presents no difficulties at all in using the intensity method. Reactivity levels are much lower than the common mode rejection indices of the intensity meter, even for Δr = 15 mm. It is therefore not necessary in this case to use the 60 mm spacer at low frequencies.

4.8.7 Case 6: sound insulation test on P220P(150A)110P brick wall containing Window 9,5L(500A)10S

The analysis in Table 4.25 shows that no difficulties should arise with the intensity method, provided that the 60 mm spacer is used in the 125 Hz third-octave band. The method may be applied selectively to either the window or the filler wall without having to increase the amount of absorption in the reverberation room.

Table 4.24

Validity of intensity method results according to the criteria for minimum receiving room absorption (maximum reverberation time) of Section 3.4.4. Case 5: sound insulation test on Window 9,5L(500A)10S mounted in P220P(150A)110P brick wall.

Constants: A_F = 6,67 m^2; A = 2,13 m^2; V = 414 m^3

Analysis based on requirement Lem < 2,0 dB; ΔL > 4,3 dB

Third-octave centre frequency (Hz)			125	250	500	1000	2000
Test conditions							
Reverberation times		T	6,9	5,1	5,1	5,6	4,7
Sound reduction:	Wall	R_F	48,8	54,1	65,0	73,9	77,0
	Window	R	45,8	56,4	66,2	72,9	70,9
Flanking ratio		h_F	1,6	5,3	4,1	2,5	0,8
Reactivity:	predicted	LR	7,5	9,7	8,9	7,9	5,1
	measured	LR	7,4	8,9	9,3	9,3	5,5
Instrumentation							
Phase mismatch (degrees)		ε	0,11	0,06	0,10	0,31	0,49
CMRI (Δr = 15 mm)		LRm	12,5	18,1	18,9	17,0	18,0
CMRI (Δr = 60 mm)		LRm	18,5	24,1	24,9	-	-
Minimum requirements							
Minimum Sα (Δr = 15 mm)			7,8	4,7	3,1	3,4	1,3
Minimum Sα (Δr = 60 mm)			1,7	1,1	0,8	-	-
Maximum T (Δr = 15 mm)			8,5	14,2	21,2	19,7	49,8
Maximum T (Δr = 60 mm)			38,3	58,8	87,1	-	-

Table 4.25

Validity of intensity method results according to the criteria for minimum receiving room absorption (maximum reverberation time) of Section 3.4.4. Case 6: sound insulation test on P220P(150A)110P brick wall containing Window 9,5L(500A)10S.

Constants: A_F = 2,13 m^2; A = 6,67 m^2; V = 414 m^3

Analysis based on requirement Lem < 2,0 dB; ΔL > 4,3 dB

Third-octave centre frequency (Hz)			125	250	500	1000	2000
Test conditions							
Reverberation times		T	6,9	5,1	5,1	5,6	4,7
Sound reduction:	Window	R_F	45,8	56,4	66,2	72,9	70,9
	Wall	R	48,8	54,1	65,0	73,9	77,0
Flanking ratio		h_F	0,6	0,2	0,2	0,4	1,3
Reactivity:	predicted	LR	10,0	7,7	7,9	8,6	9,9
Instrumentation							
Phase mismatch (degrees)		ε	0,11	0,06	0,10	0,31	0,49
CMRI (Δr = 15 mm)		LRm	12,5	18,1	18,9	17,0	18,0
CMRI (Δr = 60 mm)		LRm	18,5	24,1	24,9	-	-
Minimum requirements							
Minimum Sα (Δr = 15 mm)			15,6	2,7	2,4	4,2	5,4
Minimum Sα (Δr = 60 mm)			3,4	0,7	0,6	-	-
Maximum T (Δr = 15 mm)			4,2	24,2	28,0	15,7	12,2
Maximum T (Δr = 60 mm)			19,2	100,0	115,0	-	-

4.8.8 Case 7: sound insulation test on 6 mm hardboard panel mounted in 220 mm brick wall

Considering the small thickness of the panel as compared to that of the brick filler wall, it stands to reason that the panel will strongly beam direct sound into the receiving room. This is confirmed by the very low reactivity levels predicted near the panel surface. As indicated by the large values of maximum reverberation time in Table 4.26, the test could be conducted in extremely reverberant conditions.

4.8.9 Case 8: sound insulation test on 220 brick wall containing 6 mm hardboard panel

The relatively strong radiation from the flanking panel together with the reverberant nature of the receiving room, constitute extremely unfavourable conditions for the measurement of the sound intensity radiated by the brick wall. Reactivity levels in the vicinity of the wall are expected to exceed the common mode rejection index of the measurement system for Δr = 15 mm. Upon examination of the minimum requirements for receiving room absorption given in Table 4.27, it is concluded that the intensity method could only be employed in this case by using Δr = 60 mm at frequencies below 2 kHz and by increasing the amount of absorption in the receiving room.

Table 4.26

Validity of intensity method results according to the criteria for minimum receiving room absorption (maximum reverberation time) of Section 3.4.4. Case 7: sound insulation test on 6 mm hardboard panel mounted in 220 mm brick wall.

Constants: A_F = 8,3 m^2; A = 0,5 m^2; V = 414 m^3

Analysis based on requirement Lem < 2,0 dB; ΔL > 4,3 dB

Third-octave centre frequency (Hz)			125	250	500	1000	2000
Test conditions							
Reverberation times		T	6,9	5,1	5,1	5,6	4,7
Sound reduction:	Wall	R_F	40,2	43,5	51,5	58,5	63,7
	Panel	R	14,5	18,9	25,2	30,3	33,7
Flanking ratio		h_F	0,0	0,1	0,0	0,0	0,0
Reactivity:	predicted	LR	1,6	1,2	1,2	1,3	1,1
Instrumentation							
Phase mismatch (degrees)		ε	0,11	0,06	0,10	0,31	0,49
CMRI (Δr = 15 mm)		LRm	12,5	18,1	18,9	17,0	18,0
CMRI (Δr = 60 mm)		LRm	18,5	24,1	24,9	-	-
Minimum requirements							
Minimum Sα (Δr = 15 mm)			0,7	0,2	0,1	0,2	0,2
Minimum Sα (Δr = 60 mm)			0,2	0,0	0,0	-	-
Maximum T (Δr = 15 mm)			88,6	363,0	446,0	286,0	369,0
Maximum T (Δr = 60 mm)			402,0	1497,0	1832,0	-	-

Table 4.27

Validity of intensity method results according to the criteria for minimum receiving room absorption (maximum reverberation time) of Section 3.4.4. Case 8: sound insulation test on 220 mm brick wall containing 6 mm hardboard panel.

Constants: A_F = 0,5 m^2; A = 8,3 m^2; V = 414 m^3

Analysis based on requirement Lem < 2,0 dB; ΔL > 4,3 dB

Third-octave centre frequency (Hz)			125	250	500	1000	2000
Test conditions							
Reverberation times		T	6,9	5,1	5,1	5,6	4,7
Sound reduction:	Panel	R_F	14,5	18,9	25,2	30,3	33,7
	Wall	R	40,2	43,5	51,5	58,5	63,7
Flanking ratio		h_F	22,4	17,4	25,7	131,8	60,2
Reactivity:	predicted	LR	22,1	19,8	21,4	28,7	24,6
Instrumentation							
Phase mismatch (degrees)		ε	0,11	0,06	0,10	0,31	0,49
CMRI (Δr = 15 mm)		LRm	12,5	18,1	18,9	17,0	18,0
CMRI (Δr = 60 mm)		LRm	18,5	24,1	24,9	-	-
Minimum requirements							
Minimum Sα (Δr = 15 mm)			277,9	52,7	63,4	498,0	180,0
Minimum Sα (Δr = 60 mm)			61,3	12,8	15,4	-	-
Maximum T (Δr = 15 mm)			0,2	1,3	1,0	0,1	0,4
Maximum T (Δr = 60 mm)			1,1	5,2	4,3	-	-

4.9 DIAGNOSTIC SOUND TRANSMISSION ANALYSIS

4.9.1 Window 9,5L(200A)10S

The relative amounts of sound power radiated by the frame, the seal and the window pane were examined by sound intensity measurement along a line extending across the window and part of the wall. The distance between the microphone and the window surface was 50 mm.

Sound intensity levels LI and sound pressure levels LP are presented graphically in Fig. 4.10. The sound intensity levels show a marked difference with regard to the sound transmission of the wall and that of the window in the 2kHz third-octave band; a result which tallies with the sound reduction indices obtained previously (Table 4.5). Note that the LP curve, which gives some indication of the sound level perceived by auditive inspection close to the radiation sufaces, shows a rather inconclusive increase in sound level if the microphone is moved from the wall towards the centre of the window.

The result in Fig. 4.10 which was obtained by measuring at 60 mm distance intervals, indicates that the frame-and-seal combination is very effective; the radiation from this region is well below the level observed at the window pane.

A more detailed analysis of sound radiation from the frame was obtained by sound intensity measurement at 10 mm distance intervals as shown in Fig. 4.11. Upon examination of LI it is concluded that the gradual level increase across the width of the frame should be seen as a natural transition resulting from interference between the low sound power level at the wall and the higher level at the window pane. A leak anywhere on the frame would have caused a sharp level increase in the LI curve.

The analyses given in Tables 4.17, 4.22 and 4.23 indicate that reliable sound intensity measurements could be performed without any difficulty at the surfaces of the window and the filler wall under consideration. The measured levels LI in Figs. 4.10 and 4.11 may therefore be regarded as an accurate account of sound radiation along the path AA'.

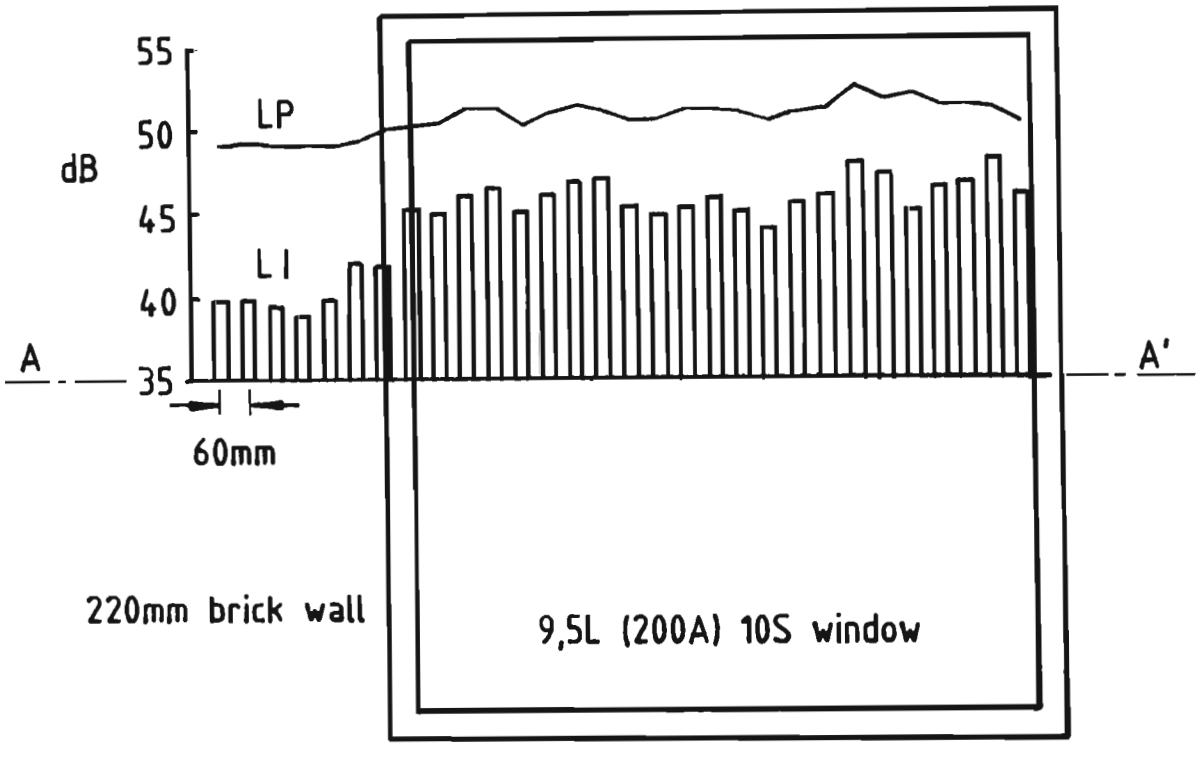

Figure 4.10

Diagnostic sound transmission analysis at the surface of window 9,5l (200A) 10S and flanking brick wall. Sound pressure levels LP and sound intensity levels LI measured along line AA' with intensity probe directed normally to the window surface. f=2kHz; distance between probe and window = 50mm.

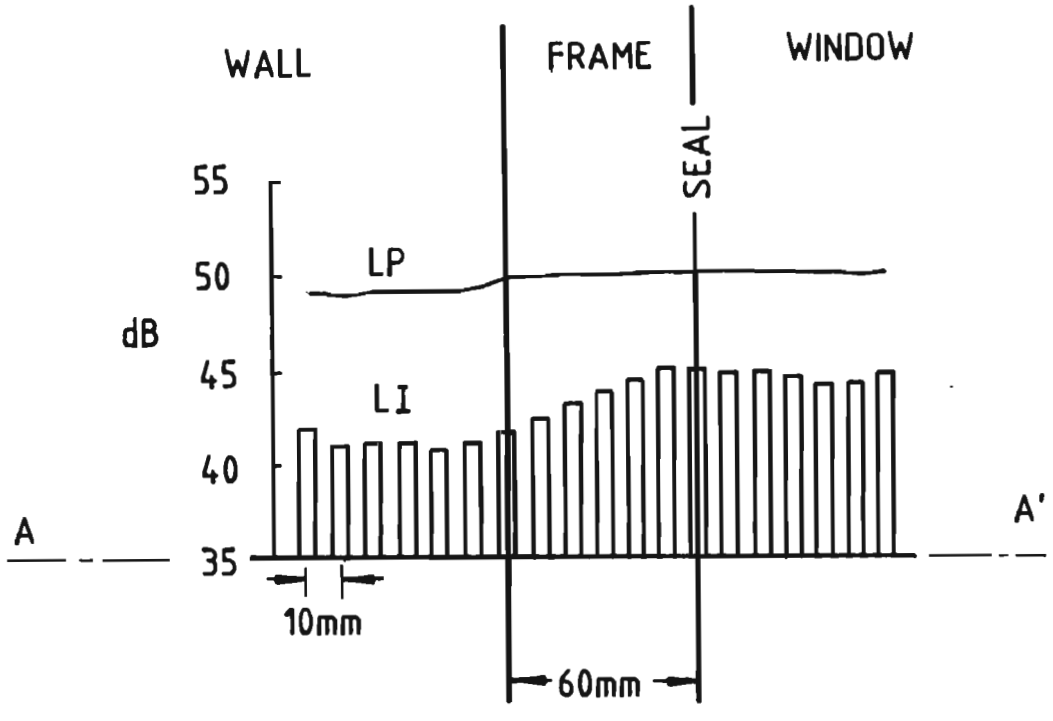

Figure 4.11

Examination of frame and seal insulation, Window 9,5L (200A) 10S. Sound pressure levels LP and sound intensity levels LI measured along line AA' with intensity probe directed normally to window surface f=2kHz

4.9.2 Window 9,5L(500A)10S

The efficiency of the seal used in this window was assessed by examination of the sound intensity level along two paths extending lengthwise along the seal at a distance of 50 mm from the window surface.

The results in Fig. 4.12(a) seem to point at non-uniformity in the sound insulation of the seal in the 1kHz third-octave band. In this case, however, where the sound radiation from the seal is low in relation to the total radiation from the window, the observed variation is of little consequence.

It would also appear that the seal is slightly more efficient along the section AA' (LI average = 20,0 dB) than along BB' (LI average = 22,0 dB). The result obtained in the 2kHz third-octave band (Fig. 4.12(b)) shows a similar difference in efficiency (12,2 dB and 14,7 dB, respectively).

4.9.3 Diagnostic analysis of the performance of a door

The sound insulation test on Door A described in Section 4.2.1 was performed in the laboratory on a prototype of a newly developed door. A production unit of this design was at a later stage encountered in a building where it was suspected of falling short of the performance attained by the prototype. Since the room containing the door was reverberant, it was decided to measure the sound insulation of the door with the source located in the reverberant room and with the relatively absorbent hallway adjacent to it acting as the receiving room. The measurement was performed with a B & K 3360 sound intensity analyzer, using Δr = 12 mm.

The result of the field test in Fig. 4.13 confirmed the suspicion that there was something wrong with the door; the decline in sound insulation at high frequencies indicated that the seal was probably leaking. Upon examination of the intensity field with a hand-held moving probe the leak was located at the bottom section of the seal.

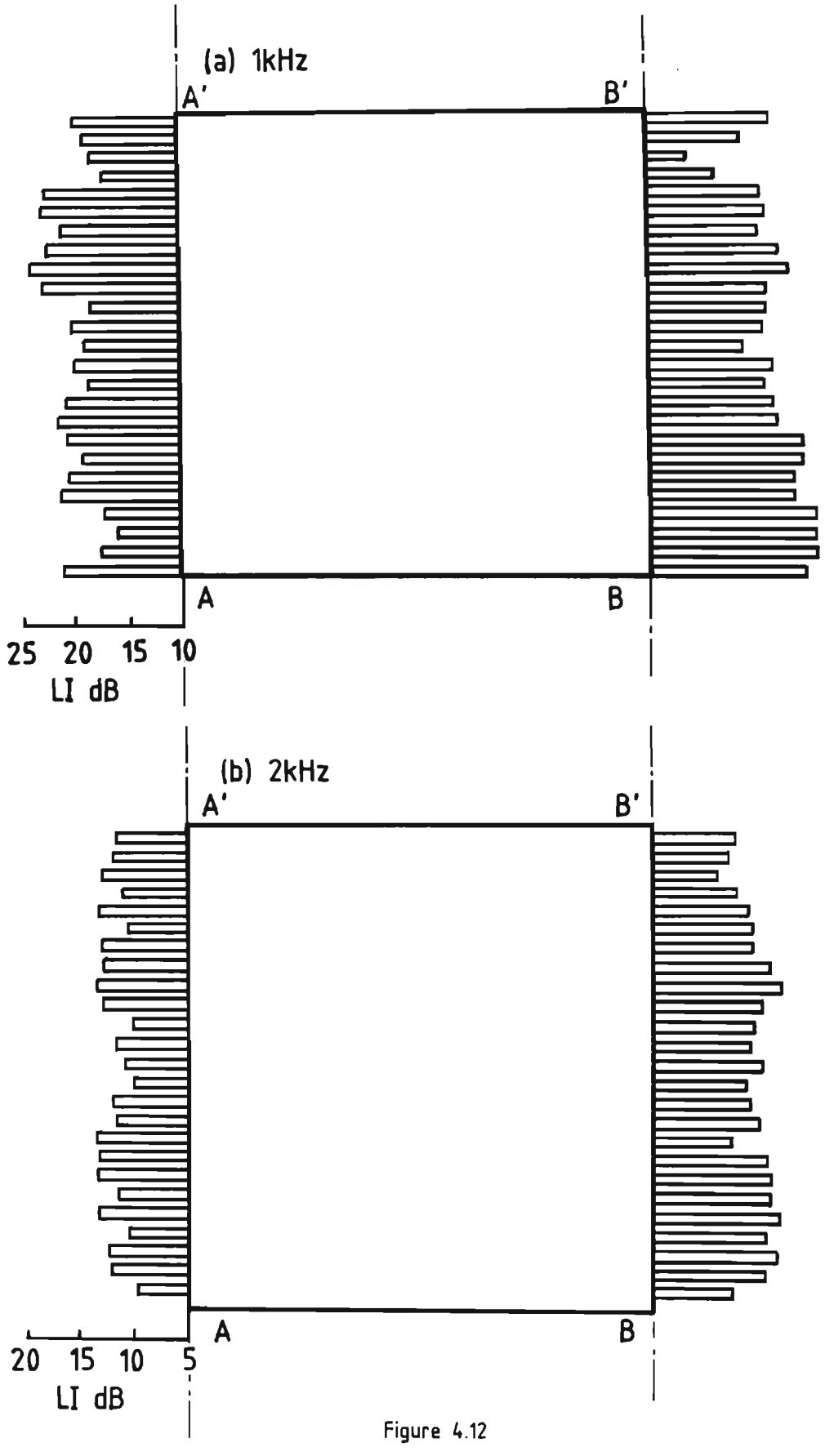

Figure 4.12

Sound intensity levels LI measured on lines AA' and BB' extending lengthwise along the seal of a window 9,5L (500A) 10S.
(a) Third-octave band centre frequency = 1kHz
(b) Third-octave band centre frequency = 2kHz.

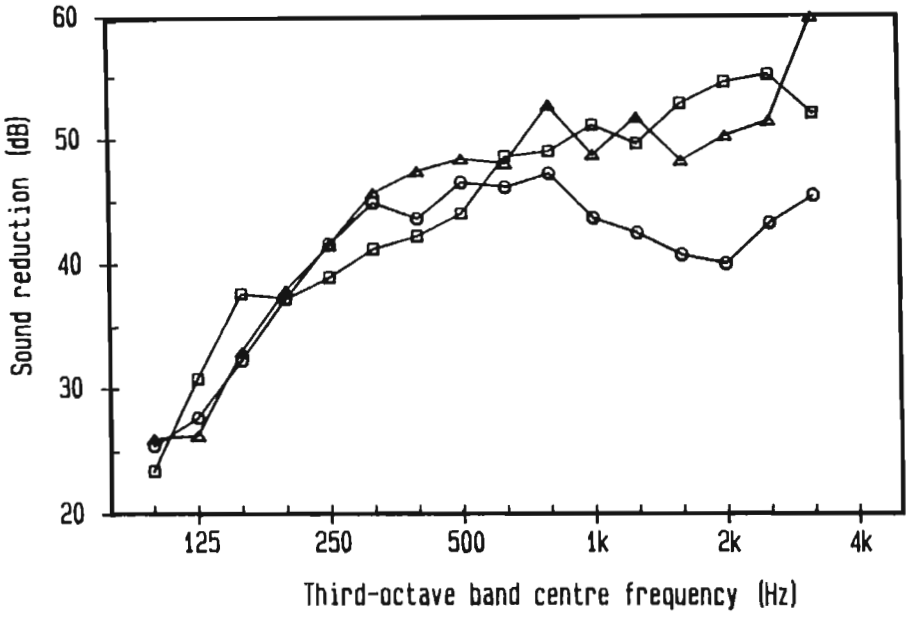

Figure 4.13

Sound reduction R of a door determined by the sound intensity method.

- □ Laboratory measurement on prototype door
- o Field measurement on production unit with faulty seal
- △ Field measurement on production unit, upper part only

Since the top section of the seal appeared to be intact, it was decided to assess the performance of the door as if the leak did not exist, by selective measurement of the sound insulation of the upper quarter section of the door. The result in Fig. 4.13 shows that, disregarding the defective seal, the production unit conformed to the performance standard set by the prototype in the laboratory test.

4.10 ASSESSMENT OF DIFFUSIVITY BY SOUND INTENSIMETRY

4.10.1 The characteristics of sound intensity fields in diffuse and non-diffuse rooms

A Brüel & Kjaer type 4204 reference sound source was successively placed in five acoustically different rooms, and the sound pressure and sound intensity levels were measured as functions of the radial distance from the source. Sound intensity was measured in octave bands using a model A80 SIM analog sound intensity meter with a microphone spacing of 15 mm.

The rooms were selected to cover the following range of acoustical properties, extending from a free field to an environment believed to be diffuse:

(1) anechoic room (free field);
(2) anechoic room containing a 1,2 x 2,5 m reflector (semi-free field);
(3) empty laboratory with absorbent ceiling (semi-reverberant);
(4) empty entrance hall, linked to staircases, passages and other rooms (reverberant, not expected to be diffuse);
(5) a reverberation room of the NPRL containing stationary diffusers (reverberant, expected to be diffuse).

Sound intensity and sound pressure levels in the 500 Hz-octave band as functions of distance from the reference source are shown in Fig. 4.14. The broken line, passing through the (1.0 m ; 0 dB) coordinate, depicts the inverse square law. All sound levels are normalized with respect to the value measured at a 1 m distance.

The intensity fluctuations observed in Fig. 4.14(b), (c) and (d) indicate a lack of directional diffusion in the corresponding ordinary rooms, while the inverse-square-law decay obtained in the reverberation room is in agreement with the expectation that, in this case, the reverberant sound field would be directionally diffuse. The reverberant part of the total sound field does not contribute to the net acoustic energy flow in the room and thus becomes "translucent" to the sound in-

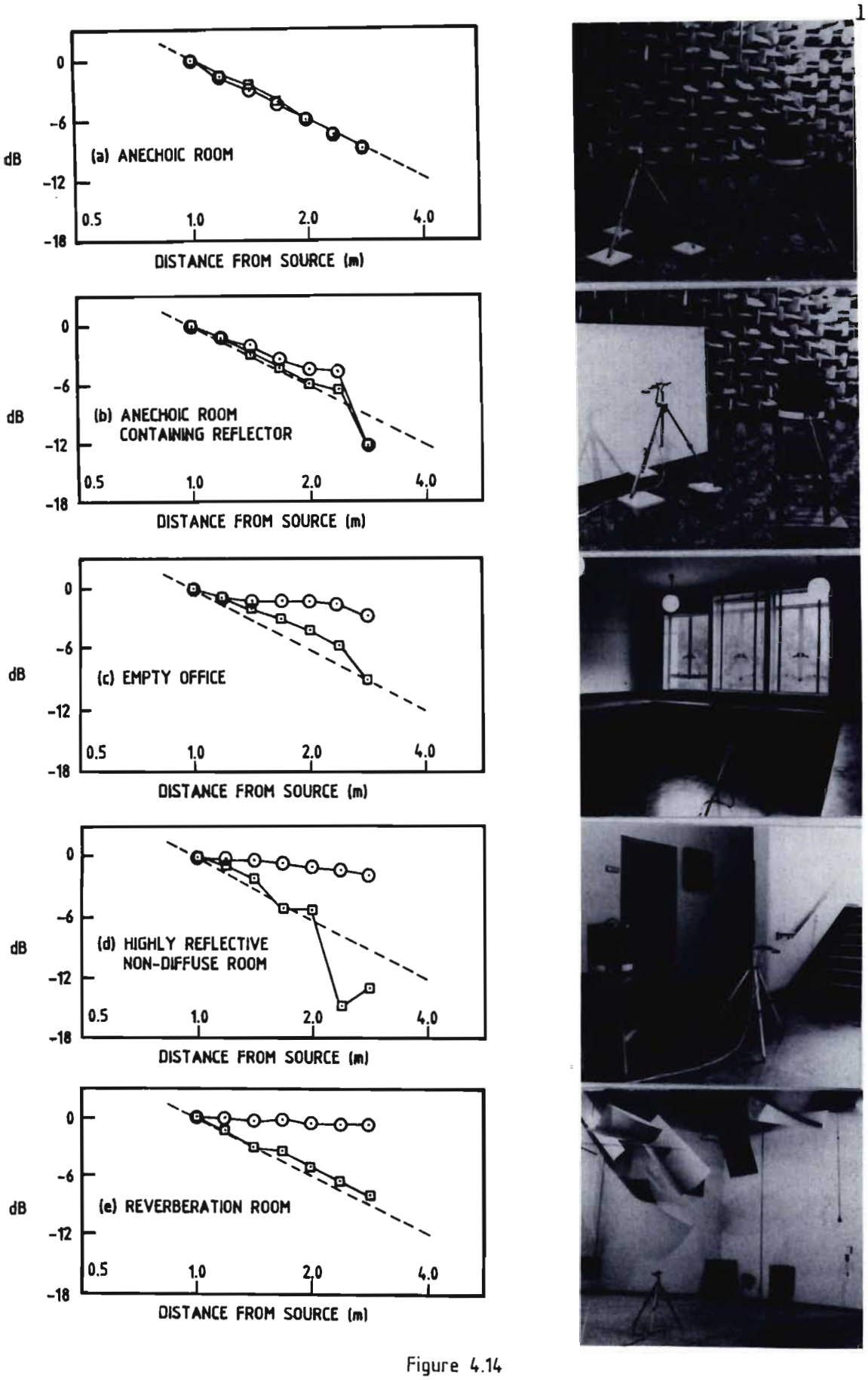

Figure 4.14

Sound intensity □ and energy density ○ in diffuse and non-diffuse fields.

tensity meter which only observes the net energy flow due to the direct sound field. In reverberant test-room practice, direct exposure of the test object to source radiation should be avoided in order to escape the distorting effect of the direct intensity field on the directionally balanced reverberant field. In this study of diffusion, intensity measurements were deliberately made in the well-defined direct field of a point source, using the apparent distortion of the reference field as an indicator for directional imbalance in the reverberant field. Thus, by sound intensity measurement, directional diffusion was examined by means of an inverse-square-law test, similar to that commonly used to check free-field conditions in anechoic rooms.

4.10.2 Diffusivity measurements in the vicinity of an open window in a reverberation room wall

The diffusivity meter described in Section 3.5.5 was used to investigate the degree of directional diffusivity along a line extending across a brick filler wall in the test aperture between the transmission test rooms employed in the previously described sound insulation tests. The filler wall contained an open window of 915 x 545 mm. Measured values of the degree of directional diffusivity d in the 125, 250 and 500 Hz octave bands, obtained with a microphone spacing Δr = 60 mm, are shown graphically in Fig. 4.15. These measurements were performed on the reverberation room side of the test aperture with absorptive material added to the adjacent room.

In a perfectly diffuse field the diffusivity would attain values d = 100 % at the wall and d = 50 % at an ideal open window. These values are well-approximated by the measured data, considering that d is expressed as a percentage. Differences between measured and theoretical values are caused by:

(a) a lack of perfect directional diffusion in the reverberation room;
(b) failure to simulate a perfect open window;
(c) the finite common mode rejection index of the sound intensity meter (Model A83 SIM).

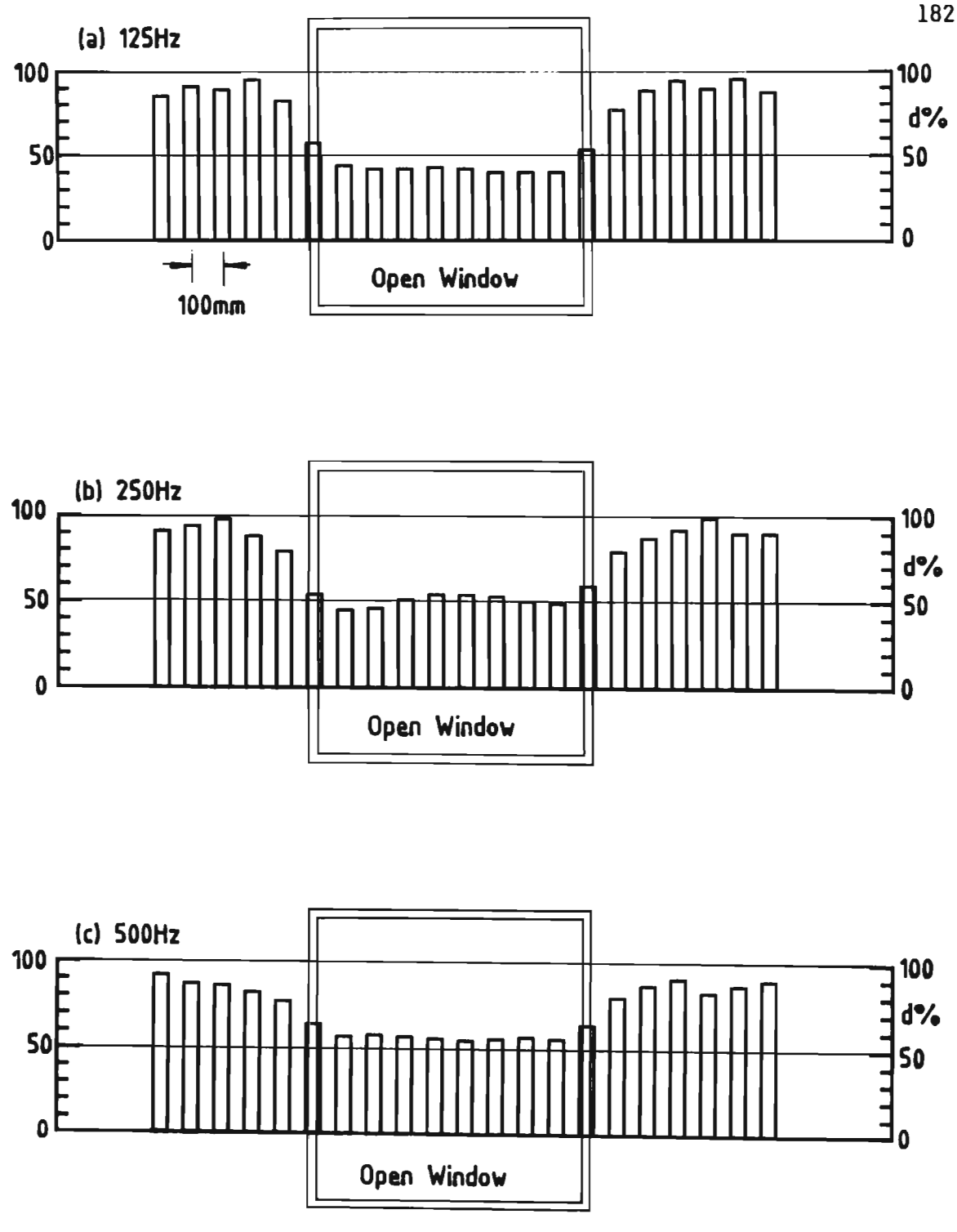

Figure 4.15

Degree of directional diffusivity d at a reverberation room wall containing an open window; measured with the direct-reading diffusivity meter described in Section 3.5.5; Δr=60mm.

(a) 125Hz octave band
(b) 250Hz octave band
(c) 500Hz octave band.

4.10.3 Application to sound transmission analysis by intensimetry

It has been shown in Section 3.5.4 that diffusivity requirements are different for sound insulation tests than for diagnostic transmission analysis by intensimetry. In the former case diffusivity is only important in relation to the source room, whereas diagnostic analysis of the transmitted power also requires a certain degree of directional diffusivity in the receiving room.

The significance of the diffusivity criteria developed in this thesis was examined by applying it to the sound transmission analyses conducted on Window 9,5L(200A)10S and described in previous sections of this chapter. Minimum requirements with respect to the intrinsic reactivity LRd and the degree of directional diffusivity d were calculated for sound insulation tests as well as diagnostic transmission analysis on the window and the 220 mm brick wall containing it. These figures are compared with the states of diffusivity which actually prevailed during the tests, determined by direct measurement with the portable diffusivity meter described in Section 3.5.5.

(a) Source room The minimum requirements with regard to LRd and d are given in Eqs. (3.142) and (3.143), respectively. For sound insulation tests $|Le| < 1{,}0$ dB yields

$$\{\ LRd > 12\ \text{dB};\quad d > 75\ \%\ \}\quad .$$

For the purpose of diagnostic transmission analysis $|Le| < 2{,}5$ dB will usually suffice, giving

$$\{\ LRd > 7\ \text{dB};\quad d > 56\ \%\ \}\quad .$$

The degree of directional diffusivity measured in the source room that was employed in the actual tests is shown in Fig. 4.16 for five positions at a height of 1,5 m above the floor in the centre region of the room. These positions lie within the volume traversed by the pressure microphone during sound insulation tests. The point (X ; Y) = (2 ; 0) lies at a distance of 2,0 m from the source which was situated on

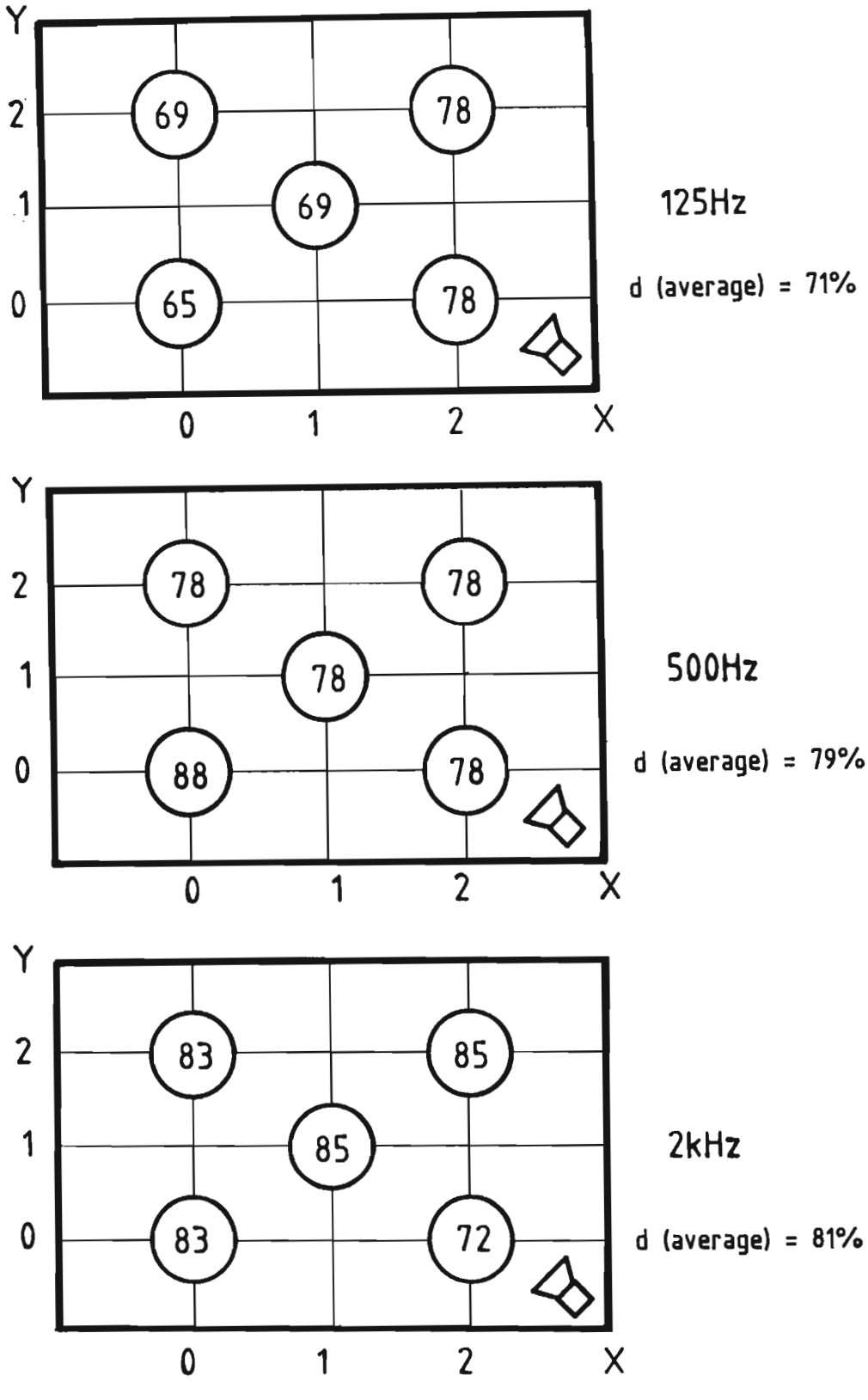

Figure 4.16

Degree of directional diffusivity d(%) measured at a height of 1,5m above the floor of the source room used for sound insulation tests on window 9,5L(200A)10S.

the floor. A microphone spacing Δr = 60 mm was used at 125 and 500 Hz while Δr = 15 mm was used at 2 kHz.

At low frequencies the diffusivity of the small room (V = 81 m^3) with its limited modal density is noticeably lower than at the higher frequencies. In the 125 Hz octave band the source room does not meet the diffusivity requirements to ensure $|Le| < 1,0$ dB for sound insulation tests. The average values measured in the room are

{ 125 Hz : LRd = 10,7 dB; d = 71 % }
{ 500 Hz : LRd = 13,4 dB; d = 79 % }
{ 2 kHz : LRd = 14,6 dB: d = 81 % }

(b) Receiving room Diffusivity requirements for diagnostic analysis of the power transmitted into the receiving room are given in Tables 4.28 and 4.29 for measurements near the surfaces of Window 9,5L(200A)10S and the associated 220 mm brick filler wall, respectively. Equations (3.148) and (3.149) were used to calculate LRd and d, respectively. These requirements are compared in the tables with the actual values measured in the receiving room at the filler wall in the absence of any transmission of sound from the source room. The room safely meets the requirements for diffusivity at all frequencies. The degree of directional diffusivity in the relatively large reverberation room (V = 414 m^3) with its large number of stationary diffusers is seen to be appreciably higher than in the source room which did not contain any diffusers.

Table 4.28

Receiving room diffusivity requirements for diagnostic sound transmission analysis by sound intensimetry, compared with values measured in NPRL reverberation room.

Test object : Window 9,5L(200A)10S in 220 mm brick filler wall.

Maximum error $|Le| < 1,0$ dB; $A = 2,13\ m^2$.

Octave-band centre frequency (Hz)		125	250	500	1000	2000
Flanking ratio	h_F	5,9	5,9	8,7	2,8	0,4
Room absorption (m^2)	$S\alpha$	9,6	13,0	13,0	11,8	14,1
Intrinsic reactivity	**LRd**					
Required; Eq. (3.148)		16,7	15,4	16,9	13,3	8,2
measured (average near wall)		18,0	20,1	20,6	22,0	25,0
Directional diffusivity	**d %**					
Required; Eq. (3.149)		85	83	86	78	61
measured (average near wall)		87	90	91	92	94

Table 4.29

Receiving room diffusivity requirements for diagnostic sound transmission analysis by sound intensimetry, compared with values measured in NPRL reverberation room.

Test object : 220 mm brick filler wall containing Window 9,5L(200A)10S.

Maximum error $|Le| < 1,0$ dB; $A = 6,7$ m^2.

Octave band centre frequency (Hz)		125	250	500	1000	2000
Flanking ratio	h_F	0,17	0,17	0,11	0,38	2,5
Room absorption (m^2)	$S\alpha$	9,6	13,0	13,0	11,8	14,1
Intrinsic reactivity	**LRd**					
Required; Eq. (3.148)		14,0	12,7	12,5	13,8	17,1
measured (average near wall)		18,0	20,1	20,6	22,0	25,0
Directional diffusivity	**d %**					
Required; Eq. (3.149)		80	77	76	80	86
measured (average near wall)		87	90	91	92	94

CHAPTER 5

CONCLUSIONS

5.1 INTRODUCTION

This thesis presented a critical examination of sound transmission analysis by sound intensimetry, which involves the measurement of sound reduction indices and diagnostic analysis of sound transmission through panels and structures. Since the intensity method of determining sound reduction indices has certain basic aspects in common with the classic two-room method, the latter was examined theoretically and applied on a comparative basis with the intensity method.

The standard formulation of the intensity method has been expanded to account for leakage error, interference effects and calibration mismatch. A theoretical framework has been developed for the evaluation of sound transmission analysis by intensimetry. Application of the newly developed criteria to practical situations demonstrated the versatility of the intensity method, but it also emphasized the importance of acoustical evaluation of test arrangements in view of the performance limitations of practical measurement systems.

Determined by the accuracy of phase matching, the common mode rejection index of the sound intensity meter is the principle limiting factor in regard to the applicability of the intensity method. In assessing the validity of test results in a given application, this property must be weighed up against the minimum requirements for the situation, calculated according to the criteria developed in Chapter 3. These requirements, which depend upon the flanking factor, the reflectivity of the receiving room and the phase matching of the measurement system, may be brought within reach of the intensity meter performance, if necessary, by adjustment of either the microphone spacing or the amount of absorption in the receiving room.

Diffusion is a fundamental requirement of the classic two-room method and, albeit to a lesser extent, of the sound intensity method as well.

Assessment of the diffusivity of test rooms is often neglected because of a lack of practical measurement techniques for this purpose. A new method of measuring the degree of directional diffusivity has been developed and demonstrated in this thesis. Based on sound intensimetry, this technique gives a direct indication of diffusivity in terms of the intrinsic reactivity of the sound field.

5.2 THE CLASSIC TWO-ROOM METHOD

Most aspects of the classic two-room method have been thoroughly investigated in the literature. The unsuitability of this method to distinguish between direct and flanking transmission, however, is seldom referred to. The reason for this, presumably, is that standard measurement practice based on the classic two-room method requires that flanking transmission is either suppressed to negligable levels, or regarded as part of the direct transmission. In certain applications, namely if selective determination of the performance of highly efficient sound insulating elements is required, the latter approach is inadequate.

Confirmed by experimental observation, error analyses showed that selective determination of direct transmission by subtraction of the experimentally determined flanking power from the total power, becomes exceedingly difficult if the flanking factor exceeds a value of approximately 1,0. This lack of sensitivity also renders the classic two-room method unsuitable for diagnostic sound transmission analysis of composite test objects.

5.3 FORMULATION OF THE INTENSITY METHOD

The standard formulation of the sound intensity method of determining sound reduction indices

$$R = LP1 - LI - 6 \quad dB \tag{5.1}$$

has been expanded to

$$R = LP1 - LI + 10 \log (A/A_2) + 10 \log (1 + \lambda S_1/8V_1) + Lc - 6 \quad dB. \quad (5.2)$$

In order of appearance, the terms introduced into Eq. (5.1) to obtain Eq. (5.2) account for the following:

(1) The difference between the commonly used plane measurement surface A and the measurement surface A_2 needed to fully cover the radiation from the surface of the test object towards the receiving room. If a plane measurement surface is used, the resulting leakage error should be minimized by locating the measurement surface as close as possible to the radiation surface. Taking this precaution, the error is usually less than 1,0 dB.

(2) The storage of reverberant energy in the interference field constituted at the boundaries of the source room. At low frequencies, sound reduction indices obtained according to the standard formulation of the intensity method are generally lower than those obtained by the classic method. Introduction of the Waterhouse correction term improves the accuracy of the estimate for the average energy density in the room. At low frequencies, where it could make a difference of more than 2 dB, application of this correction was found to resolve the commonly observed discrepancy between intensity and classic method results. As for the classic two-room method, the Waterhouse correction is of less importance in view of the partial cancellation of the source and receiving room terms.

(3) Calibration mismatch between the sound pressure and intensity measurement systems employed in determining sound reduction indices. The effect of calibration mismatch is usually less than 1,0 dB but being a systematic error, it should be eliminated. The calculation or elimination of this error depends on the design of the measurement system and its calibration procedure.

5.4 SOUND ABSORPTION BY THE TEST OBJECT

Sound absorption by the test object on the receiving room side constitutes a sink within the Gaussian surface of integration. The flux of absorbed power subtracts from the flux of power radiated by the test object, creating the impression that less than the actual amount of power is transmitted. The sound reduction index is therefore overestimated as a result of sound absorption by the test object.

In most applications, owing to the typically low sound absorption exhibited by test panels, the error is negligible. However, since the flux of absorbed power not only depends on the absorption coefficient, but on the flanking factor as well, the following situations could give rise to large absorption errors:

(1) Sound insulation tests and diagnostic analysis of highly efficient elements mounted in filler walls.

(2) Sound insulation tests and diagnostic analysis of flanking walls containing thin panels or inefficient elements.

In the aforementioned cases the absorption error may attain large values, even though the test object may be a solid hard panel such as a brick wall with an absorption coefficient of 0,04 or less. Sound absorption by the test object not only affects the accuracy of sound insulation tests; it may also create a false impression of the transmission characteristics of composite structures. It should be borne in mind that the sound intensity meter (if used within its limitations), gives an accurate account of the net situation which may simultaneously involve radiation and absorption of sound. A well-damped panel in a filler wall would radiate a uniform flux of power into an anechoic receiving room. If the receiving room is made reverberant, the panel may appear to behave quite differently in that the net radiation may appear to become smaller or even negative. The reason for this is that the rate at which sound energy is absorbed from the reverberant field, which may be excited predominantly by flanking sources, becomes comparable with the power radiated by the panel.

The risk of absorption error in a given application of sound transmission analysis may be assessed with the aid of the criteria presented graphically in Fig. 3.6.

5.5 MINIMUM REQUIREMENTS FOR SOUND TRANSMISSION ANALYSIS IN REACTIVE FIELDS

Sound insulation tests in reverberant receiving rooms require detection of low intensity levels in reactive fields. The common mode rejection index LRm has been defined in order to relate the performance of the measurement system to the reactivity LR of the sound field.

The reactivity near the surface of a test object facing a reverberant receiving room may range from ≈ 1 dB to more than 20 dB. In most cases, however, LR is found to lie within the range 6 - 12 dB. Using matched pairs of high-quality condenser microphones with a spacing of 12 mm, LRm has a typical value of 12 dB at 125 Hz, increasing to 18 dB or more at frequencies > 500 Hz. By increasing the spacing to 50 mm, a further 6 dB may be gained at all frequencies. Hence, even with a spacing of only 12 mm, it is possible to perform reliable sound transmission tests in reverberant rooms. However, in view of the extremities which may be encountered, it is important to assess each situation to establish the minimum acoustical requirements.

The reactivity near the surface of a test object in a given application may be predicted with the aid of Fig. 3.10. In order to limit the intensity error to a specified value, a safety margin LRm - LR > ΔL, calculated by Eq. (3.108), must be maintained. This is accomplished by either of the following methods:

(1) Control of LRm by using a large enough microphone spacing. In some applications this may involve the use of more than one spacer to cover the frequency range of interest. The spacing required for a particular value of LRm may be determined by calibration of the measurement system in a rigidly terminated standing wave tube, or if the phase-match error is known, by using Eq. (3.109).

(2) Control of LR by increasing the amount of absorption in the receiving room. The minimum amount of absorption may be determined with the aid of Fig. 3.11 or by means of Eq. (3.111).

These criteria may be applied to any part of the structure, as long as the surface under investigation is consistently viewed as the test object, while the remainder of the structure is regarded as a flanking path.

5.6 DIFFUSIVITY

It has been shown that the sound intensity field in the vicinity of a source in a diffuse room is identical to that in a free field. The reason is that the sound intensity in the reverberant part of a diffuse field is characterized by uniform directional distribution and zero net flow at any point. If not deflected, the direct field maintains its free-field characteristic. The extent to which the total intensity field (direct plus reverberant) approximates the free-field characteristic of the source may be used as an indicator of the degree of directional diffusivity in the reverberant field.

A quantitative method of measuring the degree of directional diffusivity has been developed and evaluated. Based on the relationship between reactivity LR and the degree of directional balance in the intensity field, this method involves the measurement of the average sound pressure level in the room as well as the magnitude of the total intensity vector at the point under consideration. A direct-reading diffusivity meter, used in conjunction with a portable sound intensity meter, has been developed and utilized in assessing diffusivity in test environments.

The main advantage of the intensity method over the directivity and correlation methods, is its comparative simplicity and directness. Moreover, being directly related to the net energy imbalance at the point under consideration, the result of the intensity method may be used quantitatively in assessing the effect of a lack of diffusivity on acoustical tests performed in a reverberant room.

The effect of a lack of directional diffusivity on the accuracy of sound transmission analysis in reactive fields has been investigated. Criteria for calculating minimum diffusivity requirements in the source and receiving rooms have been developed. In short, these amount to the following: (LRd = intrinsic reactivity; d = % directional diffusivity)

(1) Source room For a maximum error of 1,0 dB, the requirement is

$$\{ LRd \geq 12 \text{ dB} \; ; \; d \geq 75 \; \% \} \tag{5.3}$$

(2) Receiving room Due to the elimination of extraneous noise by closed-surface integration of sound intensity, a diffuse receiving room is not required for the determination of sound reduction indices by intensimetry. For the purpose of diagnostic transmission analysis, however, a certain degree of diffusivity is required. The figure, according to Eq. (3.151), increases with the surface area of the test object and with the flanking factor, and decreases with the amount of absorption in the receiving room.

6. REFERENCES

[1] H.F. Olson, U.S. Patent No. 1892644 (1932).

[2] C.W. Clapp and F.A. Firestone, J. Acoust. Soc. Am., **13**, 124-136 (1941).

[3] S. Baker, "An Acoustic Intensity Meter", J. Acoust. Soc. Am., **27**, 2, 269-273 (1955).

[4] T.J. Schultz, "Acoustic Wattmeter", J. Acoust. Soc. Am., **28**, 4, 693-699 (1956).

[5] J.F. Burger, G.J.J. van der Merwe, B.G. van Zyl and L. Joffe, "Measurement of Sound Intensity Applied to the Determination of Radiated Sound Power", J. Acoust. Soc. Am., **53**, 3, 1167-1168 (1973).

[6] B.G. van Zyl, "Bepaling van Klankdrywing met behulp van 'n Klank-intensiteitsmeter", M.Sc. thesis, University of Pretoria (1974).

[7] B.G. van Zyl and F. Anderson, "Evaluation of the Intensity Method of Sound Power Determination", J. Acoust. Soc. Am., **57**, 3, 682-686 (1975).

[8] E. Skudrzyk, "Foundations of Acoustics", (Springer-Verlag, Wien-New York, 1971).

[9] B.G. van Zyl, "The Determination of the Comparative Sound Powers Radiated by two Gillbox Machines in the Carding and Combing Section of the SAWTRI in Port Elizabeth", NPRL Report (1973).

[10] CSIR, "Sizing up Sound", Scientific Progress, **6**, 4, 3-4 (1973).

[11] B.G. van Zyl, "Sound Intensity Meter", Technical Information for Industry, **17**, 5, 1-4 (1979).

[12] H.M.M. van der Wal and B.G. van Zyl, "Laboratory and Field Measurements with an Analog Intensity Meter", Proceedings of the International Congress on Recent Developments in Acoustic Intensity Measurements, Senlis, France (1981).

[13] M+P Akoestische Adviseurs bv, "Praktische Toepasbaarheid van Methoden ter Bepaling van de Geluidimmissie ten gevolge van Industriële Inrichtingen door Emmissiemetingen", Report MVM 78.2.1, M+P Akoestische Adviseurs bv, Amstelveen, The Netherlands (1979).

[14] B.G. van Zyl, "A Portable Sound Intensity Meter: Versatile Acoustical Instrument", Technical Information for Industry, **20**, 5, 1-6 (1982).

[15] B.G. van Zyl, "A Practical Sound Intensity Meter", Paper delivered at the 10th International Congress on Acoustics, Syndey, Australia (1980).

[16] B.G. van Zyl and F. Anderson, "The Sound Intensity Meter - Diagnostic Aid to Scientist and Engineer", Proceedings of the 1980 International Symposium on Sound, Buildings and People, Durban, South Africa (1980).

[17] B.G. van Zyl and F. Anderson, "The Sound Intensity Characteristics of a Diffuse Sound Field", Paper presented at the International Symposium on Acoustics and the Quality of Life, Cape Town, South Africa (1982).

[18] B.G. van Zyl, "Theoretical and Experimental Investigation of Certain Aspects of Diffusion in Reverberation Rooms", NPRL Report FIS 274 (1982).

[19] B.G. van Zyl, F. Anderson and P.J. Erasmus, "Sound Intensity in Diffuse Sound Fields", J. Acoust. Soc. Am., **78**, 2, 587-589 (1985).

[20] B.G. van Zyl, "A Portable Sound Intensity Meter: Versatile Acoustical Instrument", Power & Plant in Southern Africa, April 1983, 11-15 (1983).

[21] B.G. van Zyl, "The Sound Intensity Meter - Diagnostic Aid to Scientist and Engineer", Pulse, February 1981, 53-54 (1981).

[22] B.G. van Zyl and F. Anderson, "Determination of Acoustical Properties by Sound Intensity Measurement", Paper delivered at the 28th Annual Conference of the South African Institute of Physics, Pretoria, South Africa (1983).

[23] B.G. van Zyl and F. Anderson, "Sound Absorption Coefficients

Determined by Sound-Intensity Measurement", S. Afr. J. Phys., **3**, 64-66 (1980).

[24] B.G. van Zyl and P.J. Erasmus, "Sound Absorption Tests by Sound Intensimetry", Proceedings of the First South African Congress on Acoustics, Pretoria, South Africa (1985).

[25] B.G. van Zyl and P.J. Erasmus, "Sound Insulation Tests by Sound Intensimetry", Proceedings of the First International Congress on Acoustics", Pretoria, South Africa (1985).

[26] B.G. van Zyl, P.J. Erasmus and G.J.J. van der Merwe, "Determination of Sound Reduction Indices in the Presence of Flanking Transmission", To be published in Applied Acoustics (1985).

[27] B.G. van Zyl and P J Erasmus, "Application of Sound Intensimetry to the Determination of Sound Reduction Indices in the Presence of Flanking Transmission", Proceedings of the 2nd International Congress on Acoustic Intensity, Senlis, France, 555-560 (1985).

[28] B.G. van Zyl and P.J. Erasmus, "Sound Transmission Analysis in Reactive Fields by Sound Intensimetry", Submitted for publication in Noise Control Engineering (1985).

[29] B.G. van Zyl, P.J. Erasmus and G.J.J. van der Merwe, "A Comparative Study of the Classic Method and the Sound Intensity Method for Determining Sound Insulation", NPRL Report FIS 320 (1985).

[30] B.G. van Zyl, "Sound Intensity - An Introduction", Newsletter of the South African Acoustics Institute, **24**, 7-8 (1984).

[31] B.G. van Zyl, "Sound Intensity - Principles of Intensimetry", Newsletter of the South African Acoustics Institute, **25**, 8-11 (1985).

[32] T.J. Schultz, P.W.Smith Jr. and C.I. Malme, "Measurement of Acoustic Intensity in Reactive Sound Field", J. Acoust. Soc. Am., **57**, 6, 1263-1268 (1975).

[33] F.J. Fahy, "Measurements with an Acoustic Intensity Meter of the Acoustic Power of a small Machine in a Room", ISVR Technical Report No. 94 (1977).

[34] F.J. Fahy, "Measurement of Acoustic Intensity using the Cross-Spectral Density of two Microphone Signals", J. Acoust. Soc. Am., 62, 4, 1057-1059 (1977).

[35] F.J. Fahy, "A Technique for Measuring Sound Intensity with a Sound Level Meter", Noise Control Engineering, 9, 3, 155-162 (1977).

[36] G. Pavic, "Measurement of Sound Intensity", J. Sound Vib., 51, 4, 533-546 (1977).

[37] J.Y. Chung, "Cross-Spectral Method of Measuring Acoustic Intensity without Error caused by Instrument Phase Mismatch", J. Acoust. Soc. Am., 64, 6, 1613-1616 (1978).

[38] W. Stahel and H.P. Lambrich, "Development of an Instrument for the Measurement of Sound Intensity and its Application in Car Acoustics", external publication, INTERKELLER AG, Zurich, Switzerland (1977).

[39] J.Y. Chung and J. Pope, "Practical Measurement of Acoustic Intensity - The Two Microphone Cross-Spectral Method", Proceedings of INTER-NOISE 78, San Francisco, CA, 893-900 (1978).

[40] T.K. Stanton and R.T. Beyer, "Complex Wattmeter Measurements in a Reactive Acoustic Field", J. Acoust. Soc. Am., 65, 1, 249-252 (1979).

[41] D.H. Munro and K.U. Ingard, "On Acoustic Intensity Measurements in the Presence of Mean Flow", J. Acoust. Soc. Am., 65, 6, (1979).

[42] R.J. Alfredson, "The Direct Measurement of Acoustic Energy in Transient Sound Fields", J. Sound Vib., 70, 2, 181-186 (1980).

[43] J.Y. Chung and D.A. Blaser, "Transfer Function Method of Measuring Acoustic Intensity in a Duct System with Flow", J. Acoust. Soc. Am., 68, 6, 1570-1577 (1980).

[44] J.K. Thompson and D.R. Tree, "Finite Difference Approximation Errors in Acoustic Intensity Measurements", J. Sound Vib., 75, 2, 229-238 (1981).

[45] A.F. Seybert, "Statistical Errors in Acoustic Intensity Measurements", J. Sound Vib., 75, 4, 519-526 (1981).

[46] O.K.O. Petterson, "A Procedure for Determining the Sound Intensity Distribution Close to a Vibrating Surface", J. Sound Vib., **66**, 626-629 (1979).

[47] G. Krishnappa, "Cross-Spectral Method of Measuring Acoustic Intensity by Correcting Phase and Gain Errors by Microphone Calibration", J. Acoust. Soc. Am., **69**, 1, 307-310 (1981).

[48] S. Gade, "Sound Intensity (Part I. Theory)", Technical Review, Brüel & Kjaer, 1982 No. 3, 3-39 (1982).

[49] S. Gade, "Sound Intensity (Part II. Instrumentation & Applications)", Technical Review, Brüel & Kjaer, 1982 No. 4, 3-32 (1982).

[50] J.C. Pascal and C. Carles, "Systematic Measurement Errors with Two Microphone Sound Intensity Meters", J. Sound Vib., **83**, 1, 53-65 (1982).

[51] A.F. Seybert, "Source Characterization Using Acoustic Intensity Measurements", Proceedings of INTER-NOISE 80, Miami, 1067-1070 (1980).

[52] J. Bucheger, W. Trethewey and H.A. Evensen, "A Selective Two Microphone Acoustic Intensity Method", J. Sound Vib., **90**, 1, 93-101 (1983).

[53] G.P. Mathur, "A Stochastic Analysis for Cross-Spectral Density Method of Measuring Acoustic Intensity", J. Acoust. Soc. Am., **74**, 6, 1752-1756 (1983).

[54] G. Rasmussen and M. Brock, "Transducers for Intensity Measurements", Proceedings of the 11th ICA, Paris, France, 177-180 (1983).

[55] P.R. Wagstaff and J.C. Henrio, "The Measurement of Acoustic Intensity by Selective Two Microphone Techniques with a Dual Channel Analyzer", J. Sound Vib., **94**, 1, 156-159 (1984).

[56] G.S.K. Wong, "Precise Measurement of Phase Difference and the Amplitude Ratio of Two Coherent Sinusoidal Signals", J. Acoust. Soc. Am., **75**, 3, 967-972 (1984).

[57] J.Y. Chung, "Funmdamental Aspects of the Cross-Spectral Method of

Measuring Acoustic Intensity", Proceedings of the International Congress on Recent Developments in Acoustic Intensity Measurement, Senlis, France, 1-10 (1981).

[58] F.J. Fahy and S.J. Elliott, "Practical Considerations in the Choice of Transducers and Signal Processing Techniques for Sound Intensity Measurement", Proceedings of the International Congress on Recent Developments in Acoustic Intensity Measurement, Senlis, France, 37-44 (1981).

[59] F.J. Fahy and S.J. Elliott, "Acoustic Intensity Measurements of Transient Noise Sources", Noise Control Engineering, **17**, 120-123 (1981).

[60] G.S.K. Wong, "Precise Measurement of Phase Difference and Amplitude ratio with an Interchange Reference Method", J. Acoust. Soc. Am., **73**, S23 (1983).

[61] G. Krishnappa, "Scattering/Diffraction Effects in the Two-Microphone Technique of Measuring Sound Intensity at Sound Incidence Angles Other than 0 °", Noise Control Engineering, **22**, 3, 96-102 (1984).

[62] J. Tichy, "Some Effects of Microphone Environment on Intensity Measurements", Proceedings of the International Congress on Recent Developments in Acoustic Intensity Measurements, Senlis, France, 25-30 (1981).

[63] G. Krishnappa, "Some Investigations of the limitations of Acoustic Intensity Measurements by Two Microphone Technique in Noise Source Identifications", Proceedings of INTER-NOISE 82, **II**, 699-702 (1982).

[64] T.W. Bartel, S.L. Yaniv and R.K. Cook, "Analog Measurement of Intensity for Bandlimited Noise in a Standing-Wave Tube", J. Acoust. Soc. Am., **76**, 5, 1573-1576 (1984).

[65] D. Pleeck and E.C.Petersen, "Real Time Sound Intensity Measurements Performed with an Analog and Portable Instrument", Proceedings of the International Congress on Recent Developments in Acoustic Intensity Measurements, Senlis, France, 53-60 (1981).

[66] O. Roth, "A Sound Intensity Real-Time Analyzer", Proceedings of the International Congress on Recent Developments in Acoustic Intensity Measurements, Senlis, France, 69-74 (1981).

[67] M.P. Waser and M.J. Crocker, "Introduction to the Two-Microphone Cross-Spectral Method of Determining Sound Intensity", Noise Control Engineering, **22**, 3, 76-85 (1984).

[68] H.A. Wolf, "Development of the Two-Microphone Cross-Spectral Method for In-Situ Sound Power Measurements", Proceedings of INTER--NOISE 82, **II**, 747-750 (1982).

[69] V.O. Knudsen, "Measurement and Calculation of Sound-Insulation", J. Acoust. Soc. Am., **2**, 1, 129-140 (1930).

[70] L.L. Beranek, "Acoustic Measurements", (John Wiley & Sons, Inc., New York, 1949).

[71] "Measurement of Sound Insulation in Buildings and of Building elements", International Standard ISO 140 I-III, International Organization for Standardization (1978).

[72] M.J. Crocker, B. Forssen, P.K. Raju and A. Mielnicka, "Measurement of Transmission Loss of Panels by an Acoustic Intensity Technique", (INTER-NOISE 80, George C. Maling, Jr., Ed. Noise Control Foundation, New York, 1980), **II**, 741-746 (1980).

[73] E. Buckingham, "Theory and Interpretation of Experiments on the Transmission of Sound Through Partition Walls", National Bureau of Standards (U.S.), Sci. Technol. Papers, **20**, 193-219 (1925).

[74] F.R. Watson, "Coefficient of Transmission of Sound", J. Acoust. Soc. Am., **1**, 202-208 (1930).

[75] V.L. Chrisler, "Measurement of Sound Transmission", J. Acoust. Soc. Am., **1**, 2, 175-180 (1930).

[76] P.E. Sabine, "Transmission of Sound by Walls", J. Acoust. Soc. Am., **1**, 2, 181-201 (1930).

[77] P. E. Sabine, "Sound Transmission Coefficient and Reduction Factors", J. Acoust. Soc. Am., **2**, 4, 506-513 (1931).

[78] W. Waterfall, "An Audiometric Method for Measuring Sound Insulation", J. Acoust. Soc. Am., **1**, 2, 209-216 (1930).

[79] R.W. Guy, A De Mey and P. Sauer, "The Effect of Some Physical Parameters upon the Laboratory Measurement of Sound Transmission

Loss", Applied Acoustics, **18**, 81-98 (1985).

[80] G. Maidanik, "Response of Ribbed Panels to Reverberant Acoustic Fields", J. Acoust. Soc. Am., **34**, 809-826 (1962).

[81] M.J. Crocker and A.J. Price, "Sound Transmission Using Statistical Energy Analysis", J. Sound Vib., **9**, 3, 469-486 (1969).

[82] A.J. Price and M.J. Crocker, "Sound Transmission Through Double Panels Using Statistical Energy Analysis", J. Acoust. Soc. Am., **3**, 1, 683-693 (1969).

[83] A.C. Nilsson, "Reduction Index and Boundary Conditions for a Wall between Two Rectangular Rooms.", Acustica, **26**, 1-23 (1972).

[84] T. Kihlman and A.C. Nilsson, "The Effects of Some Laboratory Designs and Mounting Conditions on Reduction Index Measurements", J. Sound Vib., **24**, 349-364 (1972).

[85] K.A. Mulholland, H.D. Parbrook and A. Cummings, "The Transmission Loss of Double Panels", J. Sound Vib., 6, 3, 324-334 (1967).

[86] M. Heckl, "The Tenth Sir Richard Fairey Memorial Lecture: Sound Transmission in Buildings", J. Sound Vib., **77**, 2, 165-189 (1981).

[87] J.B. Ochs, "Transmissibility Across Simply Supported Thin Plates. I. Rectangular and Square Plates with and without Damping Layers", J. Acoust. Soc. Am., **58**, 4, 832-840 (1975).

[88] A. Cummings and K.A. Mulholland, "The Transmission Loss of Finite Sized Double Panels in a Random Incidence Sound Field", J. Sound Vib., 8, 1, 126-133 (1968).

[89] W.A. Utley and B.L. Fletcher, "Influence of Edge Conditions on the Sound Insulation of Windows", Applied Acoustics, **2**, 131-136 (1969).

[90] J. Lang, "Differences Between Acoustical Insulation Properties Measured in the Laboratory and Results of Measurements in Situ", Applied Acoustics, 5, 21-37 (1972).

[91] R.E. Jones, "Effects of Flanking and Test Environment on Lab-Field Correlations of Airborne Sound Insulation", J. Acoust. Soc. Am., **57**, 5, 1138-1149 (1975).

[92] A.C.C. Warnock, "Influence of Specimen Frame on Sound Transmission Loss Measurement", Applied Acoustics, 15, 307-314 (1982).

[93] M.C. Bhattacharya and R.W. Guy, "The Influence of the Measuring Facility on the Measured Sound Insulating Property of a Panel", Acustica, 26, 344-347 (1972).

[94] T. Mariner, "Critique of the Reverberant Room Method of Measuring Air-Borne Sound Transmission Loss", J. Acoust. Soc. Am., 33, 3, 1131-1139 (1961).

[95] P.V. Brüel, "The Enigma of Sound Power Measurements at Low Frequencies", Technical Review, Brüel & Kjaer, 1978 No. 3, 3-39 (1978).

[96] H. Larsen, "Reverberation Process at Low Frequencies", Technical Review, Brüel & Kjaer, 1978 No. 4, 3-41 (1978).

[97] H.Larsen, "Power Based Measurements of Sound Insulation", Technical Review, Brüel & Kjaer, 1980 No. 3, 3-22 (1980).

[98] P. De Tricaud, "Impulse Techniques for the Simplification of Insulation Measurement Between Dwellings", Applied Acoustics, 8, 245-256 (1975).

[99] K.W. Goff, "The Application of Correlation Techniques to Some Acoustic Measurements", J. Acoust. Soc. Am., 27, 2, 236-246 (1955).

[100] P.D. Schomer, "Measurement of Sound Transmission Loss by Combining Correlation and Fourier Techniques", J. Acoust. Soc. Am., 51, 4, 1127-1141 (1971).

[101] J.A. Macadam, "The Measurement of Sound Radiation from Room Surfaces in Lightweight Buildings", Applied Acoustics, 9, 103-118 (1976).

[102] A.N. Burd, "The Measurement of Sound Insulation in the Presence of Flanking Paths", J. Sound Vib., 7, 13-26 (1968).

[103] E. Meyer et al., "A Tentative Method for the Measurement of Indirect Sound Transmission in Buildings", Acustica, 1, 17-28 (1951).

[104] M.J. Crocker and F.M. Kessler, "Noise and Noise Control Volume II", (CRC Press, Inc., Boca Raton, Florida, 1982).

[105] L.L. Beranek, "Acoustics", (McGraw-Hill Book Company, Inc., New York, 1954).

[106] J.D. Irwin and E.R. Graf, "Industrial Noise and Vibration Control", (Prentice-Hall, Inc., Englewood Cliffs, New York, 1979).

[107] L.E. Kinsler and A.R. Frey, "Fundamentals of Acoustics", (John Wiley & Sons, Inc., New York, 1962).

[108] H. Kuttruff, "Room Acoustics", (Allied Science Publishers Ltd., London, 1973).

[109] R.W. Young, "Sabine Reverberation Equation and Sound Power Calculations", J. Acoust. Soc. Am., **31**, 7, 912-921 (1959).

[110] D.K. Cheng, "Analysis of Linear Systems", (Addison-Wesley Publishing Company, Inc., Reading, Massachusetts, 1966).

[111] R.J. Donato, "Direct-Energy Density in Transmission-Loss Measurements", J. Acoust. Soc. Am., **40**, 1, 1-3 (1966).

[112] R.K. Cook, et al., "Measurement of Correlation Coefficients in Reverberant Sound Fields", J. Acoust. Soc. Am., **27**, 6, 1072-1077 (1955).

[113] R.V. Waterhouse, "Interference Patterns in Reverberant Sound Fields", J. Acoust. Soc. Am., **27**, 2, 247-258 (1955).

[114] M.J. Crocker and A.J. Price, "Noise and Noise Control Volume I", (CRC Press, Inc., Cleveland, Ohio 44128, 1975).

[115] R. Waterhouse, "Noise Measurement in Reverberant Rooms", J. Acoust. Soc. Am., **54**, 4, 931-934 (1973).

[116] T.W. Bartel. S.L. Yaniv and D.R. Flynn, "Use of 'Corner Microphones' for Sound Power Measurements in a Reverberation Chamber", J. Acoust. Soc. Am., **74**, 6, 1794-1800 (1983).

[117] A. de Bruijn, "Influence of Diffusivity on the Transmission Loss of a Single-Leaf Wall", J. Acoust. Soc. Am., **47,** 3, 667-675 (1970).

[118] L.W. Sepmeyer, "Computed Frequency and Angular Distribution of Normal Modes of Vibration in Rectangular Rooms", J. Acoust. Soc. Am., **37,** 3, (1965).

[119] V.M.A. Peutz, "The Sound Energy Density in a Room", Proceedings of the 6th International Congress on Acoustics, Tokyo, Japan, E-165-168, E-5-2 (1968).

[120] M.M. Carroll, "Steady-State Sound in an Enclosure with Diffusely Reflecting Boundary", J. Acoust. Soc. Am., **64,** 5, 1424-1428 (1978).

[121] K. Fujiwara, "Steady State Sound Field in an Enclosure with Diffusely and Specularly Reflecting Boundaries", Acustica, **54,** 266-273 (1984).

[122] R.N. Miles, "Sound Field in a Rectangular Enclosure with Diffusely Reflecting Boundaries", J. Sound Vib., **92,** 2, 203-226 (1984).

[123] C.G. Balachandran and R.W.Robinson, "Diffusion of the Decaying Sound Field", Acustica, **19,** 5, 245-257 (1967/68).

[124] V.R. Thiele, "Richtungsverteilung und Zeitfolge der Schalldrückwürfe in Räumen", Acustica, **3,** 291-302 (1953).

[125] E. Meyer, "Definition and Diffusion in Rooms", J. Acoust. Soc. Am., **26,** 630-634 (1954).

[126] E. Meyer and R. Thiele, "Raumakustische Untersuchungen in Zahlreichen Konzertsälen und Rundfunkstudios unter Anwendung Neuerer Messverfahren", Acustica, **6,** 425-444 (1956).

[127] A.D. Broadhurst, "An Acoustical Telescope for Architectural Acoustic Measurements", Acustica, **46,** 299-310 (1980).

[128] A.D. Broadhurst, "Sparse Volume Array for Architectural Acoustic Measurements", Acustica, **50,** 1, 33-38 (1982).

[129] P. Dämmig, "Zur messung der Diffusität von Schallfelderen durch Korrelation", Acustica, **7**, 387-399 (1957).

[130] F. Kohmer and M. Krnack, "Der Einfluss der Fläche des Prüfmaterials auf die Diffusität des Schallfeldes im Hallraum und auf den Schallabsorptionsgrad", Acustica, **11**, 405-413 (1961).

[131] E.C. Wente, "Characteristics of Sound Transmission in Rooms", J. Acoust. Soc. Am., **7**, 123-126 (1935).

[132] R.H. Bolt and R.W. Roop, "Frequency Response Fluctuations in Rooms", J. Acoust. Soc. Am., **22**, 2, 280-289 (1950).

[133] M.J. Crocker, B. Forssen, P.K. Raju and A. Mielnicka, "Measurement of Transmission Loss of Panels by an Acoustic Intensity Technique", Inter-Noise 80 Proceedings, 741-746 (1980).

[134] M.J. Crocker, P.K. Raju and B. Forssen, "Measurement of Transmission Loss of Panels by the Direct Determination of Transmitted Acoustic Intensity", Noise Control Engineering, **17**, 1, 6-11 (1981).

[135] Y.S. Wang and M.J. Crocker, "Direct measurement of Transmission Loss of Aircraft Structures Using the Acoustic Intensity Approach", Noise Control Engineering, **19**, 3, 80-85 (1982).

[136] A. Cops, "Acoustic Intensity Measurements and their Application to the Sound Transmission Loss of Panels and Walls", Proceedings of Inter-Noise 83, 567 (1983).

[137] A. Cops and M. Minten, "Comparative Study Between the Sound Intensity Method and the Conventional Two-Room Method to Calculate the Sound Transmission Loss of Wall Constructions", Noise Control Engineering, **22**, 3, 104-111 (1984).

[138] J. Roland, M. Villenave and C. Martin, "Intensimétrie Acoustique Application à la Recherche des Chemins de Transmission du Son", Report, Centre Scientifique et Technique du Bâtiment, Paris, France (1984).

[139] M.C. McGary and W.H. Mayes, "A New Measurement Method for separating Airborne and Structureborne Aircraft Interior Noise", Noise Control Engineering, **20**, 1, 21-30 (1983).

[140] A. Cops and M. Minten, "The Niche Effect in Sound Transmission Loss Measurements - A Comparison Between the Intensity and the Two-Room Method", Proceedings of Inter-Noise 84, Honolulu, 1197 (1984).

[141] A. Cops, M. Minten and H. Myncke, "Influence of the Design of Sound Transmission Rooms on the Sound Transmission Loss of Glass", Report, Laboratorium voor Akoestiek en Warmtegeleiding, Belgium (1985).

[142] S. Gade, K.B. Ginn, O. Roth and M. Brock, "Sound Power Determination in Highly Reactive Environments Using Sound Intensity Measurements", Paper delivered at Inter-Noise 83 (1983).

[143] P.H. Parkin and H.R. Humphreys, "Acoustics Noise and Buildings", (Faber and Faber, Ltd, London 1969).

APPENDIX A1

DESCRIPTION AND SPECIFICATIONS OF SOUND INTENSITY METER MODEL A83 SIM

A1.1 GENERAL DESCRIPTION

A1.1.1 Physical description Model A83 SIM, shown in Plate A1.1, is a battery-operated portable sound intensity meter developed at the NPRL of the CSIR. The dimensions of the instrument are 335 x 185 x 90 mm and it has a weight of 3,0 kg.

A1.1.2 Measurement principle Particle velocity is derived from the signals of two pressure microphones in accordance with the relationship defined in Euler's equation. The sequence of differentiation and integration, however, differs from the usual order in that subtraction is preceeded rather than followed by integration. Sound pressure is determined by averaging of the two microphone signals and the sound intensity by multiplication of the pressure and particle velocity signals. The measurement of sound intensity as shown diagrammatically in Figure A1.1, is performed by analog electronic computation.

A1.1.3 Modular composition The main functions of the system are grouped and contained in 11 modules, as shown in Fig. A1.2.

A1.1.4 Filters The system incorporates two sets of matched filters, each comprising eight octave filters (centre frequencies from 63 Hz to 8 kHz) as well as dBA and LINEAR networks. dBA-weighting complies with IEC recommendation 179 in the frequency range 10 Hz to 10 kHz. Octave filters meet requirements for ANSI Class II filters.

A1.1.5 Averaging facilities In addition to using FAST or SLOW meter response, averaging may be performed by linear integration of the instantaneous intensity signal over fixed periods of either 10 s or 32 s.

A1.1.6 Signal output/input (record/playback) facilities. Input/output facilities provided at various stages in the computation process simplify calibration, test, recording and playback procedures.

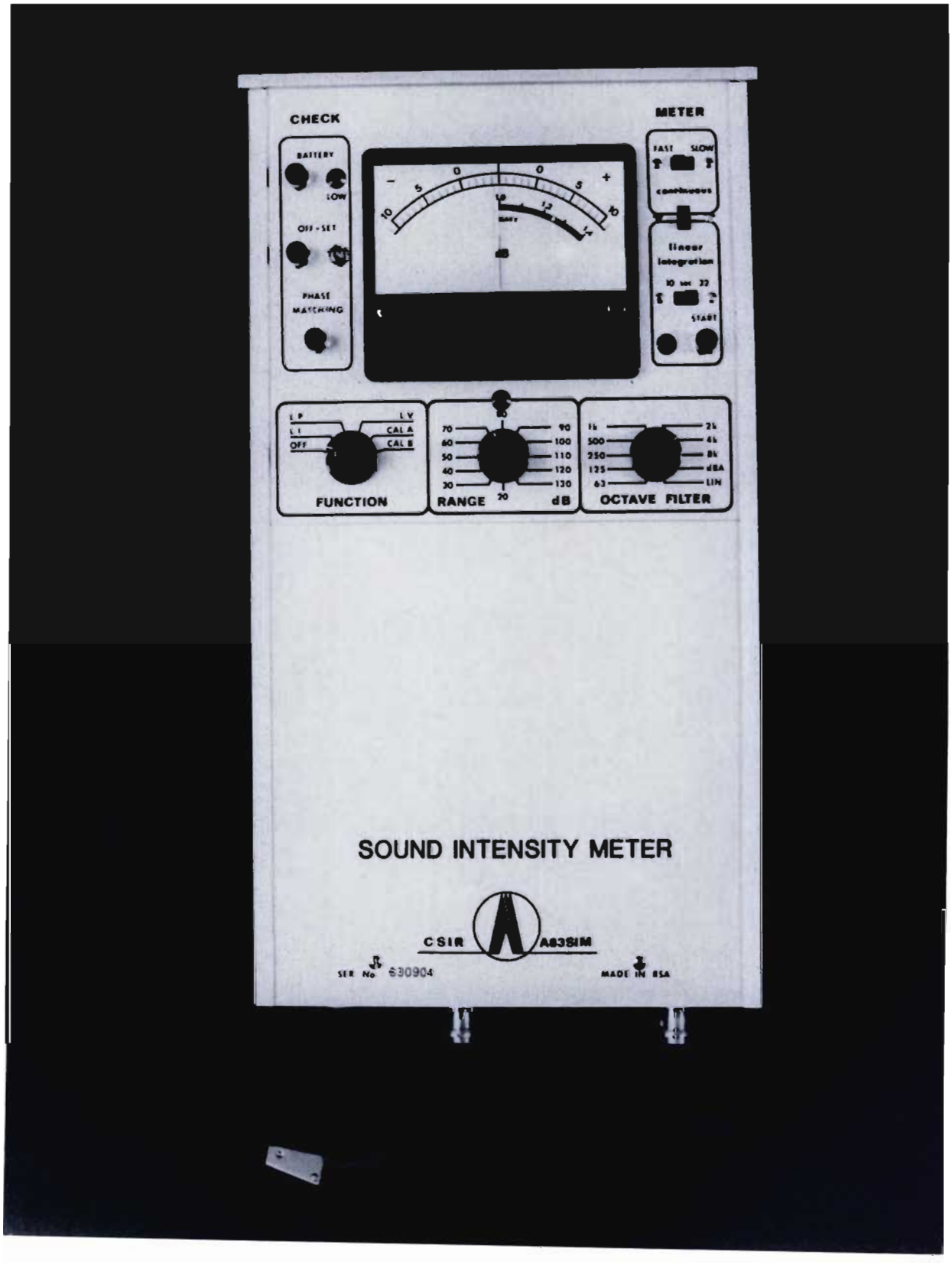

Plate A1.1

Sound intensity meter model A83 SIM

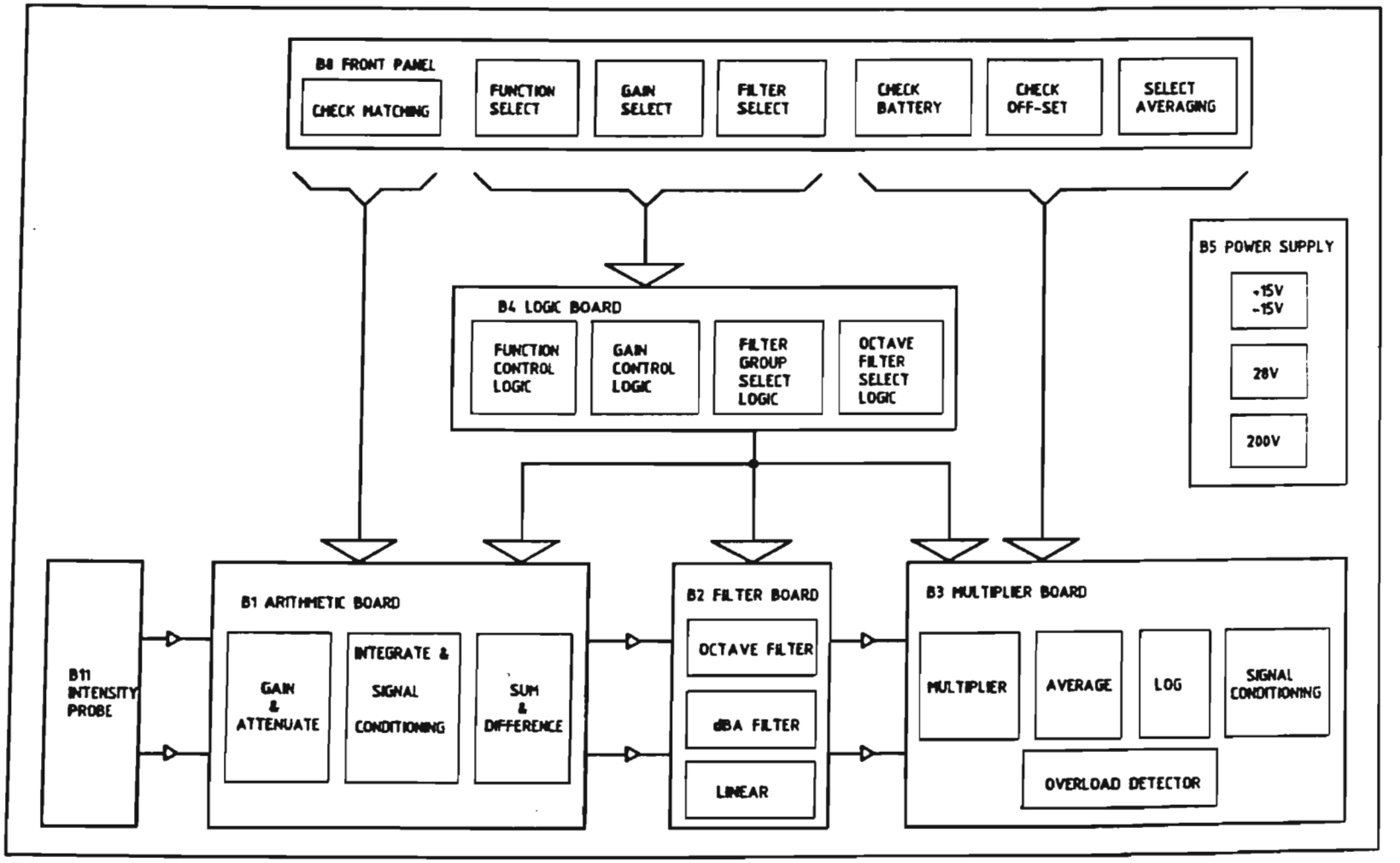

Figure A1.1

Block diagram of sound intensity meter Model A83 SIM

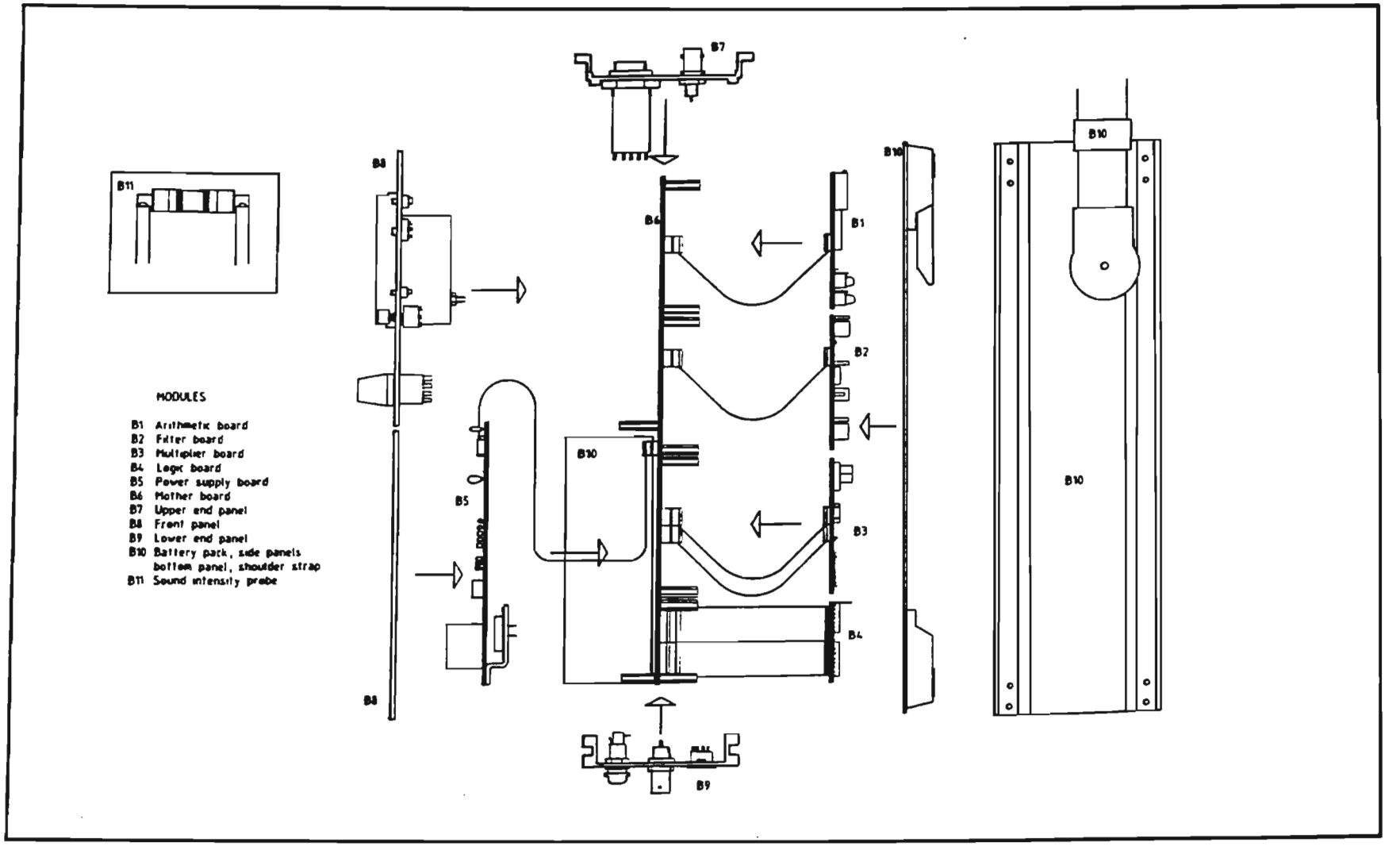

Figure A1.2

Expanded side view showing modular composition of sound intensity meter Model A83 SIM

A1.1.7 Functions The following functions may be selected:

(1) Sound intensity level (re $10^{-12}W/m^2$)
(2) Particle velocity level (re 50×10^{-9}nm/s)
(3) Pressure level, microphone A (re 20×10^{-6} Pa)
(4) Pressure level, microphone B (re 20×10^{-6} Pa)

A1.1.8 Intensity probe Model A83 SIM is used with either of the following two probes:

(1) Brüel & Kjaer type 3519 sound intensity probe.
(2) NPRL intensity probe comprising two sets of phase-matched Brüel & Kjaer type 4165 condenser microphones and 2619 preamplifiers contained in an adjustable clamp. Cylindrical spacers are used to stabilize the microphones in their spaced positions and to reduce interference effects. The NPRL-probe is shown in Plate A1.2.

Performance figures presented in this appendix were measured with the intensity meter fitted with the latter probe.

A1.2 CALIBRATION

A1.2.1 Regular calibration The microphones are calibrated with the aid of a pistonphone. This ensures calibration of all functions, provided system gain setting corresponds with selected microphone spacing.

A1.2.2 Optional adjustment of relative calibration level Particle velocity gain can be adjusted to attain calibration for $\rho c \neq 400$ mks rayls, if required. Calibration is performed by means of an electronic calibrator A83 CAL 2 which generates two accurately defined phase-shifted signals.

A1.2.3 System performance checks Special functions and facilities are incorporated in the system to enable accurate **in situ** assessment and optimization of system performance. This ensures accurate differentia-

Plate A1.2

Sound intensity probe used with sound intensity meter Model A83 SIM

tion and integration and provides for optimum gain and phase matching of the electronic system.

A1.3 SPECIFICATIONS

A1.3.1 Frequency response The frequency response curves of the complete system shown in Fig. A1.3(a) - (c) were determined in an anechoic room with the intensity probe placed at a distance of 0,75 m from a loudspeaker driven by a sine-wave signal. A reference microphone and a compressor-feedback system were used to attain a frequency - independent sound pressure level at the measurement point.

A1.3.2 Directional response The directional characteristics of the sound intensity meter as measured in an anechoic chamber are shown in Fig. A1.4.

A1.3.3 Common mode rejection index The common mode rejection indices LRm of the system listed in Table A1.1 were obtained by measuring the sound pressure level LP and the sound intensity level L Im in a rigidly terminated standing wave tube excited with broad-band random noise. LRm was calculated from

$$L_{Rm} = L_P - L_{Im} \quad \text{dB} \tag{A1.1}$$

Table A1.1

Common mode rejection indices LRm of model A83 SIM sound intensity meter for different microphone spacings Δr.

Δr (mm)	Octave band centre frequency (Hz) 63	125	250	500	1000	2000	4000	8000
9	6,0	10,3	15,5	17,0	15,0	16,0	18,0	15,0
15	8,2	12,5	18,0	19,0	17,0	18,0	20,0	-
60	14,1	18,6	24,0	25,1	23,0	-	-	-

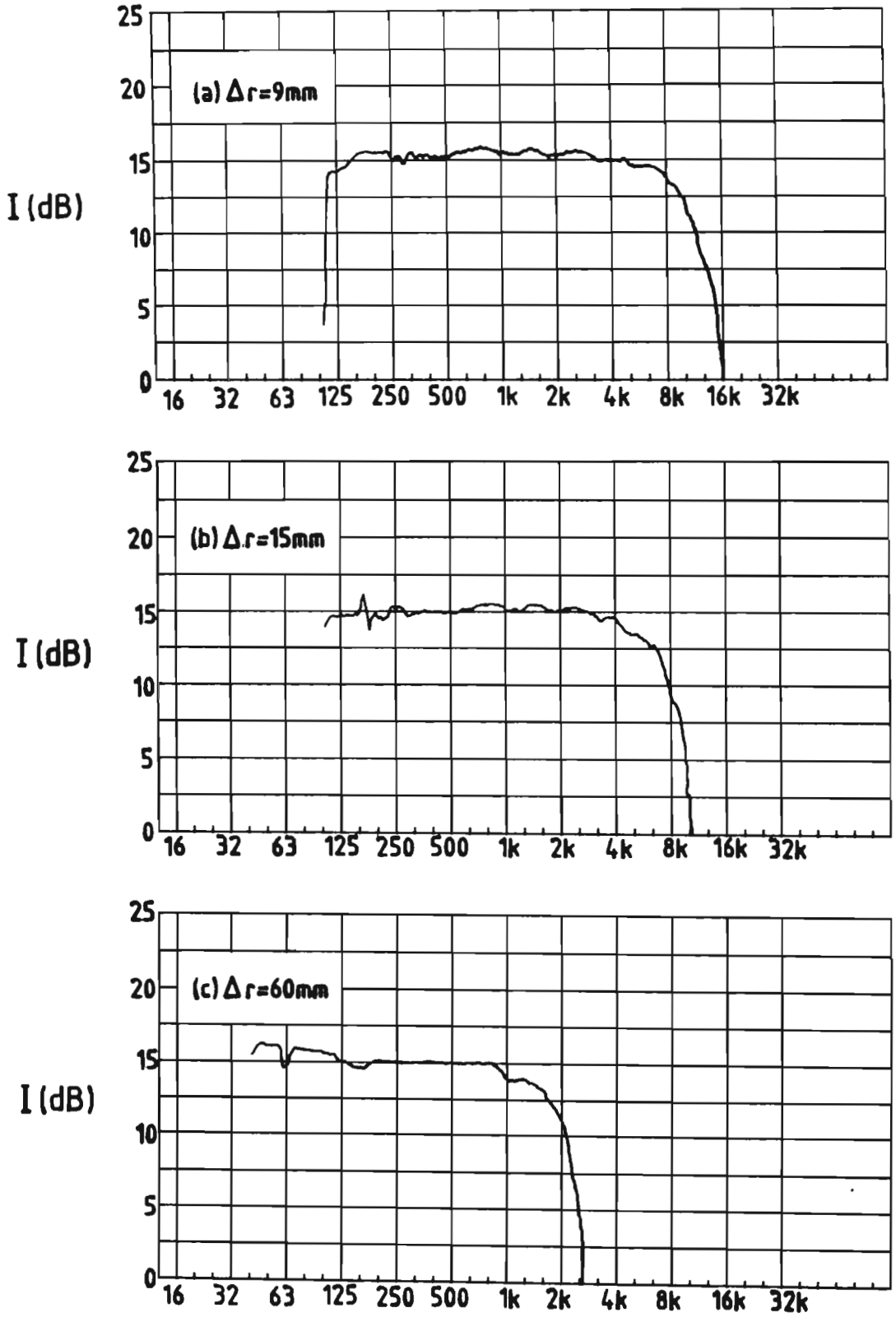

Figure A1.3

Frequency response of sound intensity meter Model A83 SIM.
Intensity probe: 2X B&K4165 microphones + 2X B&K2619 preamplifiers.

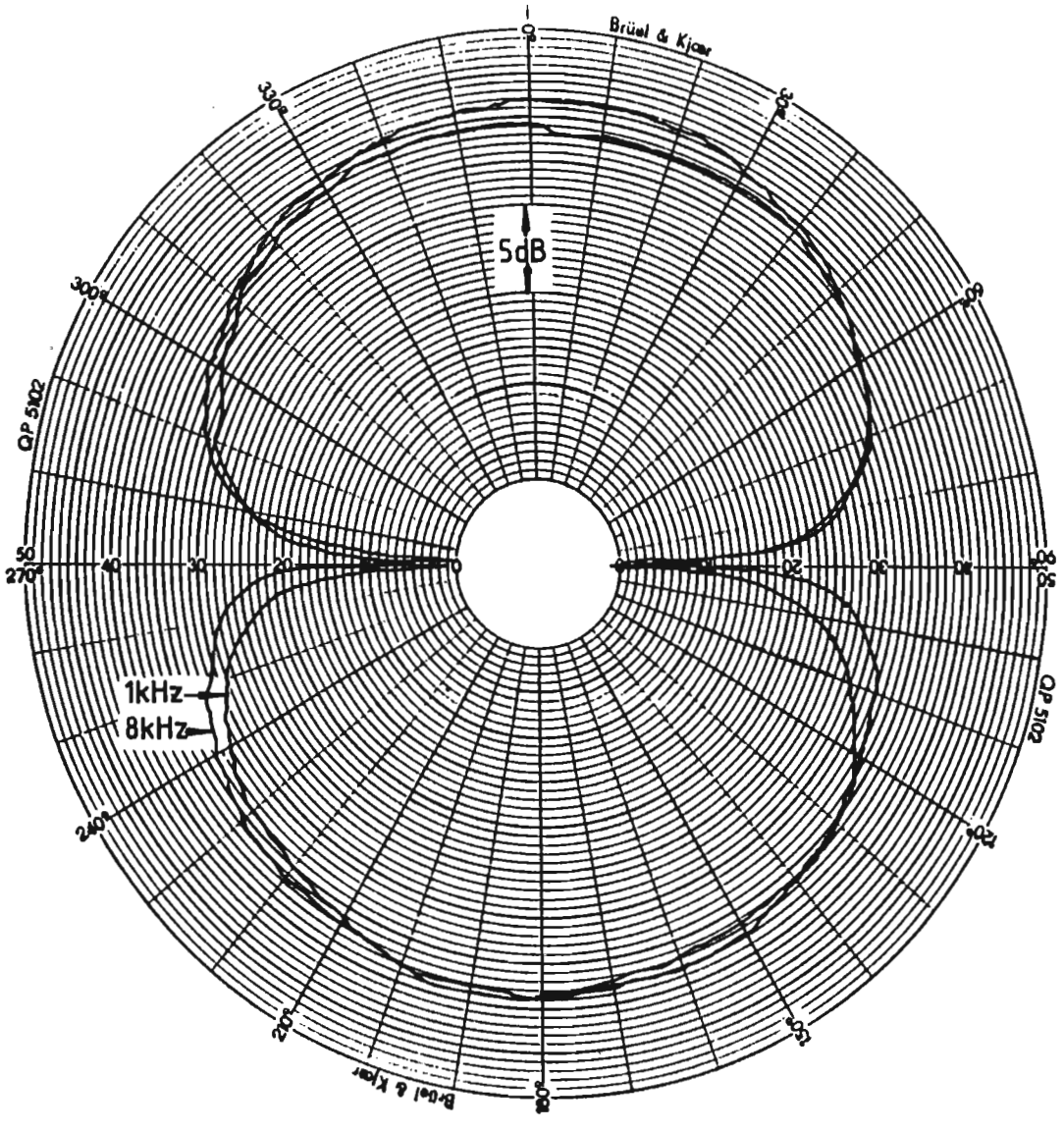

Figure A1.4

Directional intensity response of model A83 SIM.
Probe: 2X B&K4165 microphones + 2X B&K2619 preamplifiers.
Δr = 15mm.

A1.3.4 Dynamic range The maximum level (pressure, particle velocity and sound intensity) is 140 dB relative to standard reference levels P_0 = 20 x 10^{-6} Pa, U_0 = 50 x 10^{-9} nm/s and I_0 = 10^{-12} W/m^2. Minimum levels measured with the probe placed in a quiet anechoic chamber are listed in Table A1.2.

Table A1.2

Sound intensity meter Model A83 SIM

Equivalent octave-band sound pressure level LP, particle velocity level LV and sound intensity level LI (dB) due to inherent system noise (microphones included). Δr = microphone spacing.

Δr (mm)	Function	Octave band centre frequency (Hz) 63	125	250	500	1000	2000	4000	8000
9	LP	25	20	<15	<15	<15	<15	<15	<15
	LV	58	49	41	33	26	21	17	16
	LI	30	20	<15	<15	<15	<15	<15	<15
15	LV	54	45	37	29	22	17	<15	-
	LI	25	18	<15	<15	<15	<15	<15	-
60	LV	42	<15	<15	<15	<15	-	-	-
	LI	20	<15	<15	<15	<15	-	-	-